

Electronic Thesis and Dissertation Repository

9-25-2020 2:00 PM

Assessment of the Performance of Field-Scale Bioretention Systems to Reduce Phosphorus Loads from Urban Stormwater

Jaeleah J. Goor, *The University of Western Ontario*

Supervisor: Robinson, Clare E., *The University of Western Ontario*

A thesis submitted in partial fulfillment of the requirements for the Master of Engineering Science degree in Civil and Environmental Engineering

© Jaeleah J. Goor 2020

Follow this and additional works at: <https://ir.lib.uwo.ca/etd>



Part of the [Environmental Engineering Commons](#)

Recommended Citation

Goor, Jaeleah J., "Assessment of the Performance of Field-Scale Bioretention Systems to Reduce Phosphorus Loads from Urban Stormwater" (2020). *Electronic Thesis and Dissertation Repository*. 7348. <https://ir.lib.uwo.ca/etd/7348>

This Dissertation/Thesis is brought to you for free and open access by Scholarship@Western. It has been accepted for inclusion in Electronic Thesis and Dissertation Repository by an authorized administrator of Scholarship@Western. For more information, please contact wlsadmin@uwo.ca.

Abstract

High nutrient loading can degrade surface water quality worldwide. Bioretention systems are low impact development stormwater management features designed to remove pollutants, including phosphorus (P), from urban stormwater runoff. In this study, two field-scale bioretention systems installed in London, Ontario, Canada were monitored to develop detailed understanding of P behaviour and the hydro-biogeochemical mechanisms that govern overall P retention. Net retention of total P and dissolved organic P, and net release of soluble reactive P (SRP) and total dissolved P were observed. Prolonged input of road de-icing salts (NaCl) in winter and early spring may result in high P release from the bioretention systems in spring. Porewater samples revealed the distribution of SRP within the bioretention systems to be highly heterogeneous and without a monotonic decrease with depth as commonly assumed in literature, highlighting complex temporal and spatial behaviour of P and controlling biogeochemical processes within field-scale bioretention systems.

Keywords

Stormwater Management, Low Impact Development (LID), Bioretention, Green Infrastructure, Phosphorus, Road Salt, Seasonal, Field Investigations, Biogeochemical Processes, Sorption, Cold Climate

Summary for Lay Audience

Rainwater from urban areas can become polluted by nutrients (nitrogen and phosphorus) because of human activities such as lawn fertilization and animal waste. While some nitrogen and phosphorus is needed for plant and animal growth, high levels in lakes and rivers can create toxic algal blooms which cause serious public health, economic and environmental problems. Bioretention systems, sometimes called rain gardens, are designed to clean and control rainwater runoff from urban areas to protect streams, rivers, and lakes. They allow water to soak into the ground and use natural methods such as filtration to improve the water quality. However, these systems do not always perform as designed and can release high levels of phosphorus under certain conditions. It is still unclear what controls the behavior of phosphorus within bioretention systems and what conditions result in phosphorus release instead of phosphorus retention.

For this study, water samples were analyzed from the input and output of two bioretention systems in London, Ontario, Canada over an entire year. The output concentrations of the different chemical forms of phosphorus were considerably higher in spring compared to the rest of the year. This is an important finding because high phosphorus inputs to surface waters in spring can result in large toxic algal blooms in summer. Experiments in the lab were used to show that high road salt use in winter and early spring may lead to high phosphorus release from bioretention systems during late spring.

This study also investigated the processes within bioretention systems that may influence phosphorus behaviour. Porewater samples collected from within the bioretention system showed that the distribution of phosphorus was highly heterogeneous. Therefore, the processes governing phosphorus removal are complex and, in contrast to what is often thought, phosphorus removal may not increase with depth. It is possible that several processes occur simultaneously, making it challenging to predict the behaviour of phosphorus in bioretention systems. More detailed field analysis should be performed to better understand the biogeochemical processes governing phosphorus removal so that the

design of bioretention systems can be improved and the quality of lakes and rivers can be protected.

Co-Authorship Statement

While the candidate is responsible for the content of this thesis through analysis of field data and writing the drafts of all chapters, this thesis is the culmination of collaboration between Dr. Clare Robinson, Dr. Chris Smart, Julia Cantelon, and Jaeleah Goor. Clare Robinson developed the research topic, established working relationships with the City of London to construct the field site, provided suggestions for data analysis and revisions for improvements of this thesis. The co-authorship breakdown for Chapters 3 and 4 is below:

Chapter 3:

Authors: Jaeleah Goor, Clare Robinson, Chris Smart, Julia Cantelon

Contributions:

Jaeleah Goor conducted the design and installation of field monitoring equipment, collected and analyzed field water quality and quantity data, interpreted the results, and was the lead author for writing the Chapter.

Clare Robinson supervised field and column data collection and analysis, provided insight and interpretation of field and lab results, and reviewed the draft chapter.

Chris Smart assisted with the design and testing of the field bioretention monitoring systems and instrumentation, and assisted in interpretation of the field data.

Julia Cantelon conducted the column experiments and preliminary analysis of the column data.

Chapter 4:

Authors: Jaeleah Goor, Clare Robinson

Contributions:

Jaeleah Goor designed the field experiment, collected and analyzed field data, interpreted the results, and was the lead author for writing the Chapter.

Clare Robinson supervised field data collection and analysis, provided insight and interpretation of results, and reviewed the draft chapter.

Acknowledgments

I would like to express my sincere gratitude to my supervisor, Dr. Clare Robinson, for consistently providing exceptional guidance and challenging me to strive for excellence. I truly appreciate your support as the principal investigator in this project and, to a greater extent, your mentorship over the past years. Thank you for leading by example with such care and passion. Dr. Chris Smart was also critical to the success of this project. Thank you for teaching me only a fraction of your immense wisdom of environmental monitoring. Your creativity and enthusiasm for learning is inspirational.

Thank you to the City of London (Adrienne Sones and Shawna Chambers), the UTRCA (Dr. Imtiaz Shah), MOECCP (Best in Science grants) who provided financial and in-kind support which made this project possible. I would also like to recognize Caitlin Corcoran for the days you spent guiding me in the lab and teaching me your expertise on how to troubleshoot analytical machines. CEE is very fortunate to have you as a lab manager. Thanks also to the CEE graduate department including Kristen Edwards and Jason Gerhard.

Thank you to the RESTORE research group for the friendships, inspiration, and encouragement, especially Alex Duchesne and Taryn Fournie for friendships that go beyond research partners. The Bioretention Team - Julia Cantelon, Matthew Zen, Yi Liu, and Brennan Donado – thank you for your tireless effort to help in the field during extreme weather and for your great teamwork in the lab. Thank you also to the other RESTORE members who helped in the lab (Archana, Meghan, Stuart).

My parents, sisters, and Michelle were beside me throughout this journey, from sample collection in 3 am downpours, delayed family dinners, and learning to be interested in SRP analysis. I'm so thankful for who you are and the support you always provide. Special thank you, Dad, for your unconditional care and practical guidance.

To everyone else who played a direct or indirect role in this research, thank you!

Above all, all glory to Jesus for unending grace in my failures, for providing the strength I rely on daily, and for being the source of my joy.

Dedication

To Oma, Nana, and Grandpa.

You set the foundation for our family in faith and in love.

Table of Contents

Abstract.....	ii
Summary for Lay Audience.....	iii
Co-Authorship Statement.....	v
Acknowledgments.....	vii
Dedication.....	viii
Table of Contents.....	ix
List of Tables.....	xii
List of Figures.....	xiii
Chapter 1.....	1
1 Introduction.....	1
1.1 Research Background.....	1
1.2 Research Objectives.....	4
1.3 Thesis Outline.....	5
1.4 References.....	6
Chapter 2.....	10
2 Literature Review.....	10
2.1 Phosphorus in the environment.....	11
2.1.1 Forms of phosphorus and transformations.....	12
2.2 Bioretention system design and benefits.....	15
2.2.1 Low impact development stormwater management.....	15
2.2.2 Bioretention system design.....	17
2.3 P retention in bioretention systems.....	21
2.4 Seasonal changes in P retention in bioretention systems and cold climate considerations.....	24

2.5	Geochemical mechanisms governing phosphorus behaviour within porewater...	27
2.6	Research gaps.....	29
2.7	References.....	31
Chapter 3.....		41
3	Seasonal performance of bioretention systems in reducing phosphorus loads from urban stormwater in cold climates	41
3.1	Introduction.....	41
3.2	Methodology	46
3.2.1	Field-scale monitoring	46
3.2.2	Laboratory column experiments	54
3.3	Results and Discussion	57
3.3.1	Seasonal performance of field-scale bioretention systems	57
3.3.2	Potential factors governing seasonal variability in P retention and release	68
3.3.3	Influence of road salt (sodium chloride) on P release.....	73
3.4	Conclusion	77
3.5	References.....	79
Chapter 4.....		89
4	Spatial variability in the behavior of soluble reactive phosphorus within field-scale bioretention systems.....	89
4.1	Introduction.....	89
4.2	Methods.....	93
4.3	Results and Discussion	98
4.3.1	SRP distribution in bioretention systems.....	98
4.3.2	Relationship between SRP and other dissolved constituents.....	101
4.3.3	Relationship between SRP and soil moisture fluctuations	106

4.4 Conclusions.....	108
4.5 References.....	110
Chapter 5.....	117
5 Summary and Recommendations.....	117
5.1 Summary.....	117
5.2 Recommendations.....	119
5.3 References.....	121
Appendices.....	122
Appendix A: Supporting information on field bioretention system monitoring.....	122
Appendix B: Analytical methods for the determination of water quality parameters	127
Appendix C: P concentrations and mass loading.....	128
Appendix D: Statistical analysis of effluent P concentrations and loads.....	132
Appendix E: Statistical analysis for seasonal porewater samples.....	140
Appendix F: Calculations for SRP release at the column and field scales	143
Appendix G: Supplementary material for soil moisture content monitoring.....	146
Appendix H: Distribution and statistical analysis of dissolved constituents in porewater.....	150
Curriculum Vitae	155

List of Tables

Table 2-1: TP trigger ranges for surface waters in Canada (Canadian Council of Ministers of the Environment, 2004)	12
Table 2-2: Bioretention Design Guidelines Used in Southern Ontario (LID SWM Planning and Design Guide, 2020)	20
Table 3-1: Design details of monitored bioretention systems	47

List of Figures

Figure 2-1: Schematic of P cycling and transformation in soil environments.....	13
Figure 2-2: Impacts of urbanization and increased impervious surface areas on hydrology..	17
Figure 2-3: Cross-section of a typical bioretention system	19
Figure 3-1: Monitoring equipment layout in the bioretention systems, influent V-notch weir, compound effluent weir with pressure transducer and sampling port and installed MacroRhizon samplers collecting porewater during precipitation events.....	49
Figure 3-2: Set up for column experiments conducted to evaluate effect of high de-icing salt loading on P retention-release from the bioretention media.	55
Figure 3-3: Event influent and effluent water volumes and calculated percentage volume reductions for the East bioretention system from November 2018 to January 2020.....	58
Figure 3-4: Influent and effluent concentrations for TP, TDP, DOP, SRP for the East and Center bioretention systems from November 2018 to October 2019.	60
Figure 3-5: Cumulative mass of TP, TDP, DOP, and SRP in the influent and effluent for the East bioretention system from November 2018 to October 2019. The orange, blue, pink and yellow shaded regions represents Fall, Winter, Spring and Summer seasons, respectively, and the error bars represent the uncertainty in the influent and effluent water volume calculations.	63
Figure 3-6: Correlation between porewater Al and SRP, Fe and SRP, Mn and SRP, and Ca and SRP for four precipitation events over the monitoring period in the East and Center bioretention systems.....	66
Figure 3-7: Correlation between TP, TDP, DOP, and SRP mass retention and precipitation depth.....	71

Figure 3-8: Chloride concentrations in influent (road runoff), effluent of the East bioretention system, and the effluent of the Center bioretention system from November 2018 to October 2019 on a logarithmic scale.	72
Figure 3-9: Correlation between porewater Na and SRP, Cl and SRP for six precipitation events over the monitoring period.	73
Figure 3-10: Cumulative TP and SRP released over time during first (wet 1) and second (wet 2) wet periods for the salt column (road runoff spiked with NaCl influent) and control column (road runoff influent).	75
Figure 4-1: Cross-section of bioretention system showing the layout of porewater samplers and volumetric water content sensors installed in the East and Center bioretention systems.	96
Figure 4-2: Porewater SRP concentrations for profiles in the East and Center bioretention system from summer and fall 2019.....	100
Figure 4-3: Porewater SRP and dissolved Al, Fe, and Mn from all profiles and depths in the East and Center bioretention systems collected on 10 June, 19 August, and 2 October 2019.	102
Figure 4-4: Porewater SRP, Al, and Fe concentrations along the Upstream, Middle, and Downstream profiles in the Centre bioretention system during precipitation events on 19 August and 2 October 2019.	105
Figure 4-5: pH and ORP measurements for the Upstream, Middle and Downstream profiles in the Center bioretention system during precipitation events on 19 August and 2 October 2019.....	106
Figure 4-6: Volumetric water content in the Centre bioretention system in the topsoil layer (5 cm depth), and in the bioretention media layer (at 40 cm and 100 cm depths) with precipitation depth	108

Chapter 1

1 Introduction

1.1 Research Background

Anthropogenic activities, including urbanization, can significantly degrade water quality worldwide (Le Moal et al., 2019; Steffen et al., 2014; Watson et al., 2016). Elevated mass input of nutrients, particularly phosphorus (P), to surface waters can result in eutrophication and harmful algal blooms, which can lead to hypoxic conditions in some cases. These impacts have severe and negative environmental, social and economic consequences (Smith et al., 2019). In Lake Erie, one of the world's largest freshwater bodies and an important water resource, increasing proliferation of harmful algal blooms over the last decade prompted the Canadian and United States governments to commit to a 40% reduction of spring total P (TP) and soluble reactive P (SRP) loads to the lake (from 2008 levels) (Environment and Climate Change Canada and Ontario Ministry of the Environment and Climate Change, 2018). SRP, the most biologically available form of P, is generally considered to be the primary cause for accelerated eutrophication in freshwaters (Environment and Climate Change Canada and Ontario Ministry of the Environment and Climate Change, 2018; International Joint Commission, 2014). P loading from diffuse sources such as agriculture (manure and inorganic fertilizer) as well as sources in urban areas including stormwater runoff are challenging to quantify and mitigate (Steffen et al., 2014; Watson et al., 2016). Nevertheless, there is an urgent need to reduce P loads from these diffuse sources to restore and protect the quality surface water bodies, including Lake Erie.

Urban stormwater runoff is the sixth largest source of impairments for lakes, ponds, and reservoirs in the United States (United States Environmental Protection Agency, 2004). Urban stormwater management priorities over the last thirty years have expanded to focus on sustainability with an effort to restore pre-development hydrology and improve the quality of stormwater entering downstream water bodies (Credit Valley Conservation and Toronto and Region Conservation Authority, 2010; Ontario Ministry of the

Environment, 2003). Low impact development (LID) features are becoming increasingly popular as a best management practice for stormwater management (Eger et al., 2017; Hager et al., 2019). These small-scale, site-specific installations are designed to treat urban stormwater runoff near the source, improve water quality, and reduce peak flows, using natural and passive methods to mimic pre-development hydrological conditions (Credit Valley Conservation and Toronto and Region Conservation Authority, 2010; Eckart et al., 2017; Eger et al., 2017; Hager et al., 2019).

Bioretention systems, a common LID feature, are increasingly being installed in many locations worldwide. The performance of these systems with respect to P removal has been investigated with studies, typically based on influent and effluent monitoring only, reporting varying results. Some studies indicate field bioretention systems decrease total P (TP) concentrations and loads, while others report an increase in TP concentrations and loads (Carpenter and Hallam, 2010; Debusk and Wynn, 2011; Khan et al., 2012; Li and Davis, 2009). While less frequently studied, yet also important, removal of different forms of P (SRP, dissolved organic P) in bioretention systems is also variable (Hager et al., 2019; Mangangka et al., 2015; Passeport et al., 2009). This inconsistent performance of bioretention systems highlights the need to generate fundamental understanding of the processes that govern P retention in these systems. Although column and mesocosm studies have identified possible P removal mechanisms to explain P behaviour in bioretention systems (Davis, 2007; Geronimo et al., 2015; Hsieh et al., 2007), the experiments neglect the complexity of real field conditions. To optimize bioretention systems for P removal, there is a need for detailed evaluation of the behaviour of P, and its different forms (particulate P, SRP, dissolved organic P [DOP]), in field-scale bioretention systems to generate fundamental understanding of the processes governing P retention.

In cold climates, the performance of bioretention systems with respect to P removal have been shown to vary seasonally due to changes in temperature, precipitation depth, freeze-thaw cycles, reduced vegetation growth, dormant biological functions, and/or high input of road de-icing salts (typically NaCl) (Ding et al., 2019; Kazemi et al., 2018; Paus et al.,

2016; Roseen, 2009; Shrestha et al., 2018). However, studies examining the effects of seasonality are limited to laboratory-scale (column or mesocosm) experiments, or to field-scale studies which focus only on comparisons of the performance of bioretention systems in winter and summer (neglecting or limiting understanding of seasonal changes in fall and spring). Furthermore, these studies generally monitor for TP and PP, while simultaneous analysis of other forms of P, including SRP, is limited. There is a need to investigate the seasonal variability of the retention of different forms of P (TP, SRP, and DOP) within field-scale bioretention systems installed in cold climates, as the timing of P release from bioretention systems is important considering that spring P loads to surface waters have been implicated in the proliferation of harmful algal blooms in summer (Irvine et al., 2019).

As described above, prior studies examining P retention in field bioretention systems generally only conduct influent and effluent monitoring and therefore provide limited insight into processes governing the fate and transport of P in bioretention systems. While there is a common notion that SRP retention in bioretention systems is governed by adsorption-desorption to Al- and Fe- oxides (Liu and Davis, 2014; Lucas and Greenway, 2011; Marvin et al., 2020), and particulate P retention is governed by physical filtration and sedimentation processes (Hsieh et al., 2007; Li and Davis, 2014; Mahmoud et al., 2019), the high reported variability in P retention in bioretention systems suggests that this may be an over-simplification of P behaviour in field-scale systems. As such, examining the distribution P within the bioretention media, as well the distribution of constituents that can affect P behaviour, may provide important insights into the mechanisms governing P fate and transformations. Understanding of these mechanisms is needed to optimize the design of bioretention systems for P retention including assessing the suitability of different amendments that may be added to the engineered soil media to enhance P retention.

1.2 Research Objectives

This research aims to address knowledge gaps related the performance of field-scale bioretention systems installed in cold climates in reducing P loads in urban stormwater. There is currently considerable variability in the performance of field-scale bioretention systems in TP and SRP retention, with some studies reporting high release of P loads from bioretention systems to downstream watersheds. Specifically, the objectives of this study are to:

1. Assess the seasonal performance of bioretention systems installed in cold climates in retaining P, including the different forms of P (PP, DOP, SRP).
2. Evaluate the effect of high road salt loading on P retention and release from the bioretention media.
3. Evaluate the spatial distribution of SRP within field bioretention systems and identify possible hydro-biogeochemical processes that influence SRP retention and release.

The findings of this study are needed to optimize bioretention system design and reduce P loads from stormwater to downstream surface waters by improving fundamental understanding of the spatiotemporal behaviour of P within these systems. While this study is limited to the monitoring of two field-scale bioretention systems in cold climates, the findings may be applicable to other climates and LID stormwater management systems aiming to reduce P loading.

1.3 Thesis Outline

This thesis is written in “Integrated Article Format”. A brief description of each chapter is presented below:

Chapter 1: Introduction to the research topic, background information, motivation for research, and the study objectives.

Chapter 2: Synthesis of literature to provide background understanding of stormwater management, bioretention system design, and P transformations in the natural environment and within bioretention systems. This chapter also highlights the available literature on the temporal and spatial distribution of P retention in bioretention systems.

Chapter 3: An in-depth analysis on the seasonal performance of field-scale bioretention systems to retain the different forms of P in cold climates. The seasonality and the mechanisms that govern this behaviour including the potential impacts of high road salt inputs are investigated and supported with column experiments.

Chapter 4: The spatial distribution of SRP within two field bioretention systems are examined and related dissolved-phase constituents and soil moisture dynamics are used to identify the potential hydro-biogeochemical processes governing SRP behaviour in the systems.

Chapter 5: Summarizes the results and conclusions from the study and provides recommendations for future research.

1.4 References

- Carpenter, D.D., Hallam, L., 2010. Influence of planting soil mix characteristics on bioretention cell design and performance. *J. Hydrol. Eng.* 15, 404–416.
[https://doi.org/10.1061/\(ASCE\)HE.1943-5584.0000131](https://doi.org/10.1061/(ASCE)HE.1943-5584.0000131)
- Credit Valley Conservation, Toronto and Region Conservation Authority, 2010. *Low Impact Development Stormwater Management Planning and Design Guide*. Toronto, Ontario.
- Davis, A.P., 2007. Field Performance of Bioretention: Water Quality. *Environ. Eng. Sci.* 24, 1048–1064. <https://doi.org/10.1089/ees.2006.0190>
- Debusk, K.M., Wynn, T.M., 2011. Storm-water bioretention for runoff quality and quantity mitigation. *J. Environ. Eng.* 137, 800–808.
[https://doi.org/10.1061/\(ASCE\)EE.1943-7870.0000388](https://doi.org/10.1061/(ASCE)EE.1943-7870.0000388)
- Ding, B., Rezanezhad, F., Gharedaghloo, B., Van Cappellen, P., Passeport, E., 2019. Bioretention cells under cold climate conditions: Effects of freezing and thawing on water infiltration, soil structure, and nutrient removal. *Sci. Total Environ.* 649, 749–759. <https://doi.org/10.1016/j.scitotenv.2018.08.366>
- Eckart, K., McPhee, Z., Bolisetti, T., 2017. Performance and implementation of low impact development – A review. *Sci. Total Environ.* 607–608, 413–432.
<https://doi.org/10.1016/j.scitotenv.2017.06.254>
- Eger, C.G., Chandler, D.G., Driscoll, C.T., 2017. Hydrologic processes that govern stormwater infrastructure behaviour. *Hydrol. Process.* 31, 4492–4506.
<https://doi.org/10.1002/hyp.11353>
- Environment and Climate Change Canada, Ontario Ministry of the Environment and Climate Change, 2018. *Canada-Ontario Lake Erie Action Plan*.
- Geronimo, F.K.F., Maniquiz-Redillas, M.C., Kim, L.H., 2015. Fate and removal of nutrients in bioretention systems. *Desalin. Water Treat.* 53.
<https://doi.org/10.1080/19443994.2014.922308>

- Hager, J., Hu, G., Hewage, K., Sadiq, R., 2019. Performance of low-impact development best management practices: A critical review. *Environ. Rev.* 27, 17–42.
<https://doi.org/10.1139/er-2018-0048>
- Hsieh, C., Davis, A.P., Needelman, B.A., 2007. Bioretention Column Studies of Phosphorus Removal from Urban Stormwater Runoff. *Water Environ. Res.* 79, 177–184. <https://doi.org/10.2175/106143006X111745>
- International Joint Commission, 2014. A Balanced Diet for Lake Erie: Reducing Phosphorus Loadings and Harmful Algal Blooms. Report of the Lake Erie Ecosystem Priority. Ottawa, Ontario.
- Irvine, C., Macrae, M., Morison, M., Petrone, R., 2019. Seasonal nutrient export dynamics in a mixed land use subwatershed of the Grand River, Ontario, Canada. *J. Great Lakes Res.* 45, 1171–1181. <https://doi.org/10.1016/j.jglr.2019.10.005>
- Kazemi, F., Golzarian, M.R., Myers, B., 2018. Potential of combined Water Sensitive Urban Design systems for salinity treatment in urban environments. *J. Environ. Manage.* 209, 169–175. <https://doi.org/10.1016/j.jenvman.2017.12.046>
- Khan, U.T., Valeo, C., Chu, A., van Duin, B., 2012. Bioretention cell efficacy in cold climates: Part 2 - water quality performance. *Can. J. Civ. Eng.* 39, 1222–1233.
<https://doi.org/10.1139/l2012-111>
- Le Moal, M., Gascuel-Oudou, C., Ménesguen, A., Souchon, Y., Étrillard, C., Levain, A., Moatar, F., Pannard, A., Souchu, P., Lefebvre, A., Pinay, G., 2019. Eutrophication: A new wine in an old bottle? *Sci. Total Environ.* 651, 1–11.
<https://doi.org/10.1016/j.scitotenv.2018.09.139>
- Li, Davis, A., 2009. Water quality improvement through reductions of pollutant loads using bioretention. *J. Environ. Eng.* 135, 567–576.
[https://doi.org/10.1061/\(ASCE\)EE.1943-7870.0000026](https://doi.org/10.1061/(ASCE)EE.1943-7870.0000026)
- Li, L., Davis, A.P., 2014. Urban stormwater runoff nitrogen composition and fate in bioretention systems. *Environ. Sci. Technol.* 48. <https://doi.org/10.1021/es4055302>

- Liu, J., Davis, A.P., 2014. Phosphorus speciation and treatment using enhanced phosphorus removal bioretention. *Environ. Sci. Technol.* 48. <https://doi.org/10.1021/es404022b>
- Lucas, W.C., Greenway, M., 2011. Phosphorus Retention by Bioretention Mesocosms Using Media Formulated for Phosphorus Sorption: Response to Accelerated Loads. *J. Irrig. Drain. Eng.* 137, 144–153. [https://doi.org/10.1061/\(ASCE\)IR.1943-4774.0000243](https://doi.org/10.1061/(ASCE)IR.1943-4774.0000243)
- Mahmoud, A., Alam, T., Yeasir A. Rahman, M., Sanchez, A., Guerrero, J., Jones, K.D., 2019. Evaluation of field-scale stormwater bioretention structure flow and pollutant load reductions in a semi-arid coastal climate. *Ecol. Eng.* X 1, 100007. <https://doi.org/10.1016/j.ecoena.2019.100007>
- Mangangka, I.R., Liu, A., Egodawatta, P., Goonetilleke, A., 2015. Performance characterisation of a stormwater treatment bioretention basin. *J. Environ. Manage.* 150, 173–178. <https://doi.org/10.1016/j.jenvman.2014.11.007>
- Marvin, J.T., Passeport, E., Drake, J., 2020. State-of-the-Art Review of Phosphorus Sorption Amendments in Bioretention Media: A Systematic Literature Review. *J. Sustain. Water Built Environ.* 6. <https://doi.org/10.1061/JSWBAY.0000893>
- Ontario Ministry of the Environment, 2003. Stormwater Management Planning and Design Manual.
- Passeport, E., Hunt, W.F., Line, D.E., Smith, R.A., Brown, R.A., 2009. Field study of the ability of two grassed bioretention cells to reduce storm-water runoff pollution. *J. Irrig. Drain. Eng.* 135, 505–510. [https://doi.org/10.1061/\(ASCE\)IR.1943-4774.0000006](https://doi.org/10.1061/(ASCE)IR.1943-4774.0000006)
- Paus, K.H., Muthanna, T.M., Braskerud, B.C., 2016. The hydrological performance of bioretention cells in regions with cold climates: Seasonal variation and implications for design. *Hydrol. Res.* 47, 291–304. <https://doi.org/10.2166/nh.2015.084>
- Roseen, R.M., 2009. Seasonal Performance Variations for Storm-water management

- systems in cold climate conditions. *J. Environ. Eng.* 3, 128–137.
[https://doi.org/10.1061/\(ASCE\)0733-9371\(2009\)135:3\(1280](https://doi.org/10.1061/(ASCE)0733-9371(2009)135:3(1280)
- Shrestha, P., Hurley, S.E., Wemple, B.C., 2018. Effects of different soil media, vegetation, and hydrologic treatments on nutrient and sediment removal in roadside bioretention systems. *Ecol. Eng.* 112, 116–131.
<https://doi.org/10.1016/j.ecoleng.2017.12.004>
- Smith, R.B., Bass, B., Sawyer, D., Depew, D., Watson, S.B., 2019. Estimating the economic costs of algal blooms in the Canadian Lake Erie Basin. *Harmful Algae* 87, 101624. <https://doi.org/10.1016/j.hal.2019.101624>
- Steffen, M.M., Belisle, B.S., Watson, S.B., Boyer, G.L., Wilhelm, S.W., 2014. Status, causes and controls of cyanobacterial blooms in Lake Erie. *J. Great Lakes Res.* 40, 215–225. <https://doi.org/10.1016/j.jglr.2013.12.012>
- United States Environmental Protection Agency, 2004. National Water Quality Inventory: Report to Congress, 2004.
- Watson, S.B., Miller, C., Arhonditsis, G., Boyer, G.L., Carmichael, W., Charlton, M.N., Confesor, R., Depew, D.C., Höök, T.O., Ludsin, S.A., Matisoff, G., McElmurry, S.P., Murray, M.W., Peter Richards, R., Rao, Y.R., Steffen, M.M., Wilhelm, S.W., 2016. The re-eutrophication of Lake Erie: Harmful algal blooms and hypoxia. *Harmful Algae* 56, 44–66. <https://doi.org/10.1016/j.hal.2016.04.010>

Chapter 2

2 Literature Review

Bioretention systems are a form of low impact development stormwater management control designed to attenuate and delay the quantity and improve the quality of urban stormwater runoff. Bioretention systems are designed for stormwater quantity control and total suspended solids removal while many systems are also designed to remove heavy metals and nutrients such as nitrogen [N] and phosphorus [P] from stormwater. The performance of bioretention systems to provide stormwater quantity control has been well demonstrated (Géhéniau et al., 2015; Hunt et al., 2012; Khan et al., 2012; Paus et al., 2015; Trowsdale and Simcock, 2011) but their ability to provide water quality improvements is inconsistent, especially with respect to nutrients (N and P) (Hager et al., 2019; Kratky et al., 2017; Li and Davis, 2016; Mahmoud et al., 2019) Furthermore, the impact of cold climate factors on the water quality performance of bioretention systems is not well understood.

Numerous studies have focused on evaluation and optimization of bioretention systems including examination of their hydraulic performance, nutrient retention, heavy metal retention, as well as factors that contribute to the overall performance of these systems at the column, mesocosm, and field scales. As the overarching objective of this thesis is to evaluate the performance of bioretention systems in retaining phosphorus (P) in cold climates and the factors affecting this performance, this chapter reviews current knowledge on P in the environment, bioretention system design, factors and processes governing P retention and release in bioretention systems, and factors affecting bioretention system performance in cold climates.

2.1 Phosphorus in the environment

Phosphorus (P) is an essential element for life in terrestrial and aquatic environments (Mackey et al., 2019). However, excessive P loads to surface waters caused by anthropogenic activities can lead to eutrophication and threaten surface water quality around the world (Le Moal et al., 2019). Eutrophic conditions can lead to proliferation of harmful algal blooms and hypoxic events and in doing so threaten drinking water sources, public health, biodiversity, and the recreational, fishing and tourism industries (Fowdar et al., 2017; Steffen et al., 2014; Watson et al., 2016). Although the direct economic costs of these impacts are often quantified as millions in equivalent annual cost (Smith et al., 2019), the total financial burden of impaired water quality due to eutrophication, including health, environmental and socio-economic impacts, is challenging to accurately evaluate (Le Moal et al., 2019).

P is often the limiting nutrient for aquatic vegetation growth in freshwater systems as N:P ratios are generally high (Berge et al., 2017; Blecken et al., 2010; Mackey et al., 2019). The growth rate of vegetation in freshwater systems is generally a function of P inputs as N sources are generally abundant while the supply of P to aquatic environments is limited to the rate of weathering for rock, natural P recycling, with P inputs from anthropogenic activities (Mackey et al., 2019). As such, water quality management efforts in freshwater environments often focus on limiting P inputs (Environment and Climate Change Canada and Ontario Ministry of the Environment and Climate Change, 2018; International Joint Commission, 2014; Smith et al., 2019; Swedish Environmental Protection Agency, 2000). For instance in Lake Erie, one of the largest freshwater lakes worldwide and an important water resources, the Canadian and United States governments have committed to a 40% reduction in spring total phosphorus (TP) and soluble reactive phosphorus (SRP) loads to the lake by 2025 (from 2008 levels) (Environment and Climate Change Canada and Ontario Ministry of the Environment and Climate Change, 2018; International Joint Commission, 2014; Smith et al., 2019). This is a challenging target to meet as non-point and diffuse sources including agriculture, septic systems, landfills, and urban stormwater are now considered to be the main sources of TP and SRP to the lake. In 2004, it was estimated that approximately 20% of lakes in the United States were

impaired by excessive levels of nutrients, making nutrients the third top cause of lake impairments after mercury and polychlorinated biphenyls (PCBs) (United States Environmental Protection Agency, 2004). Further, urban stormwater was estimated to be the main cause of water quality impairment for approximately 9% of the impaired streams in the United States (United States Environmental Protection Agency, 2004). As the impact of P loads on the aquatic ecosystem depends on the specific conditions of a surface water body, there is no single maximum P concentration limit in Canada for surface waters. Instead, TP trigger ranges have been provided for water bodies with different trophic levels to indicate concentrations that may be a concern for water quality (Table 2-1).

Table 2-1: TP trigger ranges for surface waters in Canada (Canadian Council of Ministers of the Environment, 2004)

Trophic Status	Canadian Trigger Ranges Total phosphorus ($\mu\text{g}\cdot\text{L}^{-1}$)
Ultra-oligotrophic	< 4
Oligotrophic	4-10
Mesotrophic	10-20
Meso-eutrophic	20-35
Eutrophic	35-100
Hyper-eutrophic	> 100

2.1.1 Forms of phosphorus and transformations

Total phosphorus (TP) can be separated into particulate P (PP) and dissolved P.

Particulate P is the fraction of P that is attached to particles and is retained on a $0.45\mu\text{m}$ filter (Ellison and Brett, 2006). Dissolved or soluble P is the P remaining in solution once it has been filtered, and can be either organic or inorganic. Colloidal P is included in this definition of soluble P (Mackey et al., 2019). Dissolved organic P (DOP) is from P-containing organic matter. Although there are slight differences in structure, reactivity, and analysis methods, dissolved inorganic P can be referred to as orthophosphate (PO_4 -

P), phosphate, and soluble reactive phosphorus (SRP). Environmental conditions such as pH, temperature, and the presence of oxygen can alter the state in which P exists, which may then influence its behaviour (reactivity, transport) and impact in natural environments (Mackey et al., 2019; Wang et al., 2013). For example, SRP and some DOP forms are the most bioavailable forms of P that are taken up by vegetation and contribute to algal blooms (Komlos and Traver, 2012; LeFevre et al., 2015; Li and Brett, 2013).

The fate of P in the environment is complex as it is typically highly associated with sediments through sorption and precipitation reactions, but also taken up and released by biological processes (Boström et al., 1988) (Figure 2-1). The fate and transport of P in the subsurface (porous media) depends on several factors such as historical P loading which can lead to sediments (e.g., adsorption sites) becoming saturated with P over time, sediment type, pH, redox conditions, and availability of cations that will co-precipitate with P. Transformations between the different forms of P (PP, DOP, SRP) also plays an important role in the fate and transport of P.

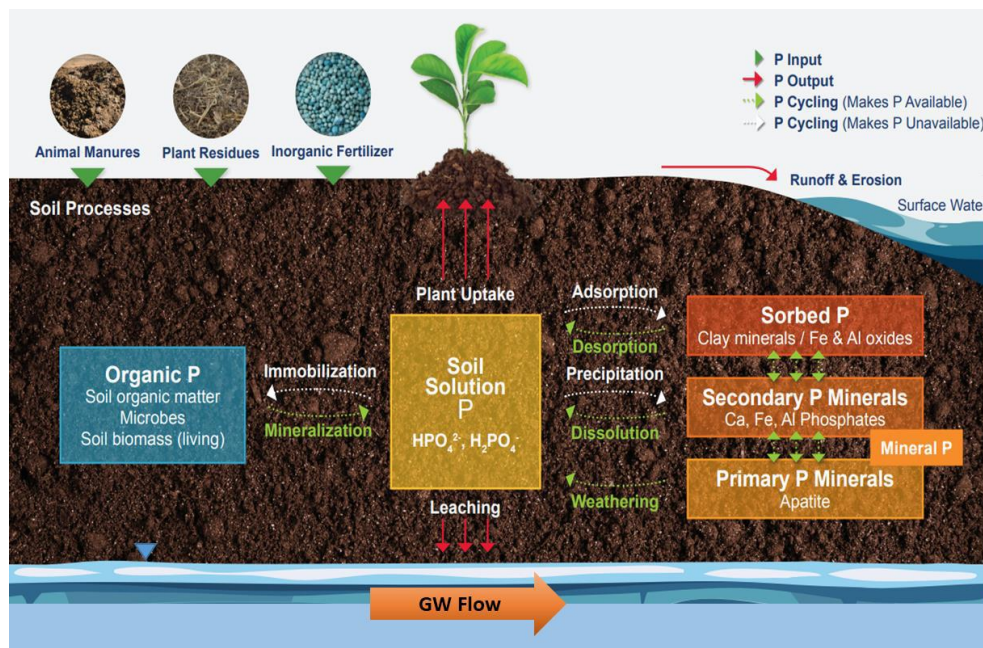


Figure 2-1: Schematic of P cycling and transformation in soil environments (Prasad and Chakraborty, 2019).

In the subsurface, mineralization transforms organic P from the sediment (vegetation and organisms) to SRP (Denich et al., 2003). SRP can be released from organic compounds containing varying amounts of C, O, and P by enzymes and/or bacteria (Cooper et al., 1991). The process of mineralization and release of DIP from cellular material occurs relatively quickly after the death of cells, leading to high conversion rates between organic and inorganic P compared to other processes which occur on longer time scales (Mackey et al., 2019). In reverse to the mineralization process, plants can draw inorganic P from the subsurface in the growing season, convert it into organic P, and store P within their biomass (Mackey et al., 2019). This process temporarily immobilizes phosphorus until harvest or die-off when mineralization occurs.

Release of P into porewater can also occur through weathering of primary P minerals such as apatite, and dissolution of secondary P minerals. Physical and chemical weathering of P minerals can release both organic and inorganic P to the porewater (Mackey et al., 2019). Secondary phosphate minerals can also precipitate when high concentrations of Ca^{2+} in calcareous sediments, and Fe^{3+} and Al^{3+} in acidic environments bind with PO_4^{3-} in super-saturated concentrations to precipitate out of solution (Mackey et al., 2019; Marvin et al., 2020; Prasad and Chakraborty, 2019; Yan et al., 2016). Precipitation of Ca, Fe, and Al phosphates is a slower and more permanent transformation compared to adsorption or mineralization (Prasad and Chakraborty, 2019) as these minerals are generally stable in the environment, resulting in a long-term retention of SRP (Mackey et al., 2019). However, this process is sensitive to changes in pH, temperature, redox conditions, and cation concentrations (Mackey et al., 2019; Parsons et al., 2017; Prasad and Chakraborty, 2019).

SRP may also be adsorbed onto clay minerals and Al, Fe, and Mn oxide minerals, decreasing porewater SRP concentrations. For this process to occur, phosphate (PO_4) ions physically bond to the surface of the solid phase (Mackey et al., 2019). This process is limited by the sorption capacity of the soil (i.e. available surface sorption site). As such, once the sorption capacity of the soil is reached, the soil may not have the capacity to further retain P (Li & Davis, 2016). Soils with higher clay contents often have greater SRP sorption capacity due to the increased surface area (Prasad and Chakraborty, 2019).

Adsorption is a fast and reversible process, leading to temporary P stores in the soil which can then be up-taken by plants, or desorbed from the soil, depending on in situ conditions (Prasad and Chakraborty, 2019). High dissolved Fe, Al and Mn concentrations often co-exist with high dissolved SRP concentrations because dissolution of these metal oxides causes release of these metal ions and SRP to porewater (Liu & Davis, 2014; Marvin et al., 2020; Yan et al., 2016). Dissolution of these metal oxide minerals and associated desorption of SRP is often triggered by the onset of reducing condition, temperature, or pH changes (Baken et al., 2015; Huang et al., 2011). Alternatively, in the absence of metal oxide dissolution, SRP can also desorb from these mineral surfaces in response to pH changes or competitive sorption processes (Parsons et al., 2017).

2.2 Bioretention system design and benefits

2.2.1 Low impact development stormwater management

Urbanization significantly alters the natural hydrology in a watershed. Increased area of impervious surfaces reduce infiltration and evapotranspiration while increasing runoff and peak discharge rates. The natural hydrograph dramatically changes from pre- to post-development. Urban stormwater runoff is also a leading cause of the degradation of streams and aquatic ecosystems (Moore et al., 2017). Common pollutants found in urban stormwater include P species (PP, DOP, SRP), nitrogen species (TKN, ON, NH₄, NO_x), suspended solids, chloride, pathogens (*E. coli* and fecal coliform), pesticides, metals (including Pb, Zn, Cu, Cr, As, Cd, Ni, and Al) and petroleum hydrocarbons (Kayhanian et al., 2012; LeFevre et al., 2015; Li and Davis, 2009; McManus and Davis, 2020; Passeport et al., 2009; Wilson et al., 2015). Until the 1990's, the focus of conventional stormwater management systems, such as storm sewer networks and detention ponds, was to offset the hydrologic effects of urbanization (Credit Valley Conservation and Toronto and Region Conservation Authority, 2010a). With the release of the 2003 Stormwater Management Planning and Design Manual in Ontario, this focus was broadened to include water quality treatment and erosion control. Traditional methods such as stormwater detention ponds often do not provide sufficient water quality treatment (Moore et al., 2017). Urban stormwater management practices now emphasize

sustainability and include considerations for climate change, restoration of pre-development water budgets, and a focus on low impact development (Credit Valley Conservation and Toronto and Region Conservation Authority, 2010a; Kordana and Słyś, 2020).

Low impact development (LID) stormwater management systems have been designed as source-control methods to treat urban stormwater runoff as close to the source as possible and to avoid the delivery of excessive peak flows and contaminant loadings to downstream watersheds (Akhter et al., 2020; Eckart et al., 2017; Moore et al., 2017). Green roofs, permeable pavement, bioretention systems, and infiltration trenches are all LID technologies that are being used to help restore the predevelopment hydrograph (Figure 2-2) (Dietz, 2007). These systems are often integrated into existing natural features and are designed to prevent runoff through strategic vegetation and reduced surface imperviousness (Credit Valley Conservation and Toronto and Region Conservation Authority, 2010a). As LID features are not designed to meet stormwater management targets for flood control on their own, they can be used in combination with traditional stormwater control measures (Credit Valley Conservation and Toronto and Region Conservation Authority, 2010a).

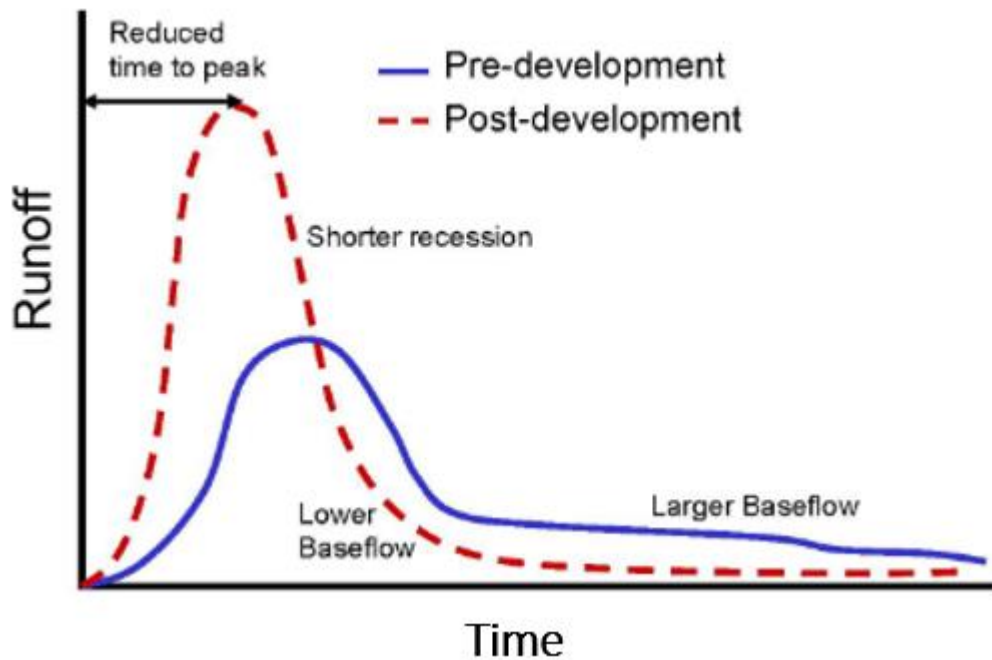


Figure 2-2: Impacts of urbanization and increased impervious surface areas on hydrology (Liu et al., 2014)

2.2.2 Bioretention system design

Bioretention systems are small-scale LID stormwater management systems used for attenuating and delaying, as well as improving the quality of urban stormwater. They can also be referred to as infiltration swales, rain gardens, bioswales, or stormwater filters (Moore et al., 2017). Through passive, natural processes, bioretention systems treat stormwater close to its source and help restore pre-development hydrology and water quality (Credit Valley Conservation and Toronto and Region Conservation Authority, 2010a). Bioretention systems are often engineered to receive stormwater from impervious areas such as roads, parking lots, and downspouts and are designed to infiltrate the water into the ground, reducing the magnitude and increasing the delay of peak flows while removing both dissolved and particulate pollutants (Hsieh et al., 2007). While bioretention systems provide some hydraulic retention benefits, they are often not

designed to infiltrate and capture large precipitation events (Credit Valley Conservation and Toronto and Region Conservation Authority, 2010b)

Bioretention systems are typically designed with a 0.05 - 0.15 m layer of mulch or topsoil on the surface (Figure 2-3). This surface layer provides a growth medium for vegetation and can also contribute to improved water quality. A 1 to 1.25 m deep layer of engineered soil media typically supports the topsoil/mulch layer and provides capacity for water quality treatment. Below the engineered media is a layer of pea gravel to separate the media from the gravel storage layer below (Credit Valley Conservation and Toronto and Region Conservation Authority, 2010b). Some bioretention systems, particularly those installed in areas where the infiltration rate of the native soil is less than 15 mm/hr (clays and silts), include an underdrain. This perforated pipe is embedded in the lower gravel layer and transports excess infiltrated water to a traditional storm sewer network (Credit Valley Conservation and Toronto and Region Conservation Authority, 2010a).

Stormwater infiltrating through a bioretention system may be infiltrated directly into the subsurface in locations with naturally high infiltration rates. Depending on the local stormwater priorities and specifications of the site, bioretention systems may also be lined. Overflow pipes are also used to limit the depth of ponded water on the bioretention system surface to 150-200 mm by creating a by-pass to the underdrain or storm sewer network. Finally, the surface of bioretention systems can be planted with a variety of vegetation for aesthetic purposes and to provide additional pollutant retention capacity (Davis et al., 2006; Geronimo et al., 2015).

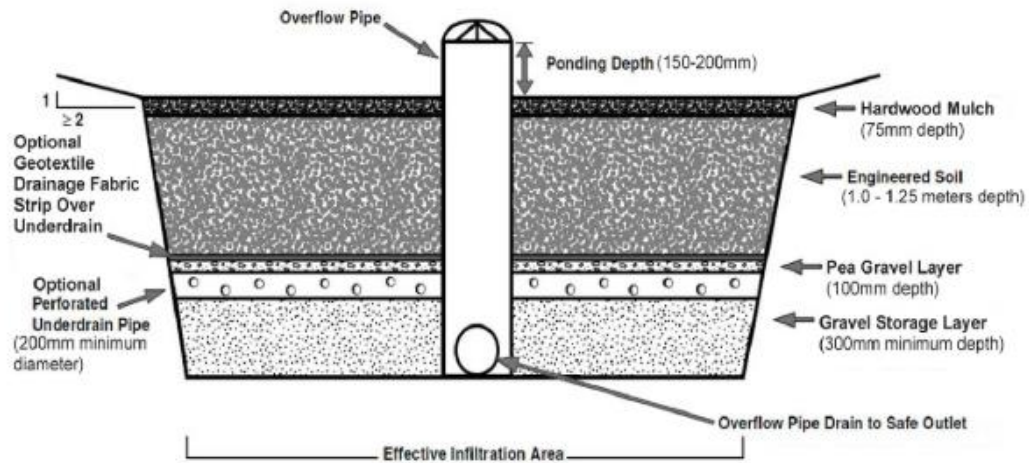


Figure 2-3: Cross-section of a typical bioretention system (Credit Valley Conservation and Toronto and Region Conservation Authority, 2010b)

The engineering soil media used in bioretention systems is generally a mix of sand, soil, and organic matter and is one of the major factors determining the overall performance of bioretention systems with respect to their ability to remove dissolved pollutants including P (Hunt et al., 2012). The specific composition of the media can be adjusted for water quality control or water quantity control and is often dependent on local stormwater management priorities. For water quality treatment including nutrient removal, the Stormwater Management Planning and Design Guide (2020) recommends that the engineered media used in bioretention systems is a pre-mixed blend of three parts sand, two-parts topsoil, and one-part organic material. Additional design guidelines commonly used in Southern Ontario are provided in **Table 2-2**. The use of a variety of organic matter sources (including wood chips, peat moss, biosolids, compost, and shredded paper) in the engineered media has been examined, with the use of non-P leaching material (as determined by sediment extraction) recommended as an important criteria for bioretention systems (Credit Valley Conservation and Toronto and Region Conservation Authority, 2010a; Jay et al., 2017; Logsdon, 2017).

Table 2-2: Bioretention Design Guidelines Used in Southern Ontario (LID SWM Planning and Design Guide, 2020)

Characteristic	Criterion
Particle-size distribution	<25% silt and clay-sized particles combined
Organic Matter	3-10% by dry weight. From compost, wood chips, peat moss, etc.
Plant-available Phosphorus	12-40 ppm. Measured by the Olsen method for P determination in soils
Cation exchange capacity	> 10 meq/100g
Saturated hydraulic conductivity	>25mm/hr to <300mm/hr, dependent on local stormwater management priorities

Amendments can also be added to the engineering soil media for enhanced water quality treatment. Appropriate selection and application of amendments requires a thorough understanding of the biogeochemical conditions and processes within field-scale bioretention systems. As sorption is generally considered to be the main mechanism governing P mobility in bioretention systems, amendments containing Al-, Fe-, and Ca-based compounds are commonly recommended as amendments to improve the sorption capacity of the media and its ability to retain P (Hunt et al., 2012; Marvin et al., 2020; O’Neill and Davis, 2012; Shrestha et al., 2018). For example, Erickson, Gulliver, & Weiss (2012) found iron filings were successful in improving SRP retention in field-scale bioretention systems and mesocosm studies completed by Lucas & Greenway (2011) reported 99% mass retention of SRP after 40 years equivalent stormwater input with Al-based water treatment residuals. Waste products from metal processing and water treatment residuals, natural materials such as soils and marine animal shells, and processed material have all been used as soil media amendments (Marvin et al., 2020). Although the majority of amendment studies have been completed in controlled laboratory column experiments, reported reductions in P concentrations and mass

loadings are highly variable with results ranging from leaching of P to complete P retention even in experiments testing the same amendments (Marvin et al., 2020). Furthermore, while the use of amendments has been found to be promising at the column-scale, construction and practical considerations (such as clogging and limited contact time) as well as more complex and dynamic environmental conditions (water saturation, redox, pH) can make the implementation of amendments in the field challenging (Marvin et al., 2020; O'Neill and Davis, 2012).

2.3 P retention in bioretention systems

Bioretention systems are popular control measures to reduce nutrient (N and P) loading from urban stormwater to downstream water bodies. However, the reported performance of bioretention systems in retaining P is highly variable, and detailed analysis of the different P forms including TP, TDP, PP, SRP, and DOP is limited at the field scale with few studies simultaneously quantifying concentrations and loads for different forms of P. While TP data can contribute to a general understanding of overall bioretention performance, it does not provide sufficient details to provide insight into the processes that govern the retention of P within bioretention systems. Previous studies have observed both increases and decreases of TP in bioretention systems based on concentrations and mass loadings. In a field study by Passeur et al. (2009), mean TP and SRP concentrations decreased between the bioretention systems inlets and outlets by 58-63% and 74-78%, respectively. However, the difference in mass loading for TP and SRP between the inlets and outlets in the same study was insignificant (Passeur et al., 2009). In contrast, another field study by Dietz & Clausen (2005) observed greater TP concentrations in the effluent compared to the influent, though effluent concentrations generally decreased over time. For the few studies that analyzed influent and effluent samples for SRP, SRP mass load removal efficiencies have been reported to vary from 90% to -400% (Hager et al., 2019; Mangangka et al., 2015). In a mesocosm study by Lucas & Greenway (2011), bioretention media with amendments was found to initially retain DOP loads and later release DOP loads, possibly due to mineralization processes. However, the only field study to our knowledge to quantify DOP loading observed a 59%

mass retention of DOP in a bioretention system using Fe- and Al- based amendments in the engineered media (Liu & Davis, 2014).

The high variability of the performance of bioretention systems with respect to P retention is partially due to the flexibility in design guidelines and the variety of engineered media mixes used (including use of amendments), climates, influent quality, and anthropogenic activities that can contribute to variable influent pollutant loads and in situ biogeochemical conditions. Several column experiments have investigated P retention-release mechanisms in bioretention media, but few studies have examined the behaviour of P and attempted to explain P transformations within field-scale bioretention systems due to the added complexities in field-scale systems, temporally limited monitoring, and lack of in situ (porewater and sediment) sampling.

Many of the mechanisms that affect P behaviour in the natural environment, including in porous media, also affect P fate and transport in bioretention systems. Several studies have observed high retention of particulate P in bioretention systems due to physical filtration and settling (Li & Davis, 2009; Liu & Davis, 2014; Marvin et al., 2020; Stagge, Davis, Jamil, & Kim, 2012). Adsorption and precipitation of secondary P minerals are thought to be the most important retention processes for dissolved P forms in bioretention systems (Liu & Davis, 2014; Lucas & Greenway, 2011; Marvin et al., 2020). O'Neill & Davis (2012) found that the ratio of oxalate-extractable Al, Fe, and P has a strong positive relationship with P sorption capacity of bioretention media suggesting that the Al and Fe content in the media is an important factor for P sorption and retention in bioretention systems. A recent mesocosm study by Song & Song (2018) observed that a large fraction of influent TP was retained in the media and then transformed into inorganic P in its exchangeable state and as Al- and Fe-phosphates. A modelling study by Li & Davis (2016) suggests that adsorption of dissolved P to Al and Fe oxides can either be slow and less reversible reactions when sorption occurs on the inner surface of the soil (micropores), or fast and reversible reactions when it occurs on the outer soil surface. The dissolved P can be adsorbed onto the outer soil surface during infiltration periods and later released back into the porewater or diffuse to the inner soil surface between precipitation events for more permanent retention (Li & Davis, 2016; Lucas & Greenway,

2011). Adsorption processes are strongly pH dependent (Bai et al., 2017; Davis et al., 2006; Lucas & Greenway, 2011), although O'Neill & Davis (2012) found the effects of pH on P adsorption to be minimal in bioretention systems within a pH range of 4.6 to 7.4. In environments with excess Ca, SRP can co-precipitate with Ca and Ca-containing compounds and remain relatively immobile unless conditions change (Li & Davis, 2016; Song & Song, 2018). Mineralization of organic matter in bioretention media is a potential source of SRP, with the possibility of additional P leaching from the upper mulch or topsoil layer (Davis, 2007; Li & Davis, 2016). Dissolution of redox-sensitive compounds containing Fe, Al, and Mn from the media may also release SRP. The importance of this mechanism is controlled by the amount of Al, Fe, and Mn oxides in the media as well as the redox and pH conditions within the bioretention system. However, it is possible that reductive dissolution of these oxide minerals may not occur even if the conditions are reducing due to limited contact time at the sediment-water interface (Dietz and Clausen, 2005). Although studies have directly investigated the role of redox reactions on N behaviour, the influence of redox conditions on P behaviour in bioretention systems is unclear.

Although vegetation uptake can contribute to P removal in bioretention systems and is considered essential in some systems (Liu et al., 2014; Valtanen, Sillanpää, & Setälä, 2017), mesocosm experiments by Lucas and Greenway (2008) found vegetation increased TP mass retention by 6 to 35% compared to barren treatments. However, Passeur et al. (2009) noted from their field study of bioretention systems in North Carolina that vegetation die-off will release P previously taken-up by plants, reducing the overall effectiveness of vegetation and contributing to possible increased seasonal P release in fall and winter. Studies have also observed reduced biological activity and P uptake during these seasons due to lower temperatures (Blecken et al., 2007; Khan, Valeo, Chu, & van Duin, 2012).

As the performance of a bioretention system with respect to P retention is based on the mass of P that is removed from stormwater input, P retention is not only a function of the chemical and biological processes occurring within the system that reduce the effluent P concentrations, but also a function of the amount of water volume retained within the

systems or infiltrating into the surrounding subsurface (Mangangka et al., 2015). As such, hydraulic behaviour is often an important determinant of the overall performance of bioretention systems to retain P (Dietz and Clausen, 2005). Reduced infiltration has been shown to limit hydraulic function and therefore, overall P retention (Roseen, 2009). In addition, a recent field study by Shrestha et al. (2018) showed that mobilization of a large fraction of TP occurred during a few larger precipitation events, suggesting the performance of bioretention systems may be highly variable even within a short time duration and that the characteristics of precipitation events (intensity, duration, precipitation depth etc.) may be important in governing P retention in bioretention systems (Mangangka et al., 2015).

2.4 Seasonal changes in P retention in bioretention systems and cold climate considerations

The overall performance of bioretention systems to retain P has also been shown to vary in response to seasonal changes in temperature, precipitation depth, and wetting and drying cycles (Hermawan et al., 2020; Shrestha et al., 2018).. Seasonal changes in cold climates are more extreme than in warmer climates and this may lead to large seasonal differences in the performance of bioretention systems with respect to retaining P. As such, the introduction of additional factors due to cold climates, including lower temperatures, freeze-thaw cycles, dormant biological functions, and high input of de-icing salt loads may cause greater seasonal differences in P retention (Blecken et al., 2007; Denich et al., 2003; Ding et al., 2019; Kakuturu & Clark, 2015; Manka, Hathaway, Tirpak, He, & Hunt, 2016). While these processes have been investigated in laboratory column experiments, their effects on the performance of field bioretention systems remain unclear. Furthermore, understanding the seasonal variability in P retention in bioretention systems is important as high SRP loads to tributaries in spring are known to contribute to the growth and proliferation of harmful algal blooms in summer (Irvine et al., 2019).

Field studies have observed that retention of the different P forms in bioretention systems may vary seasonally. Roseen (2009) observed slightly higher TP removal efficiencies in

summer (May to October) compared to winter (November to April) for their field bioretention systems installed in New Hampshire, United States but concluded decreased P removal in winter should not be a concern. More recently, seasonal release of TP in spring was observed in a field study in Montreal, Canada where effluent TP concentrations were greatest in May compared to the remainder of the year (Géhéniau et al., 2015). However, this study did not examine the different forms of P, quantify P loads, nor examine the potential factors contributing to the seasonal variability in TP release. In a study of vegetated mesocosm biofilter performance by Blecken et al. (2007), it was found that particulate P retention may not be negatively affected by low temperatures. A field study by Dietz & Clausen (2005) observed exponential decay in effluent TP concentrations in Connecticut, United States over the duration of their monitoring period from October 2002 to January 2004. After a decrease in TP in late winter, the TP concentrations were found to peak in April and continue to decrease over the remainder of the calendar year. However, since concentrations were even higher at the beginning of the study in October 2002 compared to April 2003, this decreasing trend was attributed to soil disturbance at the beginning of the monitoring period, and not seasonal variability (Dietz and Clausen, 2005). In a field-scale study on grassed swales, Stagge et al. (2012) observed pulses of TP release during a few large precipitation events during summer. These pulses of TP release may have been caused by the addition of P sources such as organic material and grass clippings during summer.

Cold climates add complexity to P behaviour in bioretention systems due to natural mechanisms including freeze-thaw cycles. Recent column experiments completed by Ding et al. (2019) showed that bioretention systems may have increased P release in winter due to freeze-thaw processes. Freeze-thaw cycles can disturb soil pore spaces and destabilize soil structure. Ding et al. (2019) suggested that larger pore spaces and hydraulically disconnected smaller pores have reduced available surface sorption locations for dissolved P, effectively reducing the soil's capacity to retain SRP (Ding et al., 2019). However, field studies in Montreal, Canada and Durham, New Hampshire recorded frost depths of 10-15 cm and to 20 cm, respectively, over winter monitoring seasons (Géhéniau et al., 2015; Roseen, 2009), while bioretention systems are often

constructed to greater depths (1 - 1.25 m), limiting the overall effects of freeze-thaw processes to a small fraction of the total soil media volume.

Urbanization in cold climates introduces further variability in bioretention performance with the application of road de-icing salts. While the role of salt (NaCl) on the release and mobility of metals in soils and in LID stormwater controls (e.g., infiltration trenches) is well known (Bäckström et al., 2004; Christopher et al., 1992; Nelson et al., 2009; Sjøberg et al., 2017), the effect of high salt loads on P retention in bioretention systems is unclear. It is possible that high Na and Cl may directly and indirectly influence P behaviour through ion exchange processes, toxicity to vegetation and microorganisms, and soil structure changes. Nevertheless, the potential role of these different impacts is unclear. This complexity is noted in laboratory column experiments conducted by Kakuturu & Clark (2015) where reduced sediment-bound TP concentrations and cation displacement in media amended with compost was observed. While they suggest that Na input due to de-icing salts could be the cause of the observed changes in TP concentrations and cation displacement, they acknowledge that these results may be coincidental due to the complexity of ion exchange processes. Another column study by Szota, Farrell, Livesley, & Fletcher (2015) showed improved TP retention with increased salt loading. Influent TDP concentrations decreased with increased salt loading despite consistent influent TP concentrations, suggesting a transformation from dissolved to particulate P in the influent, which is consistently removed in bioretention systems through filtration or sedimentation.

High Cl concentrations may cause an increase in SRP concentrations due to SRP desorption through competitive binding of negatively charged ions (McManus and Davis, 2020), or toxicity to vegetation, thereby reducing SRP uptake (Kratky et al., 2017). Bai et al. (2017) suggested from their laboratory study on wetland sediments that increasing salt concentrations can alter P adsorption as Cl competes with SRP for adsorption sites on sediments. In porewater, Cl can create complexes with positively charged metals and organic matter (Nelson et al., 2009). While this mechanism does not directly affect P retention, the reactions between Cl and metals in the porewater could indirectly increase or decrease porewater P concentrations if those metals were previously bonded to P. As

such, Cl complexation is often attributed to changes in metal retention in bioretention systems and has a lesser role in controlling P transformation and distribution (Christopher et al., 1992).

Although some studies have concluded that high NaCl loading does not affect P retention in bioretention systems (Valtanen et al., 2017), Denich et al. (2003) observed peak mobilization of TP mass after flushing of their mesocosms with road runoff with high salt concentrations. Denich et al. (2003) did not examine the timing and mechanisms governing the observed mobilization of P. In contrast, large-scale lysimeter experiments completed by Valtanen et al. (2017) in Finland subjected to natural temperature cycles and synthetic road run off with high salt concentrations did not observe any seasonal differences in SRP retention. More recently, a recent laboratory column study by McManus & Davis (2020) found effluent TP concentrations from bioretention media peaked during flushing events which occurred following high road salt (NaCl) input. presented column experiments suggesting there may be a delay in P release from bioretention media after high salt loadings. This delay was observed in TP concentrations (and loads) but they did not monitor the effect of the high salt loadings on SRP or DOP concentrations. These columns were kept at room temperature so as to remove the possible effects from freeze-thaw cycles and directly examine the effects of Na and Cl on P retention in the bioretention media. There is a need to better understand the effect of high salt loading on P retention in field-scale bioretention systems as these laboratory studies described above are not able to account for the complexity of the processes governing P behaviour in bioretention system in the natural environment.

2.5 Geochemical mechanisms governing phosphorus behaviour within porewater

Most studies of field scale bioretention systems rely on influent-effluent water quantity and quality monitoring only. In doing so, they limited insight into the in situ hydro-geochemical processes governing P retention in bioretention system. In contrast, column experiments have provided valuable understanding of geochemical processes that occur within bioretention systems that govern P retention and release, but these experiments

simplify the natural system thereby neglecting the complexity of field-scale systems. Overall, investigation of in situ processes in field bioretention systems is very limited with the temporal and spatial biogeochemical conditions within bioretention systems poorly understood. To our knowledge, Komlos & Traver (2012) is the only study to measure SRP concentrations within the porewater of a field bioretention system. The study included only a single profile of lysimeters with porewater samples collected from the surface (0 m), at the bottom of the engineered media (1.2 m), and below the bioretention system (2.4 m). While this study was able to show increasing SRP removal with depth, the spatial resolution was limited, and they did not examine the possible mechanisms governing the fate of P in the bioretention system.

Some studies have attempted to identify the processes controlling the fate of P in bioretention systems. Li & Davis (2016) developed a mechanistic steady-state plug-flow model, assuming the bioretention system is a 1D adsorption column, with the objective, in part, to critically evaluate the mechanisms of P retention and release. They found that media depth, vegetation and the media composition (high Fe and Al content and organic matter that will not leach P) have the greatest impact on P effluent concentrations. Limiting the model to adsorption and leaching processes implies that P retention is governed by a predictable and consistent mechanism that changes exponentially with depth, which may not represent the complexity of field systems, as noted by the authors. Adsorption of P to Fe- and Al- minerals was observed to be the greatest at the surface and decrease with depth (to 35 cm) based on sequential sediment extractions performed in a mesocosm study by Song & Song (2018). There is a common notion in the bioretention literature that P retention in bioretention systems is governed by the availability of adsorption sites in the media (Hsieh et al., 2007; Lucas & Greenway, 2011; Shrestha et al., 2018), however, this may be an over-simplification for field-scale systems, as indicated in the high variation of P retention efficiencies in bioretention field studies. Komlos & Traver (2012)'s sediment extraction observed greater adsorbed SRP concentrations at the surface (0-2cm depth) of areas which experienced greater infiltration (0.13 ± 0.03 mg PO₄/g dry soil) compared to the dry, control location (0.04 ± 0.001 mg PO₄/g dry soil). However, most studies which conduct sediment P extractions,

including this study, limit their analysis to the upper 30 cm of media based on previous studies focusing on heavy metals, which indicated that accumulation of metals is limited to shallow depths of the bioretention media. A recent study by Johnson & Hunt (2016) observed that P accumulated in the sediment near the forebay of the studied bioretention cell, leading to the risk of desorption and leaching of P. These studies suggest that there is some level of heterogeneity associated with P retention in bioretention systems based on the infiltration area. Furthermore, these studies observed spatial variability in solid phase P concentrations but did not consider variability in the porewater P concentrations.

Wetting and drying cycles and the associated redox conditions may also affect the behaviour of P. In riparian zones, rapid fluctuations in water saturation may result in SRP release from microbial biomass through osmotic shock (Dupas et al., 2015; Turner and Haygarth, 2001). More frequent wetting and drying cycles can increase porewater exchange which may increase SRP release. A recent study of lake sediments by Ding, Hua, & Chu (2019), observed that porewater exchange under repetitive drying and wetting cycles changes the pH and redox conditions resulting in the release of SRP and dissolved Fe to the porewater. Redox potential was measured in a field-scale rain garden study by Dietz & Clausen (2005) but the results were not interpreted with respect to how the redox conditions observed may affect the mobility of P or any other pollutants. Although redox-sensitive elements such as Al and Fe are often considered to be closely linked to P retention, the role of wetting and drying cycles on redox conditions, pH, and the mobility of P behaviour is not well understood in bioretention systems.

2.6 Research gaps

This chapter has reviewed the P behaviour in the natural environment as well prior studies that have examined the performance of bioretention system with respect to P removal from urban stormwater. The literature review highlights the large variability in results from previous field scale bioretention studies that are often based on influent-effluent monitoring only, and suggests that a more detailed understanding of the temporal and spatial variability in P within bioretention system is needed to better understand and improve the performance of these systems.

The identified knowledge gaps provide an opportunity to further research the seasonal performance of bioretention systems installed in cold climates. When evaluating the overall performance of bioretention systems to retain P, there is a need to better characterize the seasonal behaviour of the different P forms at a higher temporal resolution that includes all four seasons. Furthermore, while the impact of high NaCl loading on P retention in bioretention media has been observed in column studies, there is a need to investigate the effects of high NaCl loading on P behaviour in field-scale bioretention systems. Chapter 3 of this thesis focuses on analysing the seasonal trends in the performance of two field-scale bioretention systems in London, Ontario, Canada in retaining the different forms of P, including the potential influence of high Na and Cl loading on P retention in these systems.

The mechanisms that control the behaviour of P within field scale bioretention systems also need to be investigated to provide insight into the current black-box (influent-effluent) understanding of bioretention systems. Despite many column experiments and influent-effluent field monitoring studies, the hydro-biogeochemical processes occurring within bioretention systems are poorly understood at the field scale. The common notion that P retention in bioretention systems is governed by P adsorption processes with overall retention increasing with media depth may oversimplify the complexity of field systems. Detailed spatial analysis of the porewater within field bioretention systems is needed to improve understanding of the fate of P within these systems. Chapter 4 of this thesis investigates the spatial distribution of SRP within two field scale bioretention systems and examines the hydro-biogeochemical processes that may be governing the observed heterogeneous behaviour of SRP within these systems.

2.7 References

- Akhter, F., Hewa, G.A., Ahammed, F., Myers, B., Argue, J.R., 2020. Performance evaluation of stormwater management systems and its impact on development costing. *Water (Switzerland)* 12, 12–14. <https://doi.org/10.3390/w12020375>
- Bäckström, M., Karlsson, S., Bäckman, L., Folkesson, L., Lind, B., 2004. Mobilisation of heavy metals by deicing salts in a roadside environment. *Water Res.* 38, 720–732. <https://doi.org/10.1016/j.watres.2003.11.006>
- Bai, J., Ye, X., Jia, J., Zhang, G., Zhao, Q., Cui, B., Liu, X., 2017. Phosphorus sorption-desorption and effects of temperature, pH and salinity on phosphorus sorption in marsh soils from coastal wetlands with different flooding conditions. *Chemosphere* 188, 677–688. <https://doi.org/10.1016/j.chemosphere.2017.08.117>
- Baken, S., Salaets, P., Desmet, N., Seuntjens, P., Vanlierde, E., Smolders, E., 2015. Oxidation of iron causes removal of phosphorus and arsenic from streamwater in groundwater-fed lowland catchments. *Environ. Sci. Technol.* 49, 2886–2894. <https://doi.org/10.1021/es505834y>
- Berge, D., Fjeld, E., Hindar, A., Kaste, Ø., 2017. Nitrogen Retention in Two Norwegian Watercourses of Different Trophic Status. *Ambio* 26, 282–288.
- Blecken, G.T., Zinger, Y., Deletić, A., Fletcher, T.D., Hedström, A., Viklander, M., 2010. Laboratory study on stormwater biofiltration: Nutrient and sediment removal in cold temperatures. *J. Hydrol.* 394, 507–514. <https://doi.org/10.1016/j.jhydrol.2010.10.010>
- Blecken, G.T., Zinger, Y., Muthanna, T.M., Deletic, A., Fletcher, T.D., Viklander, M., 2007. The influence of temperature on nutrient treatment efficiency in stormwater biofilter systems. *Water Sci. Technol.* 56, 83–91. <https://doi.org/10.2166/wst.2007.749>
- Boström, B., Andersen, J.M., Fleischer, S., Jansson, M., 1988. Exchange of phosphorus across the sediment-water interface. *Hydrobiologia* 170, 229–244. <https://doi.org/10.1007/BF00024907>

- Canadian Council of Ministers of the Environment, 2004. Phosphorus: Canadian Guidance Framework for the Management of Freshwater Systems. *Can. Water Qual. Guidel. Prot. Aquat. Life* 1–5. <https://doi.org/10.1038/sj.bdj.4806729> [pii]
- Christopher, A., Strong, J.E., Mosher, P.A., 1992. Effect of Deicing Salts on Metal and Organic Matter Mobilization in Roadside Soils. *Environ. Sci. Technol.* 26, 703–709. <https://doi.org/10.1021/es00028a006>
- Cooper, J.E., Early, J., Holding, A.J., 1991. Mineralization of dissolved organic phosphorus from a shallow eutrophic lake. *Hydrobiologia* 209, 89–94. <https://doi.org/10.1007/BF00006920>
- Credit Valley Conservation, Toronto and Region Conservation Authority, 2010a. *Low Impact Development Stormwater Management Planning and Design Guide*. Toronto, Ontario.
- Credit Valley Conservation, Toronto and Region Conservation Authority, 2010b. *Low Impact Development Stormwater Management Planning and Design Guide, APPENDIX A: Low Impact Development Stormwater BMP Fact Sheets*. Toronto, Ontario.
- Davis, A.P., 2007. Field Performance of Bioretention: Water Quality. *Environ. Eng. Sci.* 24, 1048–1064. <https://doi.org/10.1089/ees.2006.0190>
- Davis, A.P., Shokouhian, M., Sharma, H., Minami, C., 2006. Water Quality Improvement through Bioretention Media: Nitrogen and Phosphorus Removal. *Water Environ. Res.* 78, 284–293. <https://doi.org/10.2175/106143005x94376>
- Denich, C., Bradford, A., Drake, K., 2003. Bioretention: assessing effects of winter salt and aggregate application on plant health, media clogging and effluent quality. *Water Qual. Res. J. Canada* 48, 387–399. <https://doi.org/10.2166/wqrjc.2013.065>
- Dietz, M.E., 2007. *Low Impact Development Practices : A Review of Current Research and Recommendations for Future Directions* 13. <https://doi.org/10.1007/s11270-007-9484-z>

- Dietz, M.E., Clausen, J.C., 2005. A field evaluation of rain garden flow and pollutant treatment. *Water, Air, Soil Pollut.* 167, 123–138. <https://doi.org/10.1007/s11270-005-8266-8>
- Ding, B., Rezanezhad, F., Gharedaghloo, B., Van Cappellen, P., Passeport, E., 2019. Bioretention cells under cold climate conditions: Effects of freezing and thawing on water infiltration, soil structure, and nutrient removal. *Sci. Total Environ.* 649, 749–759. <https://doi.org/10.1016/j.scitotenv.2018.08.366>
- Ding, J., Hua, Z., Chu, K., 2019. The effect of hydrodynamic forces of drying/wetting cycles on the release of soluble reactive phosphorus from sediment. *Environ. Pollut.* 252, 992–1001. <https://doi.org/10.1016/j.envpol.2019.06.016>
- Dupas, R., Gruau, G., Gu, S., Humbert, G., Jaffrézic, A., Gascuel-Oudou, C., 2015. Groundwater control of biogeochemical processes causing phosphorus release from riparian wetlands. *Water Res.* 84, 307–314. <https://doi.org/10.1016/j.watres.2015.07.048>
- Eckart, K., McPhee, Z., Bolisetti, T., 2017. Performance and implementation of low impact development – A review. *Sci. Total Environ.* 607–608, 413–432. <https://doi.org/10.1016/j.scitotenv.2017.06.254>
- Ellison, M.E., Brett, M.T., 2006. Particulate phosphorus bioavailability as a function of stream flow and land cover. *Water Res.* 40, 1258–1268. <https://doi.org/10.1016/j.watres.2006.01.016>
- Environment and Climate Change Canada, Ontario Ministry of the Environment and Climate Change, 2018. Canada-Ontario Lake Erie Action Plan.
- Erickson, A.J., Gulliver, J.S., Weiss, P.T., 2012. Capturing phosphates with iron enhanced sand filtration. *Water Res.* 46, 3032–3042. <https://doi.org/10.1016/j.watres.2012.03.009>
- Fowdar, H.S., Hatt, B.E., Cresswell, T., Harrison, J.J., Cook, P.L.M., Deletic, A., 2017. Phosphorus Fate and Dynamics in Greywater Biofiltration Systems. *Environ. Sci.*

- Technol. 51, 2280–2287. <https://doi.org/10.1021/acs.est.6b04181>
- Géhéniau, N., Fuamba, M., Mahaut, V., Gendron, M.R., Dugué, M., 2015. Monitoring of a Rain Garden in Cold Climate: Case Study of a Parking Lot near Montréal. *J. Irrig. Drain. Eng.* 141. [https://doi.org/10.1061/\(ASCE\)IR.1943-4774.0000836](https://doi.org/10.1061/(ASCE)IR.1943-4774.0000836)
- Geronimo, F.K.F., Maniquiz-Redillas, M.C., Kim, L.H., 2015. Fate and removal of nutrients in bioretention systems. *Desalin. Water Treat.* 53. <https://doi.org/10.1080/19443994.2014.922308>
- Hager, J., Hu, G., Hewage, K., Sadiq, R., 2019. Performance of low-impact development best management practices: A critical review. *Environ. Rev.* 27, 17–42. <https://doi.org/10.1139/er-2018-0048>
- Hermawan, A.A., Talei, A., Salamatinia, B., Chua, L.H.C., 2020. Seasonal performance of stormwater biofiltration system under tropical conditions. *Ecol. Eng.* 143, 105676. <https://doi.org/10.1016/j.ecoleng.2019.105676>
- Hsieh, C., Davis, A.P., Needelman, B.A., 2007. Bioretention Column Studies of Phosphorus Removal from Urban Stormwater Runoff. *Water Environ. Res.* 79, 177–184. <https://doi.org/10.2175/106143006X111745>
- Huang, L., Fu, L., Jin, C., Gielen, G., Lin, X., Wang, H., Zhang, Y., 2011. Effect of temperature on phosphorus sorption to sediments from shallow eutrophic lakes. *Ecol. Eng.* 37, 1515–1522. <https://doi.org/10.1016/j.ecoleng.2011.05.006>
- Hunt, W.F., Davis, A.P., Traver, R.G., 2012. Meeting hydrologic and water quality goals through targeted bioretention design. *J. Environ. Eng. (United States)* 138, 698–707. [https://doi.org/10.1061/\(ASCE\)EE.1943-7870.0000504](https://doi.org/10.1061/(ASCE)EE.1943-7870.0000504)
- International Joint Commission, 2014. A Balanced Diet for Lake Erie: Reducing Phosphorus Loadings and Harmful Algal Blooms. Report of the Lake Erie Ecosystem Priority. Ottawa, Ontario.
- Irvine, C., Macrae, M., Morison, M., Petrone, R., 2019. Seasonal nutrient export dynamics in a mixed land use subwatershed of the Grand River, Ontario, Canada. *J.*

- Great Lakes Res. 45, 1171–1181. <https://doi.org/10.1016/j.jglr.2019.10.005>
- Jay, J.G., Brown, S.L., Kurtz, K., Grothkopp, F., 2017. Predictors of phosphorus leaching from bioretention soil media. *J. Environ. Qual.* 46. <https://doi.org/10.2134/jeq2017.06.0232>
- Johnson, J.P., Hunt, W.F., 2016. Evaluating the spatial distribution of pollutants and associated maintenance requirements in an 11 year-old bioretention cell in urban Charlotte, NC. *J. Environ. Manage.* 184, 363–370. <https://doi.org/10.1016/j.jenvman.2016.10.009>
- Kakuturu, S., Clark, S., 2015. Clogging Mechanism of Stormwater Filter Media by NaCl as a Deicing Salt. *Environ. Eng. Sci.* 32. <https://doi.org/https://doi-org.proxy1.lib.uwo.ca/10.1089/ees.2014.0337>
- Kakuturu, S.P., Clark, S.E., 2015. Effects of Deicing Salts on the Clogging of Stormwater Filter Media and on the Media Chemistry. *J. Environ. Eng. (United States)* 141, 1–7. [https://doi.org/10.1061/\(ASCE\)EE.1943-7870.0000927](https://doi.org/10.1061/(ASCE)EE.1943-7870.0000927)
- Kayhanian, M., Fruchtman, B.D., Gulliver, J.S., Montanaro, C., Ranieri, E., Wuertz, S., 2012. Review of highway runoff characteristics: Comparative analysis and universal implications. *Water Res.* 46, 6609–6624. <https://doi.org/10.1016/j.watres.2012.07.026>
- Khan, U.T., Valeo, C., Chu, A., van Duin, B., 2012. Bioretention cell efficacy in cold climates: Part 1 - hydrologic performance. *Can. J. Civ. Eng.* 39, 1210–1221. <https://doi.org/10.1139/l2012-110>
- Komlos, J., Traver, R.G., 2012. Long-Term Orthophosphate Removal in a Field-Scale Storm-Water Bioinfiltration Rain Garden. *J. Environ. Eng.* 138, 991–998. [https://doi.org/10.1061/\(ASCE\)EE.1943-7870.0000566](https://doi.org/10.1061/(ASCE)EE.1943-7870.0000566)
- Kordana, S., Słyś, D., 2020. An analysis of important issues impacting the development of stormwater management systems in Poland. *Sci. Total Environ.* 727. <https://doi.org/10.1016/j.scitotenv.2020.138711>

- Kratky, H., Li, Z., Chen, Y., Wang, C., Li, X., Yu, T., 2017. A critical literature review of bioretention research for stormwater management in cold climate and future research recommendations. *Front. Environ. Sci. Eng.* 11, 16.
<https://doi.org/10.1007/s11783-017-0982-y>
- Le Moal, M., Gascuel-Oudou, C., Ménesguen, A., Souchon, Y., Étrillard, C., Levain, A., Moatar, F., Pannard, A., Souchu, P., Lefebvre, A., Pinay, G., 2019. Eutrophication: A new wine in an old bottle? *Sci. Total Environ.* 651, 1–11.
<https://doi.org/10.1016/j.scitotenv.2018.09.139>
- LeFevre, G.H., Paus, K.H., Natarajan, P., Gulliver, J.S., Novak, P.J., Hozalski, R.M., 2015. Review of Dissolved Pollutants in Urban Storm Water and Their Removal and Fate in Bioretention Cells. *J. Environ. Eng.* 141.
[https://doi.org/10.1061/\(ASCE\)EE.1943-7870.0000876](https://doi.org/10.1061/(ASCE)EE.1943-7870.0000876)
- Li, B., Brett, M.T., 2013. The influence of dissolved phosphorus molecular form on recalcitrance and bioavailability. *Environ. Pollut.* 182, 37–44.
<https://doi.org/10.1016/j.envpol.2013.06.024>
- Li, Davis, A., 2009. Water quality improvement through reductions of pollutant loads using bioretention. *J. Environ. Eng.* 135, 567–576.
[https://doi.org/10.1061/\(ASCE\)EE.1943-7870.0000026](https://doi.org/10.1061/(ASCE)EE.1943-7870.0000026)
- Li, J., Davis, A., 2016. A unified look at phosphorus treatment using bioretention. *Water Res.* 90, 141–155. <https://doi.org/10.1016/j.watres.2015.12.015>
- LID SWM Planning and Design Guide Contributors, 2020. Bioretention: Filter media LID SWM Planning and Design Guide [WWW Document]. *Sustain. Technol. Eval. Progr.* URL
https://wiki.sustainabletechnologies.ca/index.php?title=Bioretention:_Filter_media&oldid=10879 (accessed 5.5.20).
- Liu, J., Davis, A.P., 2014. Phosphorus speciation and treatment using enhanced phosphorus removal bioretention. *Environ. Sci. Technol.* 48.
<https://doi.org/10.1021/es404022b>

- Liu, J., Sample, D.J., Bell, C., Guan, Y., 2014. Review and research needs of bioretention used for the treatment of urban stormwater. *Water (Switzerland)* 6, 1069–1099. <https://doi.org/10.3390/w6041069>
- Logsdon, S.D., 2017. Nutrient leaching when compost is part of plant growth media. *Water (Switzerland)* 9, 238–245. <https://doi.org/10.3390/w9070501>
- Lucas, W., Greenway, M., 2008. Nutrient Retention in Vegetated and Nonvegetated Bioretention Mesocosms. *J. Irrig. Drain. Eng.* 134, 613–623. [https://doi.org/10.1061/\(ASCE\)0733-9437\(2008\)134:5\(613\)](https://doi.org/10.1061/(ASCE)0733-9437(2008)134:5(613))
- Lucas, W.C., Greenway, M., 2011. Phosphorus Retention by Bioretention Mesocosms Using Media Formulated for Phosphorus Sorption: Response to Accelerated Loads. *J. Irrig. Drain. Eng.* 137, 144–153. [https://doi.org/10.1061/\(ASCE\)IR.1943-4774.0000243](https://doi.org/10.1061/(ASCE)IR.1943-4774.0000243)
- Mackey, K.R.M., Van Mooy, B., Cade-Menun, B.J., Paytan, A., 2019. Phosphorus dynamics in the environment, 4th ed, *Encyclopedia of Microbiology*. Elsevier Inc. <https://doi.org/10.1016/B978-0-12-809633-8.20911-4>
- Mahmoud, A., Alam, T., Yeasir A. Rahman, M., Sanchez, A., Guerrero, J., Jones, K.D., 2019. Evaluation of field-scale stormwater bioretention structure flow and pollutant load reductions in a semi-arid coastal climate. *Ecol. Eng.* X 1, 100007. <https://doi.org/10.1016/j.ecoena.2019.100007>
- Mangangka, I.R., Liu, A., Egodawatta, P., Goonetilleke, A., 2015. Performance characterisation of a stormwater treatment bioretention basin. *J. Environ. Manage.* 150, 173–178. <https://doi.org/10.1016/j.jenvman.2014.11.007>
- Manka, B.N., Hathaway, J.M., Tirpak, R.A., He, Q., Hunt, W.F., 2016. Driving forces of effluent nutrient variability in field scale bioretention. *Ecol. Eng.* 94. <https://doi.org/10.1016/j.ecoleng.2016.06.024>
- Marvin, J.T., Passeport, E., Drake, J., 2020. State-of-the-Art Review of Phosphorus Sorption Amendments in Bioretention Media: A Systematic Literature Review. *J.*

- Sustain. Water Built Environ. 6. <https://doi.org/10.1061/JSWBAY.0000893>
- McManus, M., Davis, A.P., 2020. Impact of Periodic High Concentrations of Salt on Bioretention Water Quality Performance. *J. Sustain. Water Built Environ.* 6, 1–11. <https://doi.org/10.1061/JSWBAY.0000922>
- Moore, T.L., Rodak, C.M., Vogel, J.R., 2017. Urban Stormwater Characterization, Control, and Treatment. *Water Environ. Res.* 89, 1876–1927. <https://doi.org/10.2175/106143017x15023776270692>
- Nelson, S., Yonge, D., Barber, M., 2009. Effects of Road Salts on Heavy Metal Mobility in Two Eastern Washington Soils. *J. Environ. Eng.* 135, 505–510. [https://doi.org/10.1061/\(ASCE\)EE.1943-7872\(2009\)135:7\(505\)](https://doi.org/10.1061/(ASCE)EE.1943-7872(2009)135:7(505))
- O’Neill, S.W., Davis, A.P., 2012. Water treatment residual as a bioretention amendment for phosphorus. I: Evaluation studies. *J. Environ. Eng. (United States)* 138, 318–327. [https://doi.org/10.1061/\(ASCE\)EE.1943-7870.0000409](https://doi.org/10.1061/(ASCE)EE.1943-7870.0000409)
- Parsons, C.T., Rezanezhad, F., O’Connell, D.W., Van Cappellen, P., 2017. Sediment phosphorus speciation and mobility under dynamic redox conditions. *Biogeosciences* 14, 3585–3602. <https://doi.org/10.5194/bg-14-3585-2017>
- Passeport, E., Hunt, W.F., Line, D.E., Smith, R.A., Brown, R.A., 2009. Field study of the ability of two grassed bioretention cells to reduce storm-water runoff pollution. *J. Irrig. Drain. Eng.* 135, 505–510. [https://doi.org/10.1061/\(ASCE\)IR.1943-4774.0000006](https://doi.org/10.1061/(ASCE)IR.1943-4774.0000006)
- Paus, K.H., Muthanna, T.M., Braskerud, B.C., 2015. The hydrological performance of bioretention cells in regions with cold climates: seasonal variation and implications for design. *Hydrol. Res.* <https://doi.org/10.2166/nh.2015.084>
- Prasad, R., Chakraborty, D., 2019. Phosphorus Basics: Understanding Phosphorus Forms and Their Cycling in the Soil, the Alabama Cooperative Extension System.
- Roseen, R.M., 2009. Seasonal Performance Variations for Storm-water management systems in cold climate conditions. *J. Environ. Eng.* 3, 128–137.

[https://doi.org/10.1061/\(ASCE\)0733-9371\(2009\)135:3\(1280](https://doi.org/10.1061/(ASCE)0733-9371(2009)135:3(1280)

- Shrestha, P., Hurley, S.E., Wemple, B.C., 2018. Effects of different soil media, vegetation, and hydrologic treatments on nutrient and sediment removal in roadside bioretention systems. *Ecol. Eng.* 112, 116–131. <https://doi.org/10.1016/j.ecoleng.2017.12.004>
- Smith, R.B., Bass, B., Sawyer, D., Depew, D., Watson, S.B., 2019. Estimating the economic costs of algal blooms in the Canadian Lake Erie Basin. *Harmful Algae* 87, 101624. <https://doi.org/10.1016/j.hal.2019.101624>
- Søberg, L.C., Viklander, M., Blecken, G.T., 2017. Do salt and low temperature impair metal treatment in stormwater bioretention cells with or without a submerged zone? *Sci. Total Environ.* 579, 1588–1599. <https://doi.org/10.1016/j.scitotenv.2016.11.179>
- Song, Y., Song, S., 2018. Migration and transformation of different phosphorus forms in rainfall runoff in bioretention system. *Environ. Sci. Pollut. Res.* 1–8. <https://doi.org/10.1007/s11356-018-2405-4>
- Stagge, J.H., Davis, A.P., Jamil, E., Kim, H., 2012. Performance of grass swales for improving water quality from highway runoff. *Water Res.* 46, 6731–6742. <https://doi.org/10.1016/j.watres.2012.02.037>
- Steffen, M.M., Belisle, B.S., Watson, S.B., Boyer, G.L., Wilhelm, S.W., 2014. Status, causes and controls of cyanobacterial blooms in Lake Erie. *J. Great Lakes Res.* 40, 215–225. <https://doi.org/10.1016/j.jglr.2013.12.012>
- Swedish Environmental Protection Agency, 2000. *Environmental Quality Criteria - Lakes and Watercourses.*
- Szota, C., Farrell, C., Livesley, S.J., Fletcher, T.D., 2015. Salt tolerant plants increase nitrogen removal from biofiltration systems affected by saline stormwater. *Water Res.* 83, 195–204. <https://doi.org/10.1016/j.watres.2015.06.024>
- Trowsdale, S.A., Simcock, R., 2011. Urban stormwater treatment using bioretention. *J. Hydrol.* 397, 167–174. <https://doi.org/10.1016/j.jhydrol.2010.11.023>

- Turner, B., Haygarth, P., 2001. Phosphorus solubilization in rewetted soils. *Nature* 411, 258. <https://doi.org/https://doi.org/10.1038/35077146>
- United States Environmental Protection Agency, 2004. National Water Quality Inventory: Report to Congress, 2004.
- Valtanen, M., Sillanpää, N., Setälä, H., 2017. A large-scale lysimeter study of stormwater biofiltration under cold climatic conditions. *Ecol. Eng.* 100. <https://doi.org/10.1016/j.ecoleng.2016.12.018>
- Wang, C., Zhang, Y., Li, H., Morrison, R.J., 2013. Sequential extraction procedures for the determination of phosphorus forms in sediment. *Limnology* 14, 147–157. <https://doi.org/10.1007/s10201-012-0397-1>
- Watson, S.B., Miller, C., Arhonditsis, G., Boyer, G.L., Carmichael, W., Charlton, M.N., Confesor, R., Depew, D.C., Höök, T.O., Ludsin, S.A., Matisoff, G., McElmurry, S.P., Murray, M.W., Peter Richards, R., Rao, Y.R., Steffen, M.M., Wilhelm, S.W., 2016. The re-eutrophication of Lake Erie: Harmful algal blooms and hypoxia. *Harmful Algae* 56, 44–66. <https://doi.org/10.1016/j.hal.2016.04.010>
- Wilson, C.E., Hunt, W.F., Winston, R.J., Smith, P., 2015. Comparison of Runoff Quality and Quantity from a Commercial Low-Impact and Conventional Development in Raleigh, North Carolina. *J. Environ. Eng.* 141. [https://doi.org/10.1061/\(ASCE\)EE.1943-7870.0000842](https://doi.org/10.1061/(ASCE)EE.1943-7870.0000842)
- Yan, Q., Davis, A.P., James, B.R., 2016. Enhanced Organic Phosphorus Sorption from Urban Stormwater Using Modified Bioretention Media: Batch Studies. *J. of Environmental Engineering* 142 (4), 1152–1161. [https://doi.org/10.1061/\(ASCE\)EE.1943-7870](https://doi.org/10.1061/(ASCE)EE.1943-7870)

Chapter 3

3 Seasonal performance of bioretention systems in reducing phosphorus loads from urban stormwater in cold climates

3.1 Introduction

Eutrophication caused by high nutrient (phosphorus [P] and nitrogen [N]) inputs from anthropogenic sources degrades surface waters worldwide (Steffen et al., 2014; Street, 2014). Eutrophication can lead to harmful algal blooms and hypoxic events which threaten drinking water sources, public health, biodiversity, and the recreational, fishing and tourism industries (Fowdar et al., 2017; Steffen et al., 2014; Watson et al., 2016). Although N and P are both required for plant growth (Le Moal et al., 2019), P is generally the limiting nutrient for eutrophication in freshwaters, and therefore the focus of nutrient management efforts in freshwater environments (Berge et al., 2017; Swedish Environmental Protection Agency, 2000). Reducing nutrient loads to surface waters requires management of all the contributing sources. Non-point nutrient sources including urban stormwater runoff remain particularly challenging to quantify and mitigate. Urban stormwater runoff can deliver various contaminants to downstream watersheds including P, N, total suspended solids, pathogens, heavy metals, and chloride (He et al., 2010; Hwang and Weng, 2015; Kayhanian et al., 2012). Although conventional stormwater management systems (such as stormwater ponds and constructed wetlands) can improve the water quality of urban stormwater runoff, they are often designed primarily for water quantity control and total suspended solids removal. As such, low impact development (LID) stormwater systems have become an increasingly popular alternative or addition to conventional stormwater management systems for water quality control and to enhance the protection of downstream watersheds.

LID systems are small-scale, site-specific installations that treat stormwater runoff near the source using passive, natural processes to mimic the pre-development hydrology and

reduce peak flows. One popular type of LID system is bioretention systems which are vegetated depressions designed to accept stormwater runoff from impervious areas. Typically, runoff is infiltrated through a 0.1 - 0.15 m layer of mulch or topsoil (to support plant growth) before infiltrating through engineered soil media (typically 1 - 1.25 m deep (Credit Valley Conservation and Toronto and Region Conservation Authority, 2010)). As the runoff percolates through the media it can be treated by physical (filtration), chemical (precipitation, sorption, ion exchange), and biological (plant uptake, microbial degradation) processes (Hsieh et al., 2007a). While the performance of bioretention systems for improving water quality is influenced by the engineering design (e.g., sizing relative to catchment area, presence of an underdrain) and vegetation selection (Hermawan et al., 2020), the performance strongly depends on the composition of the engineered media (Davis, 2007). The media generally contains a mixture of sand, soil, and organic matter with the specific composition often based on local stormwater management priorities (e.g., water quantity or water quality control) (LID SWM Planning and Design Guide Contributors, 2020). While prior studies, mostly laboratory based, have demonstrated that various Al-, Ca-, and Fe-based amendments can be added to the media to enhance P removal (Marvin et al., 2020; O'Neill and Davis, 2012; Palmer et al., 2013), the performance of the amendments with respect to P removal is affected by pH, redox and water saturation changes within the system; this results in practical challenges for field application and inconsistent P removal (Marvin et al., 2020).

Numerous laboratory column, mesocosm, and field-scale studies have evaluated the performance of bioretention systems (or media) with respect to their ability to remove P from infiltrating stormwater. Although column and mesocosm experiments provide important insights into possible P removal mechanisms (Geronimo et al., 2015; Hsieh et al., 2007b; Li and Davis, 2016), the complexity of real environmental conditions can impact P removal in bioretention systems. These complexities include, for instance, irregular precipitation and temperature patterns, seasonality, hydrogeology and native soil conditions, and anthropogenic activities (such as road salt and fertilizer application, construction, and road use frequency). In part because of these complexities, but also due to the use of different media mixtures between studies, field investigations have shown

variable performance of bioretention systems with respect to their ability to reduce total P (TP) concentrations and loads. Some studies have shown that bioretention systems can decrease TP concentration in stormwater (Jiang et al., 2017; Liu and Davis, 2014; Lucke and Nichols, 2015; Passeport et al., 2009; Roseen, 2009), and others have combined TP concentration changes with water quantity measurements to show TP mass load reductions (Carpenter & Hallam, 2010; Davis, 2007; Debusk & Wynn, 2011; Jiang, Li, Li, Li, & Chen, 2017; Liu & Davis, 2014; Mangangka, Liu, Egodawatta, & Goonetilleke, 2015). However, other studies have shown TP concentration increases (Khan et al., 2012a; Li et al., 2011; Li and Davis, 2009), and TP mass load increases from bioretention systems (Dietz and Clausen, 2006, 2005; Li et al., 2011; Li and Davis, 2009).

TP is made up of particulate P (PP) and total dissolved P (TDP). The latter can be further divided into dissolved organic P (DOP), and dissolved inorganic P, commonly referred to as soluble reactive P (SRP). To improve P retention in bioretention systems it is essential to understand how the systems perform with respect to the different forms of P. Compared to TP, fewer field studies have examined SRP retention and release in bioretention systems. This is in spite of SRP being the bioavailable form of P that is taken up by plants and aquatic biota and therefore of key concern for downstream water quality impairment (Prestigiacomo et al., 2016). The few studies that have measured SRP show, similar to TP, varying results with respect to SRP concentration and load reduction in bioretention systems (Hager et al., 2019; Mangangka et al., 2015; Passeport et al., 2009). In addition to understanding SRP retention and release in bioretention systems, it is also important to understand the fate of DOP as this form can also be bioavailable to phytoplankton and therefore contribute to eutrophication (Li & Brett, 2013). Also, understanding the fate of DOP together with SRP provides greater insight into the overall P cycle in bioretention systems (Joshi et al., 2015). While laboratory batch experiments have reported DOP sorption in bioretention media with added amendments (Yan et al., 2016), the only field study (to our knowledge) to quantify DOP influent and effluent loads found a 59% mass reduction of DOP in a bioretention system amended with Fe- and Al-based water treatment residuals (Liu and Davis, 2014). It is unclear if this DOP mass reduction occurs more broadly in field bioretention systems, including those

without added media amendments, and how the load reductions may vary temporally. Therefore, there is a need to better quantify the retention and release of the different forms of P, especially SRP and DOP, in field scale bioretention systems including how this varies over time.

The performance of bioretention systems in decreasing TP and SRP concentrations and loads have been shown to vary over time with seasonality and precipitation depth driving variability (Shrestha et al., 2018). Understanding the seasonal performance of bioretention systems is important because the timing of TP and SRP release to downstream watersheds can play a critical role in cyanobacterial blooms (Irvine et al., 2019). Seasonal changes including precipitation, evapotranspiration, temperature, and vegetation life cycles can affect P transformations in bioretention systems, and thus P retention and release (Hermawan et al., 2020). Roseen (2009) found overall higher TP concentrations in summer influent and effluent compared to winter influent and effluent at their field site in New Hampshire with a slightly higher removal efficiency ($RE = 1 - \text{effluent concentration}/\text{influent concentration} \times 100$) in summer (19%) compared to winter (13%). Passeport et al. (2009) similarly found higher SRP removal in spring and summer (from March 20 to June 21 2006) compared with fall and winter (September 22, 2005 to March 20 2006) attributing this to plant decay, grass mowing, and organic matter decomposition in the fall.

Cold climate winter conditions add further complexities to the effects of seasonality on P retention in bioretention systems. In cold climates, the use of road de-icing salts and freeze-thaw cycles have been shown to alter the biogeochemical reactions in the bioretention media, and alter the structure of the media and its hydraulic performance (Ding et al., 2019; Kazemi et al., 2018). Laboratory column and mesocosm experiments have examined the effects of temperature, high de-icing salt (sodium chloride) loading, and freeze-thaw cycles on P retention in bioretention media, but the impact of cold climate conditions on the P retention, including the different forms of P, in field scale bioretention systems remains unclear. While laboratory experiments have shown that lower temperatures may increase SRP adsorption resulting in less SRP released from

sediments due to differences in adsorption and desorption reaction rates (Sánchez and Boll, 2005), the influence of temperature remains unclear for field scale systems. For instance, a study by Brown, Birgand, & Hunt (2013) found effluent TP concentrations to be greater with higher temperatures but found no significant correlation between effluent SRP and temperature. More recently, Manka, Hathaway, Tirpak, He, & Hunt (2016) observed no temperature effect on P retention in field bioretention systems. Using column experiments, Ding et al., (2019) showed that freeze-thaw cycles may decrease the media's capacity to remove P by increasing overall pore sizes as well as the number of isolated small pore sizes – this in turn may reduce the surface area for P adsorption (Ding et al., 2019). While the column experiments conducted by Ding et al., (2019) used high salt (NaCl) concentrations in the influent to simulate realistic cold climate conditions, they did not directly examine whether the high salt loading contributed to P release from the media.

It is expected that high salt concentrations may affect P retention in bioretention systems with a recent study by Mullins et al. (2020) that monitored field scale infiltration trenches in Pittsburgh, PA showing that high salt loading (which they characterized using Na concentrations) may have influenced seasonal trends in heavy metal and N mobility. While they did not measure P concentrations or loads, they suggested the high salt loads altered the redox conditions, ion exchange capacity, and caused chloride complexation – these changes are also expected to influence the fate of P. More recently, column experiments by McManus & Davis (2020) found effluent TP concentrations peaked during flushing events which occurred after direct salt input suggesting that high salt loads may produce a delayed release P. Building on these recent studies, data from field bioretention systems are required to investigate how salt loading may affect the release of P, and its different forms, over time while considering the wide range of conditions (such as variable salt loading patterns, freeze thaw cycles and variable precipitation patterns) to which installed bioretention systems are exposed in cold climates. As the amount and timing of de-icing salt application can be modified (provided road safety conditions are met), it is important to understand the role of Cl⁻ and Na-based salts on P retention in bioretention systems installed in cold climates. Identifying of the effects of salt loading

on P behaviour may also provide further insight into the variable performance of field-scale bioretention systems with respect to P retention.

The objective of this study was to evaluate the seasonal variability in the retention of P and its different forms (TP, TDP, DOP, and SRP) in field bioretention systems installed in a cold climate. Based on the findings from the field investigation, the second study objective was to evaluate the effect of high road salt (sodium chloride) loading on P retention and release from the bioretention media. The first objective was addressed by monitoring two large (46 - 53 m²) bioretention systems located adjacent to a major arterial road in London, Ontario, Canada. Influent and effluent water quantity and quality were analyzed together with porewater samples collected from within the bioretention systems over a 12-month period. The second objective was addressed by conducting laboratory column experiments designed to evaluate the isolated influence of high salt loading on P release from bioretention media in controlled conditions without other complicating environmental factors such as the freeze-thaw cycle, temperature changes, or plant growth-decay. The findings from this study aim to provide valuable new insights needed to enhance LID system design and mitigate the water quality impacts of urbanization on groundwater and surface water.

3.2 Methodology

3.2.1 Field-scale monitoring

3.2.1.1 Site Description

Two bioretention systems located along a major arterial road (Sarnia Road) in London, Ontario, were monitored in this study. London is in the Great Lakes and St. Lawrence lowlands climate region and has an average annual precipitation of 938 mm with maximum and minimum monthly average temperatures of 20.8 and -5.6°C, respectively, based on at least 15 years of historical data (Environment and Climate Change Canada, 2019a). The two bioretention systems, referred to as the Centre and East systems, were separated by 40 m and located along the same side of the road. The bioretention systems were designed for water quantity control (maintain existing peak flows up to and

including the 100-year event) and to meet the normal water quality control for stormwater management facilities in Ontario (70% long-term suspended solids removal). The bioretention systems were constructed in October 2017 and started receiving road runoff in late August 2018.

The physical dimensions of the two bioretention systems, including the catchment area, are provided in Table 3-1. The bioretention systems were constructed with a 0.07 - 0.15 m layer of locally sourced topsoil overlying a 1 m layer of bioretention media. Beneath the media was a 0.5 m layer of gravel. The bioretention systems have a perforated underdrain due to the low permeability of the native soil (infiltration rate <15 mm/hr) (Golder Associates Ltd., 2016). The underdrain for each system discharges into a concrete monitoring chamber located at the downstream end of the system where the effluent water quantity and quality could be measured before the water is released to the stormwater drainage network. The composition of the engineered media used in the bioretention systems is 91.2% sand, 8.8% soil fines and 3.4% organic matter in the form of woodchips, resulting in an initial soil pH of 7.5 (see Appendix A, Figure A-1 for further details of preliminary media characterization) (Fisher Landscaping, 2017). This composition was based on the 2010 Low Impact Development Stormwater Management Planning and Design Guide (Credit Valley Conservation and Toronto and Region Conservation Authority, 2010).

Table 3-1: Design details of monitored bioretention systems

Bioretention system name	Catchment area (ha)	Width of bioretention system (m)	Length of bioretention system (m)	Footprint area (m²)	Ponded water storage (m³)
East	0.13	2.0	26	53	18
Center	0.12	2.0	23	46	16

3.2.1.2 Water Sample Collection and Analysis

Influent-effluent water sampling of the Centre and East bioretention systems was conducted for 24 precipitation events from 24 November 2018 to 2 October 2019 to evaluate seasonal variability in the retention and release of P. Large precipitation events that resulted in drainage from the systems were targeted for sampling and, as such, only precipitation events greater than 5 mm depth were sampled. Influent grab samples were collected from the upstream curb cut inlet of the Center system for all monitored events. When possible, a first flush runoff sample was collected in addition to a runoff sample in the middle of the precipitation event. Analysis of these samples revealed higher SRP concentrations in the first few minutes of precipitation for some events (Appendix C Figure C-2). Runoff grab samples collected mid-event were considered to be representative of the precipitation event for consistency and as the first flush effect is minor when the entire precipitation event is considered. Ponded water was also collected from the surface of both bioretention systems during all sampled precipitation events with this sample thought to represent a time-integrated influent sample over the event. SRP concentrations were similar between pond water samples from the Centre and East systems (Appendix C Figure C-2), and therefore influent data for the Center system was assumed to be representative of the runoff infiltrating the nearby East system. While slight differences in concentrations exist between road runoff and ponded surface water ((Appendix C Figure C-2), the overall study findings are the same regardless of whether road runoff or ponded surface water samples are used to represent the influent concentrations. As the ponded surface water has interacted with the soil and vegetation of the bioretention system, the road runoff samples rather than pond water samples were used in all influent-effluent comparisons as the pond water does not capture the performance of bioretention systems when directly compared with traditional stormwater management facilities.

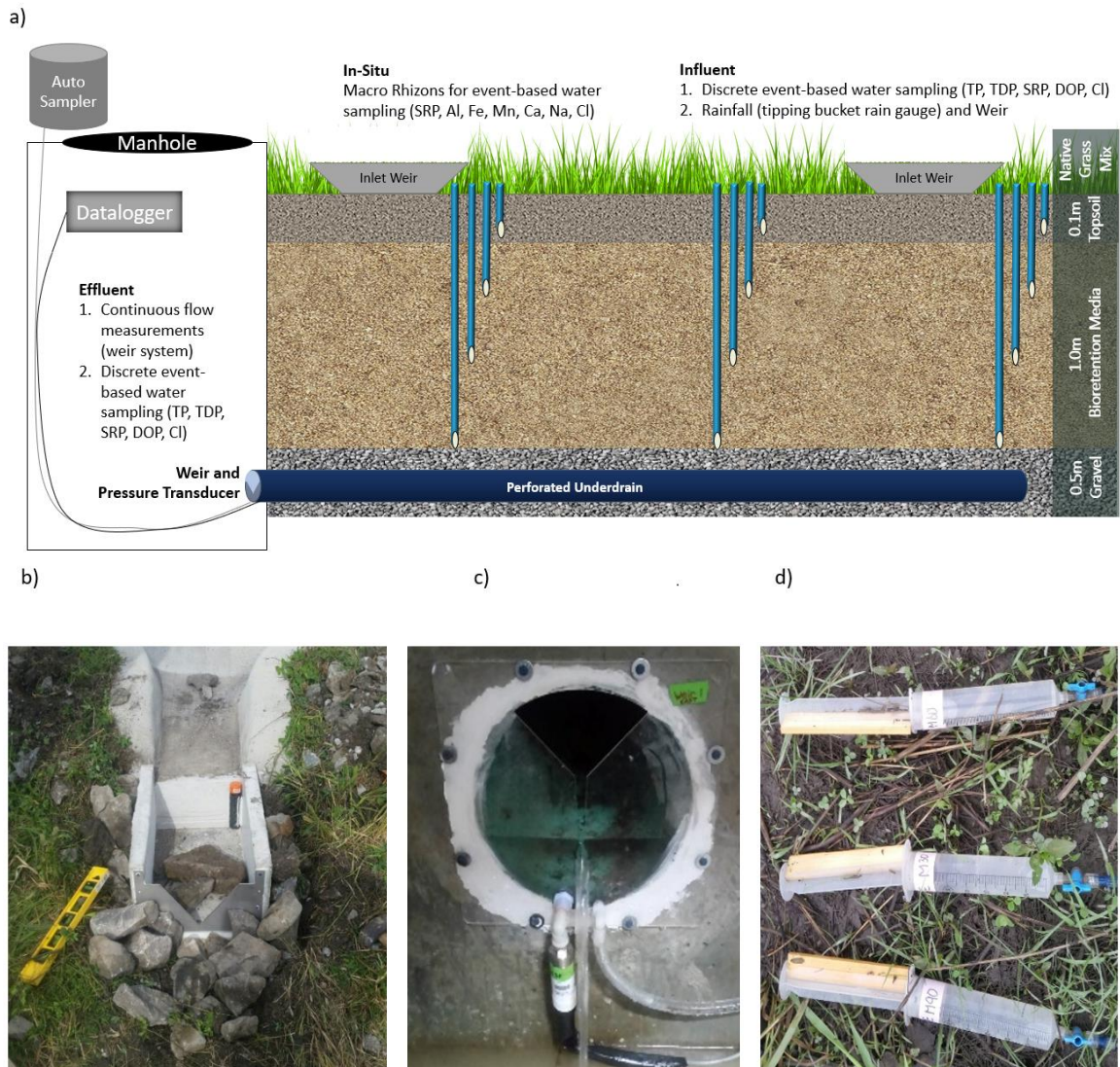


Figure 3-1: (a) Monitoring equipment layout in the bioretention systems, (b) influent V-notch weir (c) compound effluent weir with pressure transducer and sampling port (d) installed MacroRhizon samplers collecting porewater during precipitation events.

Effluent samples were collected from a sampling port located where the underdrain entered the monitoring chamber (Figure 3-1c) using an ISCO 6700 automatic sampler. Effluent samples were collected while drainage was occurring. During select precipitation events, multiple samples were collected through the drainage period (1-hour intervals) to evaluate temporal variability in the effluent water quality. This sampling

data showed that the effluent concentration was relatively stable over a drainage event and therefore a single sample collected mid-drainage was assumed to be representative of the effluent for the duration of the precipitation event (Appendix C Figure C-3).

In addition to influent-effluent sampling, porewater samples were collected from the East and Center systems during six precipitation events from March 2019 to October 2019. Three vertical arrays of MacroRhizon porewater samplers (0.15 μm ceramic screen) were installed in each bioretention system with the arrays located near the upstream and downstream inlets, and in the middle of the systems (Figure 3-1). The samplers were installed at 45-degree angles with the ports located at 0.05 m (topsoil), 0.21 m, 0.42 m, and 0.64 m depth below the ground surface. In the Centre systems, additional porewater samplers were installed vertically to 1.0 m at each profile location. Samples were collected from the MacroRhizons using 60 mL syringes and retainers that were used to apply a vacuum pressure at the beginning of each precipitation event. The vacuum pressure was applied to the porewater samplers for approximately 6 hours or overnight, until sufficient water volume was drawn into the syringes.

All samples (influent, effluent, pore water) were collected in 60 mL acid-washed HDPE sample bottles. For influent and effluent samples, one unfiltered sample (for TP analysis) and two filtered samples (all other analytes) were collected with 0.45 μm cellulose acetate membrane filters used on-site. For porewater samples, only filtered samples were collected as the samples were already filtered through the MacroRhizon 0.15 μm ceramic tips. All samples were transported back to the laboratory within two hours of collection with samples for SRP analysis refrigerated and run within 48 hours of collection, and all other samples frozen until analysis.

TP and TDP were measured on unfiltered and filtered samples, respectively, using HACH Total Phosphorus UV-Vis Method 8190 (US EPA accepted standard method 4500-P E). SRP was analyzed with LaChat QuikChem 8500 Flow Injection Analysis Machine (FIA) method 10-115-01-1-M and diluted to within the 1-100 μg P/L calibration range as needed. Quality control checks were completed with duplicates run every six to nine samples. The sample duplicates and quality control checks had high accuracy with

differences usually <2%, to a maximum of 10% difference. DOP was calculated as the difference between TDP and SRP ($DOP = TDP - SRP$). TP, TDP, and DOP concentrations are provided in mg P/L while SRP concentrations are provided in $\mu\text{g P/L}$ to the higher analytical precision of the FIA analysis ($\pm 0.005 \text{ mg/L}$). Chloride concentrations were analyzed using high-performance liquid chromatography (HPLC: Waters 432 w/ 717 plus autosampler). Porewater samples were analyzed for Al, Ca, Fe, Mn, and Na using Vista-PRO CCD Simultaneous ICP OES by Varian. Further details of the analytical methods including the QA/QC and sample storage conditions are provided in Appendix B, Table B-1.

3.2.1.3 Water Quantity Measurements

The influent and effluent water volumes were measured for the East system from November 2018 to January 2020. The total volume of stormwater influent entering the bioretention system for individual precipitation events was estimated using the measured precipitation depth, catchment area, and runoff coefficient values. Precipitation data (5-minute interval) was acquired from a City of London weather station located 4 km away from the field site. This precipitation data was validated using a Texas Electronics tipping-bucket rain gauge (model TR-525M) and a Weather Measure WEATHERtronics tipping-bucket rain gauge (model 6011-B) installed on the roof of the Claudette MacKay-Lassonde Pavilion at Western University, located 4.5 km away from the field site. For data analysis, a precipitation event was defined as precipitation that resulted in more than one bucket tip in an hour followed by six consecutive hours of no tips (Sims, et al., 2016). This definition ensured residual water in the rain gauge was not defined as a precipitation event, while also providing sensitivity to the timing of precipitation events. The runoff coefficient varies between events based on the rainfall intensity, antecedent conditions, temperature, and changes in catchment area characteristics (e.g., sediment build-up, vegetation growth). As such, to calculate the influent volumes to the bioretention system from the catchment area (55% impervious), a range in the runoff coefficient was used with 35 - 75% of water volume from medium and large storm events (> 5 mm) considered to enter the bioretention systems. This range was based on SCS Curve Number calculations (G  h  niau et al., 2015; United States Department of

Agriculture, 1986), the Ontario Stormwater Management Planning and Design Manual (Ontario Ministry of the Environment, 2003), and field influent measurements performed for select events in late 2019 - early 2020. Field influent measurements were performed using concrete weir boxes installed in the inlet curb cuts of the East system (Figure 3-1b). These weir boxes used a 75 degree V-notch weir plate designed to measure up to the maximum two-year design flow of 10 L/s from the 0.8 m curb openings (AECOM, 2016). Self-logging pressure transducers (Van Essen CTD Divers) were installed in the base of the weir boxes to measure pressure every five minutes during precipitation events. As expected, the relationship between precipitation depth and influent volumes was highly variable between monitored precipitation events. Therefore, the influent weirs were used to support a range for the runoff coefficient used with inflow calculations based on rainfall data.

To measure the effluent rate and volumes, a two-stage compound v-notch weir was installed directly onto the end of the underdrain pipe for the East system as it entered the monitoring chamber (Figure 3-1c). The weir plate was designed for a maximum flow rate of 1.7 L/s (see Appendix A, Figure A-3 for design details). Pressure was continuously measured (1 minute-interval) using a 2.0 psi FPG Honeywell differential pressure transducer fixed to the weir plate below the lower v-notch and connected to a CR10x Campbell Scientific data logger. The weir plate was tested and calibrated in the laboratory before field installation in June 2018. Field calibration was completed during the 27 August 2019 precipitation event and applied to all recorded field data along with a $\pm 5\%$ allowance for error based on calibration results. Effluent rates and volume data is unavailable from March 5-20, 2019 due to a data logger failure. The water balance was not calculated for the Centre system as a construction issue resulted in a portion of the effluent to exit the bioretention system via a crack in the monitoring chamber wall and thereby bypass the monitored underdrain.

3.2.1.4 Data Analysis

The percentage volume reduction, also referred to as the hydraulic retention efficiency, was calculated for each precipitation event using the influent and effluent volumes measured for the East bioretention system (Géhéniau et al., 2015; Khan et al., 2012b):

$$\text{Percentage volume reduction} = \frac{V_{in}-V_{out}}{V_{in}} * 100 \quad (1)$$

where V_{in} is the total influent volume (L), and V_{out} is the total effluent (underdrain) water volume (L) over one event.

The mass of TP, TDP, SRP, and DOP in the influent and effluent of the bioretention system for each event was calculated by multiplying the concentrations by the total influent and effluent water volumes measured during the precipitation event or drainage period.

$$\text{Mass Load} = C \times \sum Q \times \Delta t \quad (2)$$

where C is the representative concentration of TP, TDP, SRP, or DOP in the influent or effluent for the event ($\mu\text{g P/L}$), Q is the measured influent or effluent rate at each time step (L/s), and Δt is the interval between flow rate measurements (60 seconds). The release or retention of the different forms of P was calculated as the difference in the influent and effluent mass loads for each event. For monitored precipitation events that were completely captured by the bioretention system (i.e. no drainage) the mass release from the system was zero mg P. The mass load calculations include the uncertainty in measured influent and effluent volumes (35 - 75% of water volume and 5 % error allowance, respectively). Although this results in uncertainty in the magnitude of the annual mass loads, the overall study findings with respect to P retention-release from the bioretention systems remains the same.

For seasonal analysis, seasons were defined on the solstice/equinox basis (Passeport et al., 2009). This definition enables comparison with other studies and provides a consistent definition regardless of location. As such, our data was divided into Fall 2018

(September 23 to December 20, 2018), Winter (December 21, 2018 to March 19, 2019), Spring (March 20 to June 20, 2019), Summer (June 21 to September 22, 2019) and Fall 2019 (September 23 to December 20, 2019) for seasonal analysis.

For statistical analyses, the Shapiro-Wilk test was first performed on all datasets to determine if they were normally distributed. The Kruskal-Wallis H test was used to test whether there were statistical differences between any seasons in the concentrations and mass retentions of the different forms of P. As the Kruskal-Wallis H-test does not identify which seasons were statistically different, the Mann-Whitney U test was performed for all mass retentions and concentrations for all P forms and across the different seasons in pairs using a two-sided level of significance of 0.05. Correlations between different elements (Fe, Mn, Al, Ca, Cl, Na) and SRP concentrations in the porewater with data separated into seasons were analyzed using the Spearman rank correlation test with a p-value of 0.05 for significance. The relationship between P retention and rainfall depth was also evaluated using the Spearman rank correlation test (p-value of 0.05 for significance).

3.2.2 Laboratory column experiments

Based on the observed seasonal trends in P retention-release from the field bioretention systems, columns experiments were conducted to examine the influence of high de-icing salt (NaCl) loading on P retention-release from the bioretention media in a controlled environment. The columns (length = 0.3 m, diameter = 0.05 m) were constructed from plexiglass following best practice design recommendations (Figure 3-2) (Gibert et al., 2014). Bioretention media collected during the construction of the field bioretention systems was dry packed into the two columns. Two columns experiments were run simultaneously with different influent solutions: stormwater runoff (control column), and stormwater runoff spiked with 1.2 g/L of NaCl (salt column).

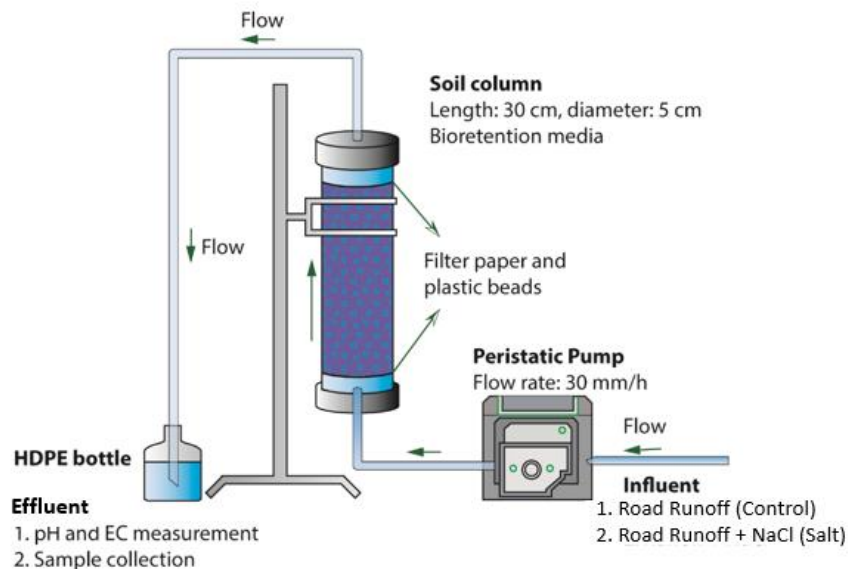


Figure 3-2: Set up for column experiments conducted to evaluate effect of high de-icing salt loading on P retention-release from the bioretention media.

Two successive wet-dry cycles were simulated in the column experiments to also examine the effect of periodic wetting-drying on P retention and release from the media. During the wet periods, influent solution was pumped bottom up through each column at the field design infiltration rate (30 mm/hr) with saturated flow maintained in the column. All column experiments were run at room temperature (22°C) eliminating the effects of other cold climate factors such as temperature and freeze-thaw cycles. The influent stormwater runoff was collected from the curb cut inlets of the field bioretention systems during precipitation events on 20 October and 27 October 2018. The runoff was stored for a maximum of 60 days in a temperature-controlled cold room (4°C). The first wet period during which there was a continuous upwards flow through the column lasted 25 days at which time electrical conductivity (EC) and TP concentrations in column effluent had reached a steady state. At this stage, the pump was switched off and the columns were allowed to drain under the influence of gravity until the soil media reached field capacity (termed dry period). Once drainage from the columns had ceased (approximately 3 days), a second wet period (23 days long) was simulated following the same procedure as the first wet period.

Discrete samples of column influent and effluent were collected at two-hour intervals at the beginning of each wet period with the sampling interval decreasing to every second day by the end of the wet period. Water samples were analyzed immediately for EC and pH using a HACH HQ40D portable multi meter and Intellical™ CDC401 and PHC201 probes for EC and pH measurements, respectively. The remaining sample volume was collected in two 60 mL HDPE bottles (one unfiltered and one filtered using 0.45 µm cellulose acetate filters). Filtered samples were refrigerated and analyzed within 48 hours for SRP (for wet period 2 only), and unfiltered samples were frozen until TP analysis. The TP and SRP analytical methods used are the same as those used for the field samples.

The cumulative mass of TP and SRP released during each wet period was compared between the salt column and control column. The cumulative mass of TP and SRP released from the column over time was calculated by summing the mass released between each sampling time period (M µg) as:

$$M = (C_{effluent} - C_{influent}) \times Q \times \Delta t \quad (3)$$

where $C_{effluent}$ is the effluent concentration (µg/L), $C_{influent}$ is the influent concentration (µg/L), Q is the flow rate (1.44 L/day), and Δt is the interval between samples (days).

3.3 Results and Discussion

3.3.1 Seasonal performance of field-scale bioretention systems

3.3.1.1 Hydraulic retention efficiency

In evaluating the performance of the bioretention systems in reducing P loads, the hydraulic retention efficiency of the systems first was evaluated first as this efficiency, together with changes in the influent-effluent P concentrations, determines the P mass load reductions. Over the monitoring period from November 2018 – January 2020 (excluding 5 - 20 March 2019 when there was a datalogger failure) there were 124 precipitation events at the field site. For 56% of these events the influent volume was completely retained (i.e., no drainage through underdrain) in the East bioretention system. The percent volume reduction was highly variable for the remaining precipitation events that had drainage (Figure 3-3). Considering all events over the monitoring period, including those with complete volume retention, the mean volume reduction was $73 \pm 28\%$. The reported standard deviations represent the variability between events as well as uncertainty associated with the influent and effluent volume calculations (based on the road runoff coefficient and sensitivity of effluent weir calibrations). The high variability in the percentage volume reduction is expected as the volume reduction for each event depends on several environmental factors including the precipitation volume and intensity (Stewart et al., 2017), antecedent conditions (Davis, 2008), infiltration rates including the formation of preferential flow paths (Carpenter and Hallam, 2010), and seepage into the surrounding native soil (Winston et al., 2016). Overall, the percentage volume reduction was larger for smaller precipitation events compared with larger events, with all events greater than 14.5 mm depth producing some drainage (see Appendix C Figure C-1). It is important to note that the percent volume reduction was negative for some events (n=11). Some of these events had large precipitation volumes, which may have resulted in an underestimation of the inflow volumes due to increased overland flow and the smaller impact of initial abstractions. Events in winter may have had additional snow and ice melt that wasn't captured by the inflow calculations. Other events started shortly after another event but greater than 6 hours after such that it was defined an

individual event. For these events, the higher effluent relative to influent was likely due to temporary water storage in the system at the start of the second event with this excess water draining during the event (Sims et al., 2019).

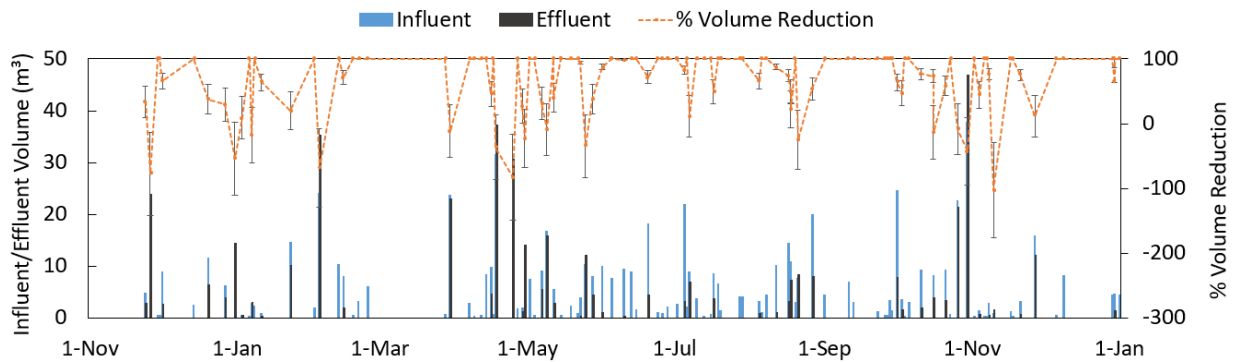


Figure 3-3: Event influent and effluent water volumes and calculated percentage volume reductions for the East bioretention system from November 2018 to January 2020.

The percentage volume reduction for individual events can also be influenced by seasonal factors. For instance, lower temperatures and decreased evapotranspiration in winter (Muthanna et al., 2008) as well as larger and more frequent precipitation events in spring have been shown to lead to lower volume reduction (Khan et al., 2012b) in these seasons compared to summer. For our study, although the percentages of volume reduction between seasons were not statistically significant due to high variability between individual events within each season (Kruskal-Wallis test, $H=3.80$, $p>0.25$), the percentage volume reduction was generally higher and less variable in summer (mean = $85 \pm 25\%$, $n = 33$) compared to the other seasons (Fall 2019 = $71 \pm 29\%$, $n = 28$; Spring 2019 = $71 \pm 28\%$, $n = 31$; Fall 2018 = $58 \pm 31\%$, $n = 7$, and Winter 2019 = $56 \pm 29\%$, $n = 17$). Importantly, of the fifteen events that had volume reductions less than 40% (excluding winter), six of these events occurred in spring, indicating lower volume reductions during this season. Finally, it is important to note that while the hydraulic performance of the bioretention systems varied seasonally through our monitoring period, these seasonal trends may change between years. For example, summer 2019 was dominated by intense thunderstorm systems which may result in different hydraulic

performance of the systems compared to wet summers with more frequent and less intense precipitation.

3.3.1.2 Influent and Effluent Concentrations

The influent and effluent concentrations of TP, TDP, SRP and DOP varied considerably between the 24 events sampled from November 2018 to October 2019. For the East bioretention system, for which the influent-effluent TP concentrations were measured for all 24 events, the mean TP concentrations in the influent (mean 0.24 ± 0.21 mg P/L) were similar to the effluent TP concentrations (mean 0.21 ± 0.14 mg P/L). The maximum influent and effluent TP concentrations were observed on 13 June 2019 (0.48 mg P/L) and 30 March 2019 (0.42 mg P/L), respectively (Figure 3-4b). Mann-Whitney U tests indicate that the effluent TP concentrations were statistically different ($U \leq 0.05$) in Spring 2019 (mean 0.23 ± 0.08 mg P/L) compared to Winter 2018 ($U=0.04$; mean 0.15 ± 0.06 mg P/L) and Summer 2019 ($U=0.01$; mean 0.15 ± 0.06 mg P/L). The reported standard deviations for concentrations indicate the variability between individual events. There was no significant difference in the effluent TP concentrations between the other seasons. In winter, the influent TP concentrations (mean 0.25 ± 0.06 mg P/L) were greater than the effluent TP concentrations (mean 0.15 ± 0.06 mg P/L). However, for the remainder of the monitoring period, effluent TP concentrations were consistently greater than the TP influent concentrations with the exception of three events. For example, in spring and summer, the mean influent TP concentrations were 0.19 ± 0.12 mg P/L and 0.11 ± 0.04 mg P/L, respectively, while the mean effluent TP concentrations were 0.23 ± 0.08 mg P/L and 0.15 ± 0.02 mg P/L, respectively. While the effluent TP concentrations for the Center bioretention system varied slightly compared with the East system, the overall seasonal trends were similar with high TP concentrations observed in the effluent of the Center bioretention system during spring (Figure 3-4). Although there is no single Canadian guideline value for P concentrations in freshwaters, TP concentrations of 0.02-0.1 mg P/L can trigger adverse ecosystem responses in meso-to hyper-eutrophic surface waters (Canadian Council of Ministers of the Environment, 2004). While the bioretention systems can be considered a very small point source, and therefore not comparable to this guideline, the effluent P concentrations from the East and Center bioretention systems

were consistently above this concentration range and may be a concern for sensitive water bodies immediately downstream of the systems.

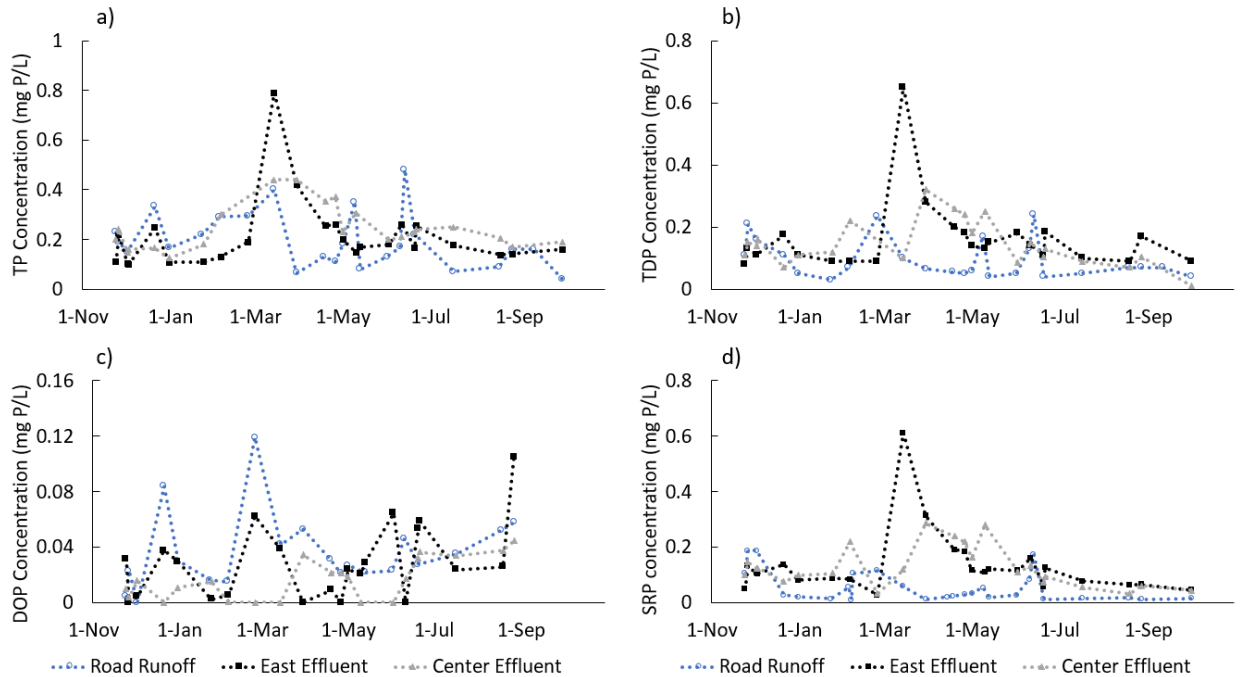


Figure 3-4: Influent and effluent concentrations for (a) TP, (b) TDP, (c) DOP, (d) SRP for the East and Center bioretention systems from November 2018 to October 2019.

A comparison of TP and TDP concentrations shows that approximately half of the TP in the influent was in particulate form ($46 \pm 28\%$) with this fraction being lower in the effluent ($23 \pm 18\%$). Consistent with prior studies, this high particulate P retention in the bioretention system is caused by physical filtration and sedimentation (Li & Davis, 2016; Liu & Davis, 2014). Considering all sampled events, influent TDP concentrations were on average lower (0.09 ± 0.06 mg P/L) relative to the effluent TDP concentrations (0.14 ± 0.05 mg P/L). Seasonal effluent TDP concentrations were statistically different (Mann-Whitney test with $U \leq 0.05$) in Spring 2019 (mean 0.18 ± 0.04 mg P/L) compared to Fall 2018 ($U=0.02$, mean 0.11 ± 0.02 mg P/L), Winter 2018 ($U=0.03$, mean 0.12 ± 0.03 mg P/L) and Summer 2019 ($U=0.03$, mean 0.11 ± 0.03 mg P/L). Comparing all other seasons (pairwise), the TDP concentrations were not significantly different. Importantly,

it can be seen in Figure 3-4b that the effluent TDP concentrations do not vary in direct response to changes in the influent TDP concentrations. This indicates that internal processes within the bioretention system are governing the TDP effluent concentrations, including the high effluent TDP concentrations observed for some individual events (e.g., 0.65 mg P/L for event on 14 March 2019). As with TP, the seasonal trend in higher spring TDP concentrations was also observed in the Center bioretention system (Figure 3-4b).

TDP includes both SRP and DOP. In comparing Figure 3-4c and d, it can be seen that the increase in TDP concentrations between the influent and effluent was predominately due to an increase in SRP between the influent and effluent rather than an increase in DOP. Considering all sampled events, effluent SRP concentrations for the East (mean 112 ± 61 $\mu\text{g P/L}$) and Centre (mean 119 ± 65 $\mu\text{g P/L}$) bioretention systems were larger compared to the mean SRP influent concentration (50 ± 55 $\mu\text{g P/L}$). Similar to TDP, temporal variability in the effluent SRP concentrations (ranging from 28 to 612 $\mu\text{g P/L}$ and 32 to 286 $\mu\text{g P/L}$ for East and Centre systems, respectively) were not driven by changes in the influent SRP concentrations (varied from 12 $\mu\text{g P/L}$ to 187 $\mu\text{g P/L}$; Figure 3-4d), indicating the importance of internal processes in governing the effluent SRP concentrations. Seasonal effluent SRP concentrations in the East system were only statistically different (Mann-Whitney test with $U \leq 0.05$) in Summer 2019 (mean 68 ± 5 $\mu\text{g P/L}$) relative to Winter 2018 ($U=0.02$, mean 98 ± 23 $\mu\text{g P/L}$) and Spring 2019 ($U=0.03$, mean 152 ± 69 $\mu\text{g P/L}$). Although the greatest SRP effluent concentrations occurred in spring, the limited number of samples collected in other seasons reduce the statistical significance of seasonal differences. However, analysis of seasonal means with standard deviations provide insight into the observed seasonal trends. The effluent SRP concentrations for both the East and Centre systems were highest in spring (Spring 2019 mean 152 ± 69 $\mu\text{g P/L}$ for East and 188 ± 56 $\mu\text{g P/L}$ for Centre) with effluent concentrations observed in early spring an order of magnitude higher than the influent concentrations (spring mean 44 ± 454 $\mu\text{g P/L}$). The effluent SRP concentrations gradually decreased over the summer for both systems with the influent and effluent concentrations comparable by Fall 2019 (Figure 3-4d). Although the effluent SRP

concentrations for the East and Center systems differed, the increase of SRP effluent concentrations in spring was similar. With SRP accounting for $80 \pm 22\%$ of TDP in the effluent, and PP in the effluent being low, the data highlight the importance of reducing SRP effluent concentrations to meet the Canadian TP guideline (0.02 - 0.1 mg P/L) for meso-to hyper-eutrophic surface waters (Canadian Council of Ministers of the Environment, 2004).

DOP concentrations ranged from below detection to 0.12 mg P/L in the influent and from below detection to 0.13 mg P/L in the effluent for the East bioretention system for the sampled events. Considering all sampled events, on average $50 \pm 25\%$ of the TDP in the influent was DOP, whereas on average only $22 \pm 20\%$ of TDP in the effluent was DOP. The observed larger fraction of effluent TDP as SRP relative to DOP, and similar fractions in the influent was also observed by Liu and Davis (2014). There was no statistical difference (Mann-Whitney statistical test with critical U-value ≤ 0.05) in DOP concentrations between the seasons for the influent and effluent concentrations. Importantly, low DOP in both influent (seasonal mean 0.04 ± 0.03 mg/L) and effluent (seasonal mean 0.03 ± 0.04 mg/L) during spring indicate that the high SRP effluent concentrations compared to the influent concentrations in spring is not simply due to transformation of influent DOP to effluent SRP. Rather, the high SRP effluent concentrations in spring come from internal P storage within the bioretention system.

3.3.1.3 P Influent and Effluent Mass Loads

The cumulative influent and effluent TP, TDP, SRP, and DOP mass loads over the monitoring period for the East bioretention system are shown in Figure 3-5. Considering all sampled events, the cumulative TP mass that entered the bioretention system (56 ± 20 g P) was similar to the cumulative TP mass in the effluent (53 ± 3 g P). The cumulative TDP and SRP influent masses were considerably lower (26 ± 10 g P and 14 ± 5 g P, respectively) than in the effluent (39 ± 2 g P and 35 ± 2 g P, respectively), indicating an overall release of TDP and SRP from the bioretention system considering all sampled events. In contrast, there was higher cumulative DOP mass in the influent (8 ± 5 g P) compared to the effluent (4 ± 0.2 g P). The total net retention or release of the different

forms of P (calculated as difference between the cumulative influent and effluent loads for all sampled events, where negative retention represents P release from the bioretention system) indicates that, as shown with the concentration data, SRP (total net release 21 ± 5.4 g P) is predominately responsible for the TDP net release from the bioretention system (total net release 12 ± 10 g P) rather than DOP (total net retention 4 ± 5 g P). The greatest masses of TP, TDP, DOP, and SRP released during an individual event were 8 ± 1 g P, 6 ± 1 g P, 0.3 ± 0.2 g P, and 7 ± 0.4 g P, respectively, highlighting the important contribution of individual large events to the overall net annual performance of the systems with respect to P retention. In contrast, the greatest TP, TDP, DOP, and SRP mass retained during an individual event were 4 ± 2 g P, 2 ± 1 g P, 0.9 ± 0.7 g P, 1.5 ± 0.6 g P, respectively (Appendix C Figure C-4).

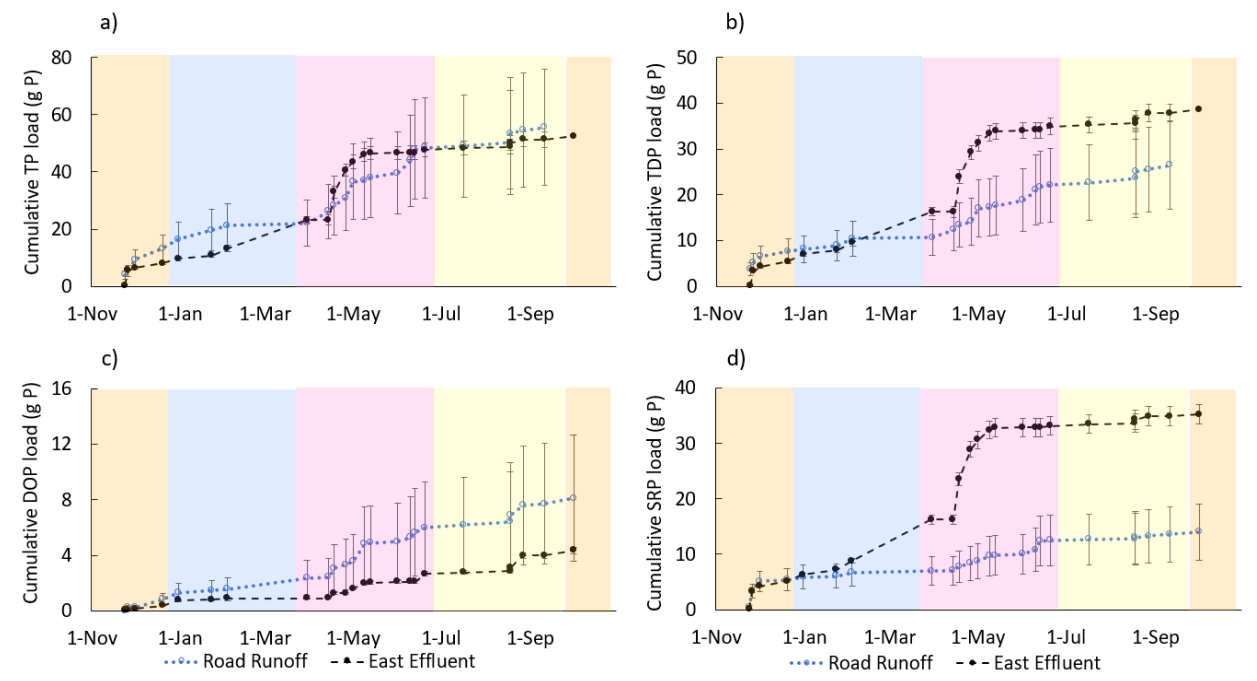


Figure 3-5: Cumulative mass of (a) TP, (b) TDP, (c) DOP, and (d) SRP in the influent and effluent for the East bioretention system from November 2018 to October 2019. The orange, blue, pink and yellow shaded regions represents Fall, Winter, Spring and Summer seasons, respectively, and the error bars represent the uncertainty in the influent and effluent water volume calculations.

The most notable feature in the cumulative TP, TDP, and SRP loads over the monitoring period is the large increase in effluent loads relative to influent loads in mid-spring compared to the remainder of the monitoring period (Figure 3-5; Spring is indicated by pink shading). Unlike the effluent loads, the cumulative influent loads do not rapidly increase in spring indicating that the source of high TP, TDP and SRP mass in the effluent is internal P stores within the bioretention system. Considering the net cumulative retention-release for each season and despite the high reported uncertainty, the net release of TP, TDP and SRP was greater in spring (6 ± 4 g P, 12 ± 2 g P, and 18.5 ± 1.0 g P, respectively) than in all other seasons. Furthermore, net retention was observed during at least one season during the monitoring period for each form of P, except for DOP which was the only P fraction for which there was net P mass retention in the bioretention system during all seasons. It is important to note that previous field studies completed in cold climates generally only focus on the differences observed between winter and summer. Our results clearly show high TP, TDP and SRP release in spring – this has previously not been shown using winter-summer seasonal classifications or in the monitoring conducted in prior studies.

While more samples were collected during spring compared to the other seasons, individual precipitation events contribute to the greater mass release during this season compared with the other seasons. For example, there was more SRP mass in the effluent on 30 March 2019 (7.4 ± 0.4 g P) than in the effluent for all precipitation events in summer and fall combined (2.1 ± 0.05 g P). This indicates that seasonal factors affecting the retention-release of TP, TDP, and SRP may have a greater impact on the overall performance of bioretention systems than factors that remain constant through the year. Finally, the cumulative effluent DOP loads increase in direct response to the influent DOP loads, suggests DOP retention-release behavior is less sensitive to seasonal variability compared to SRP.

Mann-Whitney U statistical tests were performed to test the difference (pairwise) in mass retention for each of the P forms between each season. In part due to the high variability

in P retention between individual events within each season, combined with the low number of sampled events for some seasons (Fall 2018: n=4, Winter 2019: n=4, Fall 2019: n=1), the TP, TDP, SRP and DOP mass retention in spring was not significantly different compared to the other seasons despite the sharp inflection in the cumulative effluent masses in spring for TP, TDP and SRP ($U > 0.05$; Appendix D Table D5).

Finally, note that this data analysis is limited in that only 24 precipitation events out of the total 124 events that occurred over the monitoring period were sampled. This means that the annual cumulative influent and effluent mass loads may be higher than those calculated. However, comparison of the sampled events with all events that occurred over the monitoring period indicates that the events sampled were well distributed with respect to seasonality, event size and intensity (Appendix A Figure A-5). In addition, many of the unsampled precipitation events were small events (< 5 mm) that did not result in drainage through the bioretention system and, therefore, had 100% P retention. Not including these events in the calculations may have resulted in an underestimation in the cumulative net retention of the different forms of P. However, it is possible that larger precipitation events that were not sampled due to the unpredictability of severe thunderstorms may have released more P than what was retained by these smaller events. When the cumulative seasonal net retention-release is normalized to the number of rain events sampled during each season, greater TP, TDP, SRP, and DOP release per event occurs in spring compared to all other seasons (Appendix C Table C-1).

3.3.1.4 Porewater concentrations

Porewater samples were collected from both the Center and East bioretention systems during four precipitation events over the monitoring period to provide insight into the biogeochemical processes that may contribute to the mobilization of SRP within the systems and how these processes may vary seasonally. The porewater analysis focuses on SRP rather than the other forms of P as the influent-effluent results shown above suggest that SRP is the main form of P released from the bioretention systems in comparison to DOP or PP. Porewater samples collected during the precipitation event on 30 March 2019 represent spring conditions (coinciding with the period of high SRP release), while data

for 10 June, 20 August, and 2 October 2019 represent late spring, summer, and fall, respectively (Figure 3-6). For all events, samples were analyzed for SRP and constituents known to be associated with SRP retention and release including Fe, Al, Mn, and Ca (Lucas and Greenway, 2011; Marvin et al., 2020; Mullins et al., 2020). High dissolved Fe, Al, and Mn concentrations often co-exist with high dissolved SRP concentrations because SRP adsorption to Fe-, Al-, and Mn-oxide mineral surfaces is an important SRP retention mechanism, and dissolution of these metal oxides causes release of these metal ions and SRP to porewater (Liu and Davis, 2014; Marvin et al., 2020; Yan et al., 2016). Dissolution of these metal oxide minerals is often triggered by the onset of reducing condition or pH changes. Alternatively, in the absence of metal oxide dissolution, SRP can also desorb from these mineral surfaces in response to pH changes or competitive sorption processes resulting in high porewater SRP concentrations (Parsons et al., 2017). The availability of dissolved Ca can also affect SRP retention due to co-precipitation of SRP with Ca compounds such as calcite (Li & Davis, 2016; Marvin et al., 2020).

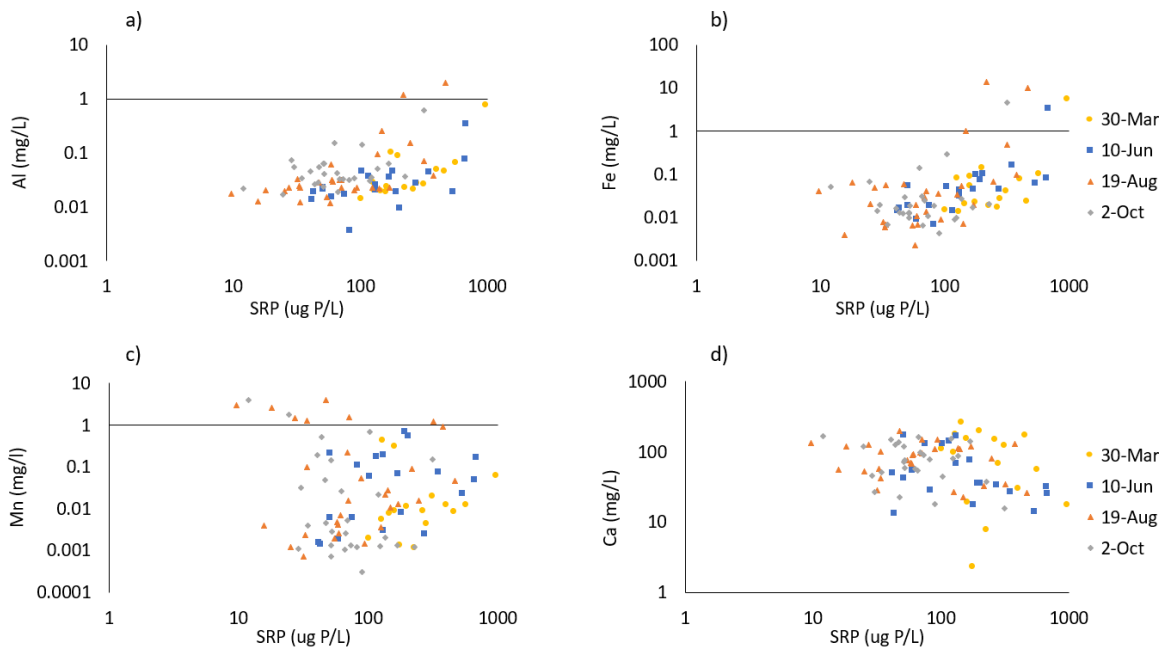


Figure 3-6: Correlation between porewater (a) Al and SRP, (b) Fe and SRP, (c) Mn and SRP, and (d) Ca and SRP for four precipitation events over the monitoring period in the East and Center bioretention systems.

The SRP porewater concentrations were significantly different between the different seasons (Kruskal-Wallis test; $H=29.5$, $p<0.05$). Consistent with the effluent SRP concentrations, the mean porewater SRP concentrations during the precipitation event on 30 March (early spring) were highest ($292 \pm 216 \mu\text{g P/L}$) with concentrations decreasing over late spring ($207 \pm 195 \mu\text{g P/L}$), into summer ($110 \pm 110 \mu\text{g P/L}$), and fall ($82 \pm 65 \mu\text{g P/L}$). Considering individual events, there was a strong significant correlation between Fe and SRP during late spring (10 June, Spearman rank correlation, $\rho=0.770$, $p=0.0001$), while the correlation between Fe and SRP is significant and moderate in summer (19 August, $\rho=0.470$, $p=0.007$) and not significant for other seasons (Appendix E Tables E-1, E-2). Significant positive correlations were also observed between Al and SRP in early spring ($\rho=0.641$, $p=0.007$), late spring ($\rho=0.513$, $p=0.021$), and summer ($\rho=0.628$, $p=0.0002$), with an insignificant correlation in fall ($\rho=0.251$, $p=0.207$). The significant positive correlations between Al, Fe, and SRP indicate that Al- and Fe- dissolution may have an important effect on SRP release in the early spring, late spring, and summer which could be influenced by changing redox and pH conditions (Li & Davis, 2016; Wang, Zhang, Li, & Morrison, 2013). For all events, Mn and SRP were not significantly correlated ($\rho<0.385$, $p>0.06$). It is possible this is due to lower abundance of Mn in the bioretention media compared with Al and Fe. Further, it is important to note while the porewater Al concentrations were significantly different between the individual sampling events ($H=9.01$, $p<0.05$), there is no statistical difference between the concentrations of Fe and Mn in the porewater between the individual events (Kruskal-Wallis test, $H= 7.24$, $p<0.1$ and $H=5.740$, $P<0.25$ for Fe and Mn, respectively). These results suggest that while dissolution of Al- and Fe- oxides may contribute to SRP release in the bioretention systems, these processes alone do not explain the greater SRP release in spring compared to the other seasons (Géhéniau et al., 2015; Muthanna et al., 2007; Paus et al., 2015).

Finally, there is no statistical difference in porewater Ca concentrations between different seasons (Kruskal-Wallis test, $H=4.200$, $p>0.1$). There is also no significant correlation between porewater Ca and SRP considering the individual events separately ($-0.43<\rho<-0.12$, $p>0.06$; Spearman rank correlation). However, the porewater Ca concentrations (2.3 to 197 mg Ca/L) are considerably higher than the SRP concentrations (10 to 3032 $\mu\text{g P}$

/L), which makes it challenging to observe the effects of P and Ca co-precipitation using porewater data alone since significant changes in SRP concentration in μg may not result in detectable changes in Ca concentrations in mg.

3.3.2 Potential factors governing seasonal variability in P retention and release

The results presented above indicate seasonal variation in the performance of the bioretention systems to retain P, with high P release occurring in spring, mostly in the form of SRP. In Southern Ontario, similar to many inland areas worldwide, high release of SRP is of particular concern as this is the bioavailable form of P that stimulates plant including algal growth. Furthermore, the field site is located in the Lake Erie Basin where high P loads to Lake Erie in spring are thought to be the key trigger for summer eutrophication and harmful algal blooms. To put into context the magnitude of the P loads released from the sampled bioretention systems, area mass loads from agriculture, which is often considered to be the highest non-point source of P loads to surface waters, are estimated to range from 0.03 to 0.05 kg P/ha/year for SRP, and between 0.23 and 0.31 kg P/ha/year for TP (Irvine et al., 2019). For our study the net equivalent areal SRP mass released (considering the bioretention system catchment area) was 0.15 ± 0.04 kg P/ha/year, and the net TP mass retained was 0.02 ± 0.1 kg P/ha/year. While there is much greater land area dedicated to agriculture compared to urban roadways, the SRP mass release from the bioretention system, which occurred predominately in spring, is a potential concern for downstream freshwater bodies that are sensitive to eutrophication.

Various factors may contribute to seasonal variability in the retention and release of P, and its different forms, in bioretention systems. Previous studies have shown that bioretention systems can have increased P release in winter due to frozen media and freeze-thaw processes (Ding et al., 2019), reduced biological activity due to lower temperatures (Blecken et al., 2007; Khan et al., 2012b), and limited hydraulic (infiltration) function (Roseen, 2009). Although not studied in field bioretention systems with respect to the behaviour of P and its different forms, cation exchange processes from high winter salt loadings are also known to mobilize metals in the subsurface (Mullins et

al., 2020), which can indirectly affect P mobility. P retention-release is also sensitive to redox and pH conditions which may vary seasonally due to biological processes including organic matter decomposition. Similar to our study, seasonal release of TP in spring was also observed in a field study in Montreal, Canada where effluent TP concentrations were greatest in May compared to the remainder of the year (Géhéniau et al., 2015). However, this study did not examine the different forms of P, nor the potential factors contributing to the seasonal variability in TP release. As mentioned above, in other bioretention studies, seasonal variability is often examined by classifying data as summer or winter without separating spring data. Roseen (2009) observed slightly higher TP removal efficiencies in summer (May to October) compared to winter (November to April) for their field scale systems installed in New Hampshire but concluded decreased P removal in winter should not be a concern. More recently, a large-scale lysimeter study in Finland suggested that SRP removal in bioretention media is consistent throughout the year, provided the bioretention systems are vegetated (Valtanen et al., 2017). The discontinuous analysis of bioretention system performance limits understanding. Although prior studies have shown seasonal variability in P load reductions, they may have overlooked the increased release of P (predominately SRP) in spring as observed at our site. As such, the factors which contribute to this observation, including the increase of de-icing road salt (NaCl) loads, remain poorly documented and understood at the field scale.

In addition to cold climate factors, variation of precipitation depths between seasons, can directly affect the retention of P in bioretention systems and result in seasonal variability of P retention (Davis, 2007). For example, precipitation depth was shown to be significantly negatively correlated with TP and SRP retention in a recent field study by Shrestha et al. (2018). In our study, the high net TP, TDP and SRP mass release in spring was caused by larger precipitation events with low percentage water volume reduction, combined with high TP, TDP and SRP effluent concentrations in spring. Considering the 24 sampled precipitation events, there was a significant moderate negative correlation between SRP retention and precipitation depth ($\rho=-0.621$, $p=0.001$, Spearman rank correlation, Figure 3-7) and TDP mass retention and precipitation depth ($\rho=-0.490$,

p=0.015). TP retention and precipitation depth were not found to be significantly correlated ($\rho=-0.177$, $p=0.407$) and there was a significant moderate positive correlation between DOP retention and precipitation depth ($\rho=0.461$, $p=0.022$). However, importantly, while SRP and TDP mass retention were negatively correlated with precipitation depth considering events for all seasons, the three large events (> 25 mm) that resulted in the highest SRP release (of the total six large events that were sampled) all occurred in spring (30 March, 18 April, and 26 April, 2019). These three events had a net SRP release of 7.1 ± 0.4 g P, 6.5 ± 0.4 g P, and 4.9 ± 0.3 g P, respectively. Furthermore, all precipitation events that released more than 1.5 g of SRP occurred in spring. This suggests that while precipitation depth influences SRP release, it may not be the primary factor with other seasonal factors contributing to the high SRP release in spring. Other seasonal processes occurring in spring in cold climates include freeze-thaw mechanisms and salt (NaCl) loading – these factors may have contributed to the observed high spring SRP release (and associated TP and TDP release).

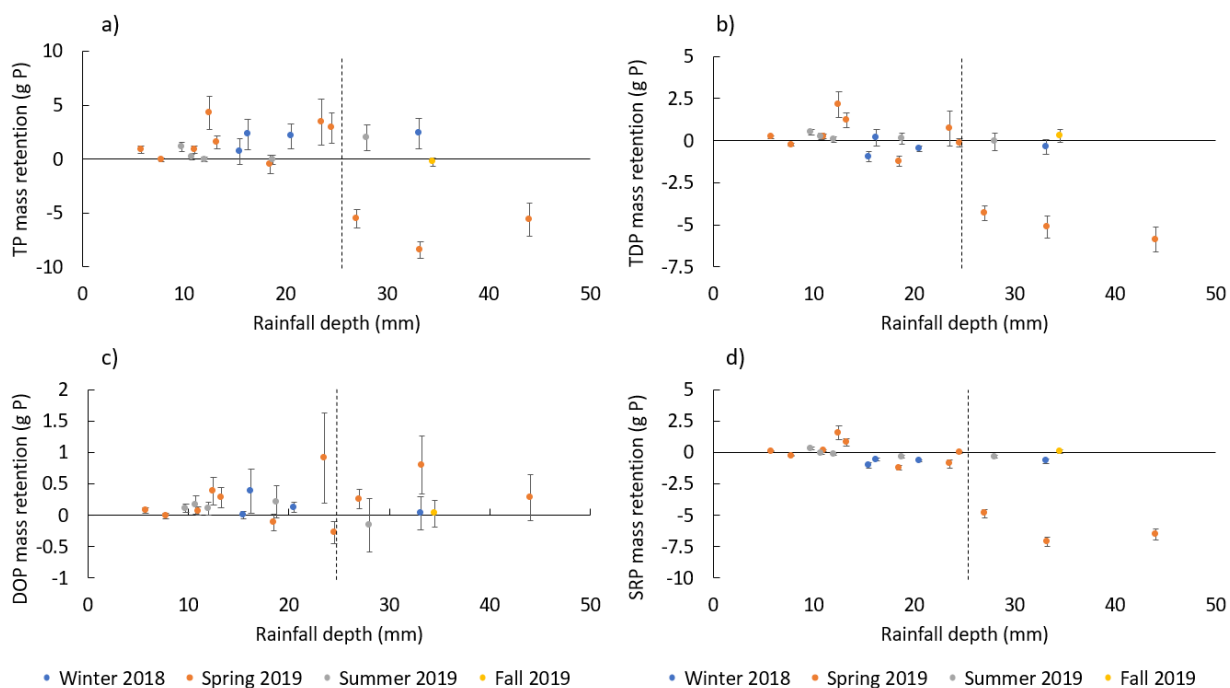


Figure 3-7: Correlation between a) TP, b) TDP, c) DOP, and d) SRP mass retention and precipitation depth. All events right of the dotted line are defined as large precipitation events (>25 mm).

The chloride (Cl) concentrations in the influent, effluent and porewater were measured to evaluate the potential role of road salt (NaCl) application on the observed seasonal variability in SRP release. In winter, brackish Cl concentrations up to 24,000 mg Cl/L were observed in the influent (Figure 3-8). By the end of spring, the influent Cl concentrations were generally below 10 mg Cl/L and were below the detection limit (2.5 mg/L) in late summer (27 August 2019). The highest effluent Cl concentrations were observed in late February-March (maximum = 3,330 mg Cl/L) - this is consistent to the timing of the high effluent SRP concentrations (Figure 3-4). The effluent Cl concentrations decreased over time but remained elevated (summer mean 95 ± 87 mg Cl/L) relative to the influent concentrations through summer. The potential relationship between high salt loading and increased release of TP and SRP from the bioretention media is consistent with some prior studies that also observed increased release of P

under the influence of road runoff with high salt concentrations (Denich et al., 2003; Géhéniau et al., 2015; Kakuturu and Clark, 2015).

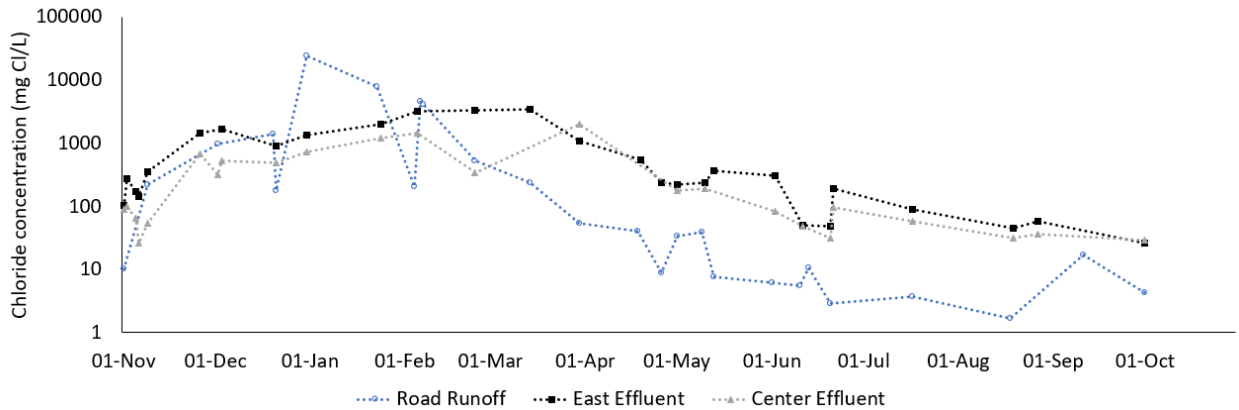


Figure 3-8: Chloride concentrations in influent (road runoff), effluent of the East bioretention system, and the effluent of the Center bioretention system from November 2018 to October 2019 on a logarithmic scale.

Porewater concentration data provides further insight into the relative influence of high salt loading on SRP release in the bioretention systems. Porewater SRP and Cl concentrations were measured for six events through the monitoring period with data available for 1 January 2019 and 7 February 2019 in addition to the four events discussed in Section 3.3.1.4. Interestingly, in spite of the high variability, mean porewater Cl concentrations were highest for the January and February events ($2,930 \pm 4,300$ mg Cl/L, and $6,920 \pm 3,200$ mg Cl/L, respectively), but the mean SRP concentrations were higher in early spring (292 ± 216 μ g P/L) compared with January (203 ± 108 μ g P/L) and February (109 ± 57 μ g P/L; Figure 3-9a). It is possible high salt loading entering the system does not have an immediate impact on SRP release from the bioretention media. The SRP release (i.e. high SRP porewater) following the peak in Cl porewater concentrations suggest that a time or mass-sensitive mechanism may be affecting the SRP release. While porewater SRP and Cl concentrations had a strong and positive correlation in late spring (10 June 2019, Spearman rank, $\rho=0.773$, $p=0.00006$), significant correlations were variable for porewater SRP and Cl, and SRP and Na concentrations for individual events across other seasons (Spearman rank, Appendix E Tables E-1, E-2)

suggesting Cl and Na may not have a direct influence the high spring SRP but rather may indirectly influence the release over a longer or delayed time (seasonal) scale. It is also possible that the mechanisms that influence this behaviour are not direct or temporally coupled.

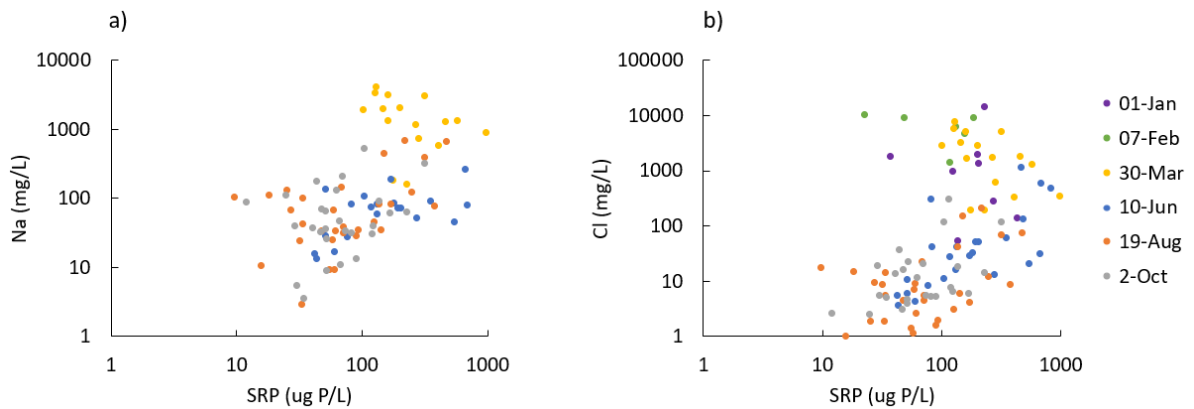


Figure 3-9: Correlation between porewater (a) Na and SRP, (b) Cl and SRP for six precipitation events over the monitoring period.

Freeze-thaw cycles may also have contributed to the high TP, TDP and SRP release from the bioretention system in spring as this process increases pore spaces and isolates smaller pores, reducing the sediment surface area available to adsorb P (Ding et al., 2019). Air temperature data indicate that the bioretention cells were undergoing freeze-thaw cycles through winter and continuing into early spring. As such it is possible that both freeze-thaw cycles and elevated NaCl concentrations may have contributed to the high SRP release in spring. However, the influence of each of these factors have not previously been evaluated independently as field investigations are not able to isolate these factors and prior laboratory experiments such as Ding et al. (2019) considered both factors simultaneously.

3.3.3 Influence of road salt (sodium chloride) on P release

Column experiments were conducted to isolate the potential influence of road salt on P retention and release from the bioretention media and evaluate whether this may have contributed to the high P, mostly in the form of SRP, release from the bioretention

systems in spring. As described above, freeze-thaw mechanisms may also be contributing to spring P release. However, freeze-thaw cycles are naturally occurring in cold climates and cannot be controlled in field installations. In contrast, road salt application has the potential to be adjusted in urban areas provided road safety conditions are met. Further, determining the effect of high salt loads on P release in bioretention systems has broader implications for understanding the impacts of salt application on P mobility in soils and groundwater in urban areas.

In this study, two column experiments were run simultaneously with one column receiving road runoff (control column) and the other column receiving road runoff spiked with salt (salt column; NaCl 1.2 g/L). Two wet-dry periods were simulated until steady-state conditions with respect to the effluent electrical conductivity and TP concentration were observed. The cumulative TP mass release results indicate that considerably more TP was released from the salt column over the first and second wet periods (15 mg and 5 mg, respectively) compared to the control column (10 mg and 2 mg, respectively; Figure 3-10a). The TP released during the first wet period was greater than the second wet period due to initial maturation (release) of TP from the media at the onset of flow through the column (Mullane et al., 2015; Willard et al., 2017). Importantly, and consistent with our field results, over the initial 20 days of the first wet period there was no difference between the cumulative TP mass released from the salt and control columns (percentage difference in cumulative TP released at day 20 = 0.3%). However, after 20 days there is a clear divergence in the cumulative TP mass released with greater TP release from the salt column compared to the control column (percentage difference in cumulative TP released at day 40 = 36%). This indicates that high salt loading may enhance TP release from the bioretention media but only after prolonged high salt input to the system.

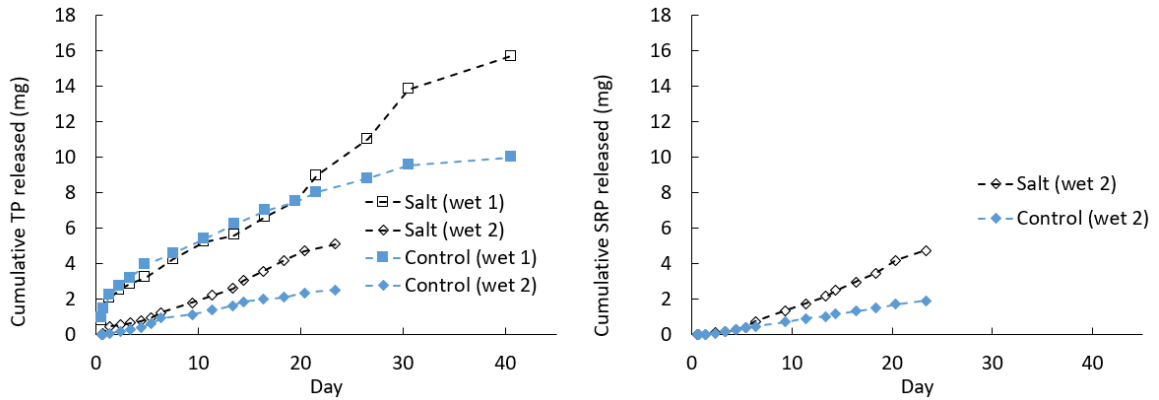


Figure 3-10: Cumulative (a) TP and (b) SRP released over time during first (wet 1) and second (wet 2) wet periods for the salt column (road runoff spiked with NaCl influent) and control column (road runoff influent).

Consistent with the first wet period, the control column and the salt column released similar TP mass until diverging after 6 days, with the salt column releasing more TP relative to the control column (Figure 3-10b). The cumulative mass of TP released from the salt column over the 23-day wet 2 period (5.1 mg) was 102% greater than the mass released from the control column (2.5 mg). SRP data was also available for the second wet period with data indicating that SRP was the major component of TP released from the salt and control columns (SRP represented 93% and 77% of the TP released over the second wet period).

Results from the column experiments are consistent with the field data which showed high Cl inputs and low TP and SRP release in winter, followed by high TP, SRP, and Cl release in spring. Combining the column results with the field data suggests that the observed TP and SRP release in spring from the field-scale bioretention systems may be due to a delayed release of SRP caused by prolonged salt inputs over the winter and spring. It is possible that there is a threshold NaCl mass input before increased P release from the bioretention media occurs. To examine this, the cumulative Cl mass input was normalized based on the total pore space volume to compare the timing of the divergence of TP release between the salt and control column with the timing of increased P release in the field bioretention systems. For this comparison, the first wet period for the column

experiments was considered (20 days of influent until divergence in TP effluent concentrations observed) as Winter 2018 was the first winter season that the bioretention systems received road runoff with de-icing salt. For the column experiments, considering the influent rate of 1.44 L/day, 0.13 L of pore space within the column, and 20 days until divergence of TP effluent concentrations, 210 pore volumes with high salt concentrations were infiltrated through the system before an increase in P release occurred. Considering this together with the field measured cumulative effluent volumes, influent Cl concentrations, and estimated 14,000L of pore space volume in the bioretention systems, the increased TP release for the field scale bioretention systems would have occurred in mid-January at the earliest (see Appendix F for details of calculations). This calculation however is based on first flush road runoff Cl concentrations which are extremely high relative to influent road runoff Cl concentrations over the entire precipitation event. When Cl concentrations from road runoff samples collected in the middle of the precipitation event are used in the calculations rather than first flush road runoff concentrations, the normalized Cl loading per pore space volume is not reached by mid-February, suggesting it is possible that the high P release in spring may be linked to the high prolonged salt loadings through the winter and spring. Although a number of assumptions were used in these calculation (e.g., no dead pore spaces, road runoff infiltrated equally across the bioretention system, homogeneity in processes governing P transformation), this preliminary analysis suggests that the high spring TP and SRP release observed in the field is comparable to the delayed enhanced TP and SRP release observed in the column experiment with high salt influent concentrations.

Our study expands on recent column experiments conducted by McManus & Davis (2020) which suggests high Cl concentrations can cause a delayed release of TP due to desorption and inhibition of sorption from to anion exchange processes. However, our study is the first to illustrate the potential delayed increased release of SRP, and associated TP and TDP forms, in field bioretention systems due to prolonged road salt application. Field monitoring over a year permitted observation of the timing and seasonal patterns of increased P release in spring, based on both concentrations and mass loads, under natural conditions. Although the precise timing of this peak P release will

vary based on actual precipitation volumes, road salt application rates, media composition, and age of bioretention systems, the potential effect of Na and Cl on P behaviour in bioretention system including the delay between salt application and high P release is important for understanding and evaluating the overall performance of these systems in cold climates.

While Cl was used in our analysis to track the road salt (NaCl) in the field bioretention systems and column experiments, it is important to note that high Na together with the high Cl input to the bioretention systems may have contributed to the high observed spring P release. For instance, high Cl concentrations may directly cause SRP desorption through anion exchange processes (McManus and Davis, 2020) and can be toxic to vegetation, thereby reducing the potential for P uptake (Kratky et al., 2017). In comparison, high Na concentrations can negatively impact the media's cation exchange capacity, and soil exchange pools, while decreasing the soil's stability (Suarez et al., 2008). Cation exchange processes are expected to have an indirect effect on P sorption as Na^+ can exchange with Ca^+ and other cations and bind to SRP. High exchangeable Na^+ can also mobilize organic matter from sediment (Christopher et al., 1992), and it is possible that the mineralization of organic matter may have contributed to the high SRP release in spring. In addition, high Na^+ and Cl^- concentrations in the bioretention system may affect the microbial community, and therefore P removal efficiencies (Yuan et al., 2007).

3.4 Conclusion

Field-scale bioretention systems installed in London, Ontario were observed to have a cumulative net retention of TP and DOP but high net release of TDP and SRP over a year-long monitoring period based on both concentrations and mass loading calculations. The majority of P release, mostly in the form of SRP, occurred during a few spring precipitation events, with effluent TP, TDP and SRP concentrations and loads decreasing into the summer and fall compared to spring. The observed timing of P release in spring is of concern considering that high spring P loadings are thought to be a key factor in summer harmful algal blooms and hypoxic conditions in downstream water bodies

(Irvine et al., 2019). Combining the field results with column experiments suggest that prolonged high road de-icing salt (NaCl) loads through winter and spring may have contributed to the high spring P release from the field scale bioretention systems with a delay between the initiation of high salt inputs and increased P release from the bioretention systems. Although other factors may also contribute to P retention-release mechanisms in the bioretention systems (e.g. redox conditions, precipitation reactions, and pH), their effects on net annual P retention may be overwhelmed by the effects of high NaCl loading. It is recommended further research be conducted to examine the long-term impacts of high salt loading on P retention-release behaviour in bioretention systems, including monitoring over consecutive winters and in mature bioretention systems. Further, more detailed porewater and sediment analysis is required using field- and laboratory-based studies to clearly identify the underlying mechanisms controlling P retention-release. Overall, this study provides new insights into the seasonal performance of bioretention systems installed cold climates with respect their ability to retain P, including its different forms, as well as the potential impacts of road salt application. This information is needed to enhance LID system design and mitigate the water quality impacts of urbanization on downstream groundwater and surface water.

3.5 References

- AECOM, 2016. Bioretention Design Brief: Sarnia Road Improvements- Hyde Park to Beaverbrook Avenue. London, Ontario.
- Berge, D., Fjeld, E., Hindar, A., Kaste, Ø., 2017. Nitrogen Retention in Two Norwegian Watercourses of Different Trophic Status. *Ambio* 26, 282–288.
- Blecken, G.T., Zinger, Y., Muthanna, T.M., Deletic, A., Fletcher, T.D., Viklander, M., 2007. The influence of temperature on nutrient treatment efficiency in stormwater biofilter systems. *Water Sci. Technol.* 56, 83–91.
<https://doi.org/10.2166/wst.2007.749>
- Brown, R.A., Birgand, F., Hunt, W.F., 2013. Analysis of consecutive events for nutrient and sediment treatment in field-monitored bioretention cells. *Water. Air. Soil Pollut.* 224. <https://doi.org/10.1007/s11270-013-1581-6>
- Canadian Council of Ministers of the Environment, 2004. Phosphorus: Canadian Guidance Framework for the Management of Freshwater Systems. *Can. Water Qual. Guidel. Prot. Aquat. Life* 1–5. <https://doi.org/10.1038/sj.bdj.4806729> [pii]
- Carpenter, D.D., Hallam, L., 2010. Influence of planting soil mix characteristics on bioretention cell design and performance. *J. Hydrol. Eng.* 15, 404–416.
[https://doi.org/10.1061/\(ASCE\)HE.1943-5584.0000131](https://doi.org/10.1061/(ASCE)HE.1943-5584.0000131)
- Christopher, A., Strong, J.E., Mosher, P.A., 1992. Effect of Deicing Salts on Metal and Organic Matter Mobilization in Roadside Soils. *Environ. Sci. Technol.* 26, 703–709.
<https://doi.org/10.1021/es00028a006>
- Credit Valley Conservation, Toronto and Region Conservation Authority, 2010. Low Impact Development Stormwater Management Planning and Design Guide. Toronto, Ontario.
- Davis, A.P., 2008. Field Performance of Bioretention: Hydrology Impacts. *J. Hydrol.*

- Eng. 13, 90–95. [https://doi.org/10.1061/\(asce\)1084-0699\(2008\)13:2\(90\)](https://doi.org/10.1061/(asce)1084-0699(2008)13:2(90))
- Davis, A.P., 2007. Field Performance of Bioretention: Water Quality. *Environ. Eng. Sci.* 24, 1048–1064. <https://doi.org/10.1089/ees.2006.0190>
- Debusk, K.M., Wynn, T.M., 2011. Storm-water bioretention for runoff quality and quantity mitigation. *J. Environ. Eng.* 137, 800–808. [https://doi.org/10.1061/\(ASCE\)EE.1943-7870.0000388](https://doi.org/10.1061/(ASCE)EE.1943-7870.0000388)
- Denich, C., Bradford, A., Drake, K., 2003. Bioretention: assessing effects of winter salt and aggregate application on plant health, media clogging and effluent quality. *Water Qual. Res. J. Canada* 48, 387–399. <https://doi.org/10.2166/wqrjc.2013.065>
- Dietz, M.E., Clausen, J.C., 2006. Saturation to improve pollutant retention in a rain garden. *Environ. Sci. Technol.* 40, 1335–1340. <https://doi.org/10.1021/es051644f>
- Dietz, M.E., Clausen, J.C., 2005. A field evaluation of rain garden flow and pollutant treatment. *Water. Air. Soil Pollut.* 167, 123–138. <https://doi.org/10.1007/s11270-005-8266-8>
- Ding, B., Rezanezhad, F., Gharedaghloo, B., Van Cappellen, P., Passeur, E., 2019. Bioretention cells under cold climate conditions: Effects of freezing and thawing on water infiltration, soil structure, and nutrient removal. *Sci. Total Environ.* 649, 749–759. <https://doi.org/10.1016/j.scitotenv.2018.08.366>
- Environment and Climate Change Canada, 2019a. 1981-2010 Climate Normals & Averages [WWW Document]. URL http://climate.weather.gc.ca/climate_normals/index_e.html (accessed 7.21.19).
- Environment and Climate Change Canada, 2019b. Daily Data Report for January 2019 [WWW Document]. URL https://climate.weather.gc.ca/climate_data/daily_data_e.html?hlyRange=2012-03-20%7C2020-07-22&dlyRange=2012-03-20%7C2020-07-22&mlyRange=%7C&StationID=50093&Prov=ON&urlExtension=_e.html&search

Type=stnName&optLimit=yearRange&StartYear=1840&EndYear=2020&selR
(accessed 6.20.20).

Fisher Landscaping, 2017. Sarnia Road Improvements- Bioretention Soil Test Results.
London, Ontario.

Fowdar, H.S., Hatt, B.E., Cresswell, T., Harrison, J.J., Cook, P.L.M., Deletic, A., 2017.
Phosphorus Fate and Dynamics in Greywater Biofiltration Systems. *Environ. Sci.
Technol.* 51, 2280–2287. <https://doi.org/10.1021/acs.est.6b04181>

Géhéniau, N., Fuamba, M., Mahaut, V., Gendron, M.R., Dugué, M., 2015. Monitoring of
a Rain Garden in Cold Climate: Case Study of a Parking Lot near Montréal. *J. Irrig.
Drain. Eng.* 141. [https://doi.org/10.1061/\(ASCE\)IR.1943-4774.0000836](https://doi.org/10.1061/(ASCE)IR.1943-4774.0000836)

Geronimo, F.K.F., Maniquiz-Redillas, M.C., Kim, L.H., 2015. Fate and removal of
nutrients in bioretention systems. *Desalin. Water Treat.* 53.
<https://doi.org/10.1080/19443994.2014.922308>

Gibert, O., Hernández, M., Vilanova, E., Cornellà, O., 2014. Guidelining protocol for
soil-column experiments assessing fate and transport of trace organics. *Demeau* 3,
54.

Golder Associates Ltd., 2016. Geotechnical Investigation.

Hager, J., Hu, G., Hewage, K., Sadiq, R., 2019. Performance of low-impact development
best management practices: A critical review. *Environ. Rev.* 27, 17–42.
<https://doi.org/10.1139/er-2018-0048>

He, J., Valeo, C., Chu, A., Neumann, N.F., 2010. Characteristics of Suspended Solids,
Microorganisms, and Chemical Water Quality in Event-Based Stormwater Runoff
from an Urban Residential Area. *Water Environ. Res.* 82, 2333–2345.
<https://doi.org/10.2175/106143010x12681059117058>

Hermawan, A.A., Talei, A., Salamatinia, B., Chua, L.H.C., 2020. Seasonal performance

- of stormwater biofiltration system under tropical conditions. *Ecol. Eng.* 143, 105676. <https://doi.org/10.1016/j.ecoleng.2019.105676>
- Hsieh, C., Davis, A.P., Needelman, B.A., 2007a. Nitrogen Removal from Urban Stormwater Runoff Through Layered Bioretention Columns. *Water Environ. Res.* 79, 2404–2411. <https://doi.org/10.2175/106143007x183844>
- Hsieh, C., Davis, A.P., Needelman, B.A., 2007b. Bioretention Column Studies of Phosphorus Removal from Urban Stormwater Runoff. *Water Environ. Res.* 79, 177–184. <https://doi.org/10.2175/106143006X111745>
- Hwang, C.C., Weng, C.H., 2015. Effects of rainfall patterns on highway runoff pollution and its control. *Water Environ. J.* 29, 214–220. <https://doi.org/10.1111/wej.12109>
- International Joint Commission, 2014. A Balanced Diet for Lake Erie: Reducing Phosphorus Loadings and Harmful Algal Blooms. Report of the Lake Erie Ecosystem Priority. Ottawa, Ontario.
- Irvine, C., Macrae, M., Morison, M., Petrone, R., 2019. Seasonal nutrient export dynamics in a mixed land use subwatershed of the Grand River, Ontario, Canada. *J. Great Lakes Res.* 45, 1171–1181. <https://doi.org/10.1016/j.jglr.2019.10.005>
- Jiang, C., Li, J., Li, H., Li, Y., Chen, L., 2017. Field Performance of Bioretention Systems for Runoff Quantity Regulation and Pollutant Removal. *Water. Air. Soil Pollut.* 228. <https://doi.org/10.1007/s11270-017-3636-6>
- Joshi, S.R., Kukkadapu, R.K., Burdige, D.J., Bowden, M.E., Sparks, D.L., Jaisi, D.P., 2015. Organic matter remineralization predominates phosphorus cycling in the mid-bay sediments in the chesapeake bay. *Environ. Sci. Technol.* 49, 5887–5896. <https://doi.org/10.1021/es5059617>
- Kakuturu, S., Clark, S., 2015. Clogging Mechanism of Stormwater Filter Media by NaCl as a Deicing Salt. *Environ. Eng. Sci.* 32. <https://doi.org/https://doi-org.proxy1.lib.uwo.ca/10.1089/ees.2014.0337>

- Kayhanian, M., Fruchtman, B.D., Gulliver, J.S., Montanaro, C., Ranieri, E., Wuertz, S., 2012. Review of highway runoff characteristics: Comparative analysis and universal implications. *Water Res.* 46, 6609–6624.
<https://doi.org/10.1016/j.watres.2012.07.026>
- Kazemi, F., Golzarian, M.R., Myers, B., 2018. Potential of combined Water Sensitive Urban Design systems for salinity treatment in urban environments. *J. Environ. Manage.* 209, 169–175. <https://doi.org/10.1016/j.jenvman.2017.12.046>
- Khan, U.T., Valeo, C., Chu, A., van Duin, B., 2012a. Bioretention cell efficacy in cold climates: Part 2 - water quality performance. *Can. J. Civ. Eng.* 39, 1222–1233.
<https://doi.org/10.1139/l2012-111>
- Khan, U.T., Valeo, C., Chu, A., van Duin, B., 2012b. Bioretention cell efficacy in cold climates: Part 1 - hydrologic performance. *Can. J. Civ. Eng.* 39, 1210–1221.
<https://doi.org/10.1139/l2012-110>
- Kratky, H., Li, Z., Chen, Y., Wang, C., Li, X., Yu, T., 2017. A critical literature review of bioretention research for stormwater management in cold climate and future research recommendations. *Front. Environ. Sci. Eng.* 11, 16.
<https://doi.org/10.1007/s11783-017-0982-y>
- Le Moal, M., Gascuel-Oudou, C., Ménesguen, A., Souchon, Y., Étrillard, C., Levain, A., Moatar, F., Pannard, A., Souchu, P., Lefebvre, A., Pinay, G., 2019. Eutrophication: A new wine in an old bottle? *Sci. Total Environ.* 651, 1–11.
<https://doi.org/10.1016/j.scitotenv.2018.09.139>
- Li, B., Brett, M.T., 2013. The influence of dissolved phosphorus molecular form on recalcitrance and bioavailability. *Environ. Pollut.* 182, 37–44.
<https://doi.org/10.1016/j.envpol.2013.06.024>
- Li, Davis, A., 2009. Water quality improvement through reductions of pollutant loads using bioretention. *J. Environ. Eng.* 135, 567–576.

[https://doi.org/10.1061/\(ASCE\)EE.1943-7870.0000026](https://doi.org/10.1061/(ASCE)EE.1943-7870.0000026)

- Li, J., Davis, A., 2016. A unified look at phosphorus treatment using bioretention. *Water Res.* 90, 141–155. <https://doi.org/10.1016/j.watres.2015.12.015>
- Li, Sung, C., Kim, M., Chu, K.H., 2011. Assessing performance of bioretention boxes in hot and semiarid regions: Highway application pilot study. *Transp. Res. Rec.* 155–163. <https://doi.org/10.3141/2262-15>
- LID SWM Planning and Design Guide Contributors, 2020. Bioretention: Filter media LID SWM Planning and Design Guide [WWW Document]. *Sustain. Technol. Eval. Progr.* URL https://wiki.sustainabletechnologies.ca/index.php?title=Bioretention:_Filter_media&oldid=10879 (accessed 5.5.20).
- Liu, J., Davis, A.P., 2014. Phosphorus speciation and treatment using enhanced phosphorus removal bioretention. *Environ. Sci. Technol.* 48. <https://doi.org/10.1021/es404022b>
- Lucas, W.C., Greenway, M., 2011. Phosphorus Retention by Bioretention Mesocosms Using Media Formulated for Phosphorus Sorption: Response to Accelerated Loads. *J. Irrig. Drain. Eng.* 137, 144–153. [https://doi.org/10.1061/\(ASCE\)IR.1943-4774.0000243](https://doi.org/10.1061/(ASCE)IR.1943-4774.0000243)
- Lucke, T., Nichols, P.W.B., 2015. The pollution removal and stormwater reduction performance of street-side bioretention basins after ten years in operation. *Sci. Total Environ.* 536, 784–792. <https://doi.org/10.1016/j.scitotenv.2015.07.142>
- Mangangka, I.R., Liu, A., Egodawatta, P., Goonetilleke, A., 2015. Performance characterisation of a stormwater treatment bioretention basin. *J. Environ. Manage.* 150, 173–178. <https://doi.org/10.1016/j.jenvman.2014.11.007>
- Manka, B.N., Hathaway, J.M., Tirpak, R.A., He, Q., Hunt, W.F., 2016. Driving forces of effluent nutrient variability in field scale bioretention. *Ecol. Eng.* 94.

<https://doi.org/10.1016/j.ecoleng.2016.06.024>

- Marvin, J.T., Passeport, E., Drake, J., 2020. State-of-the-Art Review of Phosphorus Sorption Amendments in Bioretention Media: A Systematic Literature Review. *J. Sustain. Water Built Environ.* 6. <https://doi.org/10.1061/JSWBAY.0000893>
- McManus, M., Davis, A.P., 2020. Impact of Periodic High Concentrations of Salt on Bioretention Water Quality Performance. *J. Sustain. Water Built Environ.* 6, 1–11. <https://doi.org/10.1061/JSWBAY.0000922>
- Mullane, J.M., Flury, M., Iqbal, H., Freeze, P.M., Hinman, C., Cogger, C.G., Shi, Z., 2015. Intermittent rainstorms cause pulses of nitrogen, phosphorus, and copper in leachate from compost in bioretention systems. *Sci. Total Environ.* 537, 294–303. <https://doi.org/10.1016/j.scitotenv.2015.07.157>
- Mullins, A.R., Bain, D.J., Pfeil-McCullough, E., Hopkins, K.G., Lavin, S., Copeland, E., 2020. Seasonal drivers of chemical and hydrological patterns in roadside infiltration-based green infrastructure. *Sci. Total Environ.* 714, 136503. <https://doi.org/10.1016/j.scitotenv.2020.136503>
- Muthanna, T.M., Viklander, M., Blecken, G., Thorolfsson, S.T., 2007. Snowmelt pollutant removal in bioretention areas. *Water Res.* 41, 4061–4072. <https://doi.org/10.1016/j.watres.2007.05.040>
- Muthanna, Viklander, M., Thorolfsson, S.T., 2008. Seasonal climatic effects on the hydrology of a rain garden. *Hydrol. Process.* 22, 1640–1649. <https://doi.org/10.1002/hyp.6732>
- O’Neill, S.W., Davis, A.P., 2012. Water treatment residual as a bioretention amendment for phosphorus. I: Evaluation studies. *J. Environ. Eng. (United States)* 138, 318–327. [https://doi.org/10.1061/\(ASCE\)EE.1943-7870.0000409](https://doi.org/10.1061/(ASCE)EE.1943-7870.0000409)
- Ontario Ministry of the Environment, 2003. Stormwater Management Planning and Design Manual.

- Palmer, E.T., Poor, C.J., Hinman, C., Stark, J.D., 2013. Nitrate and Phosphate Removal through Enhanced Bioretention Media: Mesocosm Study. *Water Environ. Res.* 85, 823–832. <https://doi.org/10.2175/106143013x13736496908997>
- Parsons, C.T., Rezanezhad, F., O’Connell, D.W., Van Cappellen, P., 2017. Sediment phosphorus speciation and mobility under dynamic redox conditions. *Biogeosciences* 14, 3585–3602. <https://doi.org/10.5194/bg-14-3585-2017>
- Passeport, E., Hunt, W.F., Line, D.E., Smith, R.A., Brown, R.A., 2009. Field study of the ability of two grassed bioretention cells to reduce storm-water runoff pollution. *J. Irrig. Drain. Eng.* 135, 505–510. [https://doi.org/10.1061/\(ASCE\)IR.1943-4774.0000006](https://doi.org/10.1061/(ASCE)IR.1943-4774.0000006)
- Paus, K.H., Muthanna, T.M., Braskerud, B.C., 2015. The hydrological performance of bioretention cells in regions with cold climates: seasonal variation and implications for design. *Hydrol. Res.* <https://doi.org/10.2166/nh.2015.084>
- Prestigiacomo, A.R., Effler, S.W., Gelda, R.K., Matthews, D.A., Auer, M.T., Downer, B.E., Kuczynski, A., Walter, M.T., 2016. Apportionment of bioavailable phosphorus loads entering Cayuga Lake, New York. *J. Am. Water Resour. Assoc.* 52, 31–47. <https://doi.org/10.1111/1752-1688.12366>
- Roseen, R.M., 2009. Seasonal Performance Variations for Storm-water management systems in cold climate conditions. *J. Environ. Eng.* 3, 128–137. [https://doi.org/10.1061/\(ASCE\)0733-9371\(2009\)135:3\(1280](https://doi.org/10.1061/(ASCE)0733-9371(2009)135:3(1280)
- Sánchez, M., Boll, J., 2005. The effect of flow path and mixing layer on phosphorus release: Physical mechanisms and temperature effects. *J. Environ. Qual.* 34, 1600–1609. <https://doi.org/10.2134/jeq2004.0306>
- Shrestha, P., Hurley, S.E., Wemple, B.C., 2018. Effects of different soil media, vegetation, and hydrologic treatments on nutrient and sediment removal in roadside bioretention systems. *Ecol. Eng.* 112, 116–131.

<https://doi.org/10.1016/j.ecoleng.2017.12.004>

- Sims, A.W., Robinson, C.E., Smart, C.C., O'Carroll, D.M., 2019. Mechanisms controlling green roof peak flow rate attenuation. *J. Hydrol.* 577, 123972. <https://doi.org/10.1016/j.jhydrol.2019.123972>
- Steffen, M.M., Belisle, B.S., Watson, S.B., Boyer, G.L., Wilhelm, S.W., 2014. Status, causes and controls of cyanobacterial blooms in Lake Erie. *J. Great Lakes Res.* 40, 215–225. <https://doi.org/10.1016/j.jglr.2013.12.012>
- Stewart, R.D., Lee, J.G., Shuster, W.D., Darner, R.A., 2017. Modelling hydrological response to a fully-monitored urban bioretention cell. *Hydrol. Process.* 31, 4626–4638. <https://doi.org/10.1002/hyp.11386>
- Suarez, D.L., Wood, J.D., Lesch, S.M., 2008. Infiltration into Cropped Soils: Effect of Rain and Sodium Adsorption Ratio-Impacted Irrigation Water. *J. Environ. Qual.* 37, S-169-S-179. <https://doi.org/10.2134/jeq2007.0468>
- Swedish Environmental Protection Agency, 2000. Environmental Quality Criteria - Lakes and Watercourses.
- United States Department of Agriculture, 1986. Urban Hydrology for Small Watersheds, Soil Conservation.
- Valtanen, M., Sillanpää, N., Setälä, H., 2017. A large-scale lysimeter study of stormwater biofiltration under cold climatic conditions. *Ecol. Eng.* 100. <https://doi.org/10.1016/j.ecoleng.2016.12.018>
- Wang, C., Zhang, Y., Li, H., Morrison, R.J., 2013. Sequential extraction procedures for the determination of phosphorus forms in sediment. *Limnology* 14, 147–157. <https://doi.org/10.1007/s10201-012-0397-1>
- Watson, S.B., Miller, C., Arhonditsis, G., Boyer, G.L., Carmichael, W., Charlton, M.N., Confesor, R., Depew, D.C., Höök, T.O., Ludsin, S.A., Matisoff, G., McElmurry,

- S.P., Murray, M.W., Peter Richards, R., Rao, Y.R., Steffen, M.M., Wilhelm, S.W., 2016. The re-eutrophication of Lake Erie: Harmful algal blooms and hypoxia. *Harmful Algae* 56, 44–66. <https://doi.org/10.1016/j.hal.2016.04.010>
- Willard, L.L., Wynn-Thompson, T., Krometis, L.H., Neher, T.P., Badgley, B.D., 2017. Does it pay to be mature? Evaluation of bioretention cell performance seven years postconstruction. *J. Environ. Eng.* 143, 04017041 (10 pp.). [https://doi.org/10.1061/\(ASCE\)EE.1943-7870.0001232](https://doi.org/10.1061/(ASCE)EE.1943-7870.0001232)
- Winston, R.J., Dorsey, J.D., Hunt, W.F., 2016. Quantifying volume reduction and peak flow mitigation for three bioretention cells in clay soils in northeast Ohio. *Sci. Total Environ.* 553, 83–95. <https://doi.org/10.1016/j.scitotenv.2016.02.081>
- Yan, Q., Davis, A.P., James, B.R., 2016. Enhanced Organic Phosphorus Sorption from Urban Stormwater Using Modified Bioretention Media: Batch Studies. *J. of Environmental Engineering* 142 (4), 1152–1161. [https://doi.org/10.1061/\(ASCE\)EE.1943-7870](https://doi.org/10.1061/(ASCE)EE.1943-7870)
- Yuan, B.C., Li, Z.Z., Liu, H., Gao, M., Zhang, Y.Y., 2007. Microbial biomass and activity in salt affected soils under arid conditions. *Appl. Soil Ecol.* 35, 319–328. <https://doi.org/10.1016/j.apsoil.2006.07.004>

Chapter 4

4 Spatial variability in the behavior of soluble reactive phosphorus within field-scale bioretention systems

4.1 Introduction

Urbanization results in high stormwater flows to downstream water bodies as it alters the natural hydrologic cycle in a watershed due to increased imperviousness (Akhter et al., 2020). Urban stormwater runoff can also have high pollutant concentrations leading to downstream water quality impairment (Long et al., 2014; United States Environmental Protection Agency, 2004; Wilson et al., 2015). While conventional urban stormwater management approaches (e.g., stormwater management ponds, constructed wetlands, etc.) provide water quantity control with some water quality improvements, they do not effectively restore the pre-development water balance and typically provide limited removal of pollutants including nutrients (phosphorus [P] and nitrogen [N]) (Akhter et al., 2020; Wilson et al., 2015). As such, low impact development (LID) stormwater systems have become a popular alternative or addition to traditional stormwater management systems (Eger et al., 2017; Kordana and Słyś, 2020). LIDs are source-control methods used to treat urban stormwater runoff as close to the source as possible through natural passive methods, providing both water quality and quantity benefits (Roy et al., 2008). Bioretention systems are a common LID system designed to improve stormwater runoff quality (retention of nutrients, suspended solids, and heavy metals) and restore the pre-development hydrologic cycle in urban areas. There is an increasing need for LID systems, including bioretention systems, to remove P from stormwater as high P loads to downstream water bodies linked to eutrophication, harmful algal blooms, and in some cases, hypoxic conditions (Steffen et al., 2014; Street, 2014; Watson et al., 2016). These impacts, caused by high P loads from anthropogenic sources including urban stormwater, have large economic, ecological and societal costs (Street, 2014).

In aquatic systems, total P (TP) is present in dissolved and particulate forms. Particulate P (PP) represents the P which is bonded to particles and can be filtered out of solution.

Total dissolved P (TDP) is the fraction of P that passes through a 0.45 µm filter and can be further divided into organic and inorganic forms. Dissolved organic P (DOP) consists of P bonded to oxygen and carbon compounds and is derived from a biological source (Cooper et al., 1991; Mackey et al., 2019). Inorganic dissolved P, often called soluble reactive P (SRP), is the most bioavailable form of P that is taken up by plants and aquatic biota and is therefore of key concern for its role in eutrophication and thus downstream water quality impairment (Prestigiacomo et al., 2016).

Prior studies of field-scale bioretention systems have shown variable performance with respect to their ability to retain P, with some studies indicating bioretention systems can decrease TP loads while others show the systems can increase TP loads due to P leaching from the bioretention soil media (Carpenter and Hallam, 2010; Debusk and Wynn, 2011; Khan et al., 2012; Li and Davis, 2009). While fewer field studies have quantified SRP retention in bioretention systems, performance with respect to SRP retention has been variable (Hager et al., 2019; Mangangka et al., 2015; Passeport et al., 2009). Prior field studies investigating P (TP and/or SRP) retention typically only conduct water quality sampling of the influent and effluent, thereby treating the systems as “black boxes” and providing limited insight into the behaviour of P within the bioretention systems including the biogeochemical processes that govern P retention. While laboratory column and mesocosm studies have investigated the processes governing P retention in bioretention soil media (Ding, Rezanezhad, Gharedaghloo, Van Cappellen, & Passeport, 2019; Hsieh, Davis, & Needelman, 2007; Song & Song, 2018; Zhou, Xu, Cao, Zhou, & Song, 2016), natural field conditions introduce added complexities including, for instance, irregular precipitation and temperature patterns, seasonality, variable chemical composition of influent stormwater, complex soil moisture dynamics, and varying hydrogeology and native soil conditions. As such, laboratory experiments may not adequately simulate the in situ biogeochemical environment in field-scale systems and thus the processes governing P retention. High spatial resolution of in situ porewater sampling within field-scale bioretention systems is needed to examine the fate of P within these systems and evaluate common assumptions used in bioretention system design with respect to P retention.

P behaviour in porous media, including in bioretention systems, is complex with the fate of P controlled by various abiotic and biotic processes. P retention can occur directly by physical and biogeochemical aqueous-solid phase processes including physical filtration (for PP), adsorption to the surface of metal oxides (mostly Al and Fe oxides) and clay particles, co-precipitation with Ca under alkaline conditions, co-precipitation with Fe and Al under acidic conditions, and biological P uptake (Lucas and Greenway, 2011; Zhou et al., 2016). TP retention in bioretention systems is often attributed to the removal of PP due to physical filtration and sedimentation (Li and Davis, 2009; Liu and Davis, 2014; Marvin et al., 2020; Stagge et al., 2012). In contrast, release of both dissolved organic and inorganic P to porewater is possible through weathering of P-containing minerals, mineralization of organic matter, competitive anion exchange, dissolution of secondary P minerals (Ca, Fe, and Al phosphate minerals), and desorption from metal oxide and clay surfaces (Mackey et al., 2019; McManus and Davis, 2020; Parsons et al., 2017; Prasad and Chakraborty, 2019). Several factors may affect the behaviour of P within bioretention systems including pH, redox conditions, water saturation, sediment-bound and porewater P concentrations, availability of adsorption sites, sediment Fe and Al content, temperature, particle size distribution, vegetation, and organic matter content (Blecken et al., 2007; Dietz & Clausen, 2006; Ding, Hua, & Chu, 2019; Marvin et al., 2020; McDowell & Sharpley, 2003; Shrestha, Hurley, & Wemple, 2018; Song & Song, 2018). Some of these factors can be controlled by the composition of the engineered soil media used in a bioretention system, and therefore guidelines are available for designing the soil media composition (e.g., Sustainable Technologies Evaluation Program in Southern Ontario (LID SWM Planning and Design Guide Contributors, 2020)). In addition, several different amendments have recently been tested for addition to the soil media to optimize P retention in bioretention systems, including, for example, water treatment residuals, marine animal shells, steel slag, and alum (Lucas and Greenway, 2011; Marvin et al., 2020; O'Neill and Davis, 2012)

Based primarily on mesocosm and column studies, adsorption is generally considered to be the dominant mechanism governing the retention of TDP (DOP and SRP) within bioretention systems (Liu and Davis, 2014; Lucas and Greenway, 2011; Marvin et al.,

2020). The capacity of the media to adsorb TDP is limited by the availability of adsorption sites which is in turn governed by the composition of the soil media (specifically the Al and Fe content) (Erickson et al., 2012; Lucas and Greenway, 2011; O'Neill and Davis, 2012), and the available media volume. As such, it is often assumed that increasing the depth of a field-scale bioretention system will improve DP retention by increasing the available surface area for adsorption. For instance, soil media depths of 0.6 to 0.9 m are often recommended to provide sufficient surface area for DP adsorption (Davis, 2007; Hsieh et al., 2007; Hunt et al., 2012; Passeur et al., 2009). While laboratory experiments typically show increased P removal with soil depth (Song and Song, 2018), these studies do not consider the complexity of field conditions. Brown & Hunt (2011) did evaluate the influence of soil media depth on TP and SRP retention in field scale systems through influent-effluent monitoring. They observed no statistical difference in SRP retention between bioretention systems with 0.6 m and 0.9 m depths, although TP concentrations were found to be significantly lower in the effluent of the system with greater media depth. The higher TP retention in the system with greater media depth may have been due to physical filtration and sedimentation of PP within the deeper filter bed (Li and Davis, 2009; Marvin et al., 2020; Stagge et al., 2012).

Current understanding of P behaviour within field bioretention systems – namely retention is governed by PP filtration and adsorption of DP to metal oxides and therefore retention increases with soil media depth - may over-simplify the fate of P within field-scale bioretention systems. The high variability in P mass retention observed in previous field studies (Carpenter & Hallam, 2010; Debusk & Wynn, 2011; Dietz & Clausen, 2006; Li & Davis, 2009) suggest that the processes that control P retention and mobility in bioretention systems are complex and not well understood. The only known study to sample porewater within a field bioretention system used a single profile of suction lysimeters installed at depths of 0 m (surface), 1.2 m (bottom of bioretention media), and 2.4 m (subsurface, 1.2 m below bioretention system) (Komlos and Traver, 2012). While this study demonstrated decreasing SRP concentrations between the surface and bottom of the bioretention media, the spatial sampling resolution and chemical analytes measured was not sufficient to explore the processes governing P fate within the bioretention

systems. More detailed spatial and temporal characterization of the in situ distribution of DP and other species associated DP retention-release within bioretention systems is needed to provide insight into the processes governing the overall performance of bioretention systems in retaining P.

The objective of this study is to investigate the spatial variability in the distribution of SRP and the possible hydro-biogeochemical processes that may affect the net retention, release and transport of SRP within field-scale bioretention systems. This is achieved through detailed porewater sampling and analysis of SRP and dissolved constituents commonly associated with SRP retention (Mn, Ca, Cl, Na, Al, Mn, Fe, ORP and pH) for two large field-scale bioretention systems located in London, Ontario Canada. In situ measurements are augmented with influent-effluent water quantity and water quality sampling, and continuous soil moisture content measurements within the bioretention systems. The findings from this study are needed to optimize the design of bioretention systems, including the soil media composition, for enhanced P retention. Improved P retention within bioretention systems is needed to reduce P loads in urban stormwater runoff and thereby reduce the impact of urbanization on downstream surface waters and groundwater.

4.2 Methods

Extensive monitoring of two field-scale bioretention systems located adjacent to a major arterial road (Sarnia Road) in London, Ontario was conducted for this study. A brief description of the monitored bioretention systems is provided here with more details provided in Chapter 3 (Section 3.2.1). The two monitored systems, herein referred to as the East and Center bioretention systems, were 2 m wide by 26 m long, and 2 m wide by 23 m long, respectively. The systems have a shallow 0.1 m topsoil layer, a 1.0 m layer of engineered soil media, a 0.5 m gravel layer, and a perforated underdrain which connects to the conventional storm drain network (Figure 4-1). Road runoff enters the bioretention systems via two curb-cuts in each system, referred to as the upstream and downstream inlets based on the road topographical gradient. The composition of the soil media installed in these systems was based on the 2010 Credit Valley Conservation LID

stormwater management planning and design guidelines (Credit Valley Conservation, 2010). The soil media composition was 91.2% sand, 8.8% soil fines and 3.4% organic matter in the form of woodchips (Fisher Landscaping, 2017). The pH of the installed media was 7.4, the cation exchange capacity was 38.2 meq/100g, and the P-index for duplicate samples was 9 and 11 ppm, or 13 and 14 ppm using the bicarbonate P extraction method and the Bray method, respectively (Fisher Landscaping, 2017). The soil media P content was at or below the Credit Valley Conservation (2010) guideline of 10 to 30 ppm to minimize P leaching from the media. No testing was completed on the topsoil before installation.

Water samples were collected to characterize the influent (road runoff and pond water), effluent, and in situ porewater in the bioretention systems during precipitation events. Road runoff samples were collected from the upstream inlet of the Center system, and pond water samples were collected from the surface of the East and Center systems during 24 precipitation events from November 2018 to October 2019. For the analysis of the behaviour of SRP within the bioretention systems, pond water samples collected during precipitation events were considered to be representative of the water infiltrating the bioretention systems rather than the road runoff samples. Effluent samples were collected for most monitored precipitation events for which there was drainage through the underdrain (n=21). These samples were collected while drainage was occurring using an ISCO 6700 automatic sampler (Figure 3-1).

Influent and effluent water volumes during precipitation events were determined to calculate P mass loading and thus the overall retention of P in the bioretention systems. The influent water flow rate was calculated using precipitation data provided by the City of London from their tipping bucket rain gauge located 4 km from the field site at the Medway Arena. This precipitation data was validated by two tipping bucket rain gauges installed on the roof of the CMLP building at Western University located 4.5 km from the field site. Influent volumes were calculated by considering the catchment area (0.13 ha), catchment imperviousness (55%) and applying a runoff co-efficient of 35 – 75% of the total water volume generated from the recorded precipitation depth. A two-stage

compound weir with pressure transducer was installed on the outfall of the underdrain of the East system to measure effluent flow rates and associated volumes. This weir and pressure-transducer system was extensively tested in the laboratory before field installation and was also calibrated in the field during a precipitation event on 27 August 2019. Pressure transducer data was recorded every minute using a CR10x datalogger. More details on the water quantity measurements and calculations are provided in Chapter 3 (Section 3.2.1).

Porewater samples to measure the distribution of SRP and associated constituents were collected during 16 precipitation events from March to October 2019. In this Chapter we focus on analysis of the porewater data collected from 21 June 2019 onwards due to the potential impacts of high de-icing salt on the SRP behaviour within the bioretention systems in spring (20 March – 20 June). Porewater samples were collected using permanently installed MacroRhizon porewater samplers (0.15 μm ceramic screens at sampling location). Three vertical profiles of porewater samplers were installed in each of the bioretention systems with the profiles located near the upstream and downstream curb cut inlets and in the middle of the systems. The samplers were installed at 45-degree angles with the ports located at 0.05 m (topsoil), 0.21 m, 0.42 m, and 0.64 m depths below ground surface (Figure 4-1). The angled installations limited the formation of preferential flow pathways between the sampling location and surface. Additional MacroRhizon samplers and suction lysimeter samplers were installed vertically at each profile location in the Centre system with these samplers located at 0.9 m and 1 m depths below ground surface, respectively.

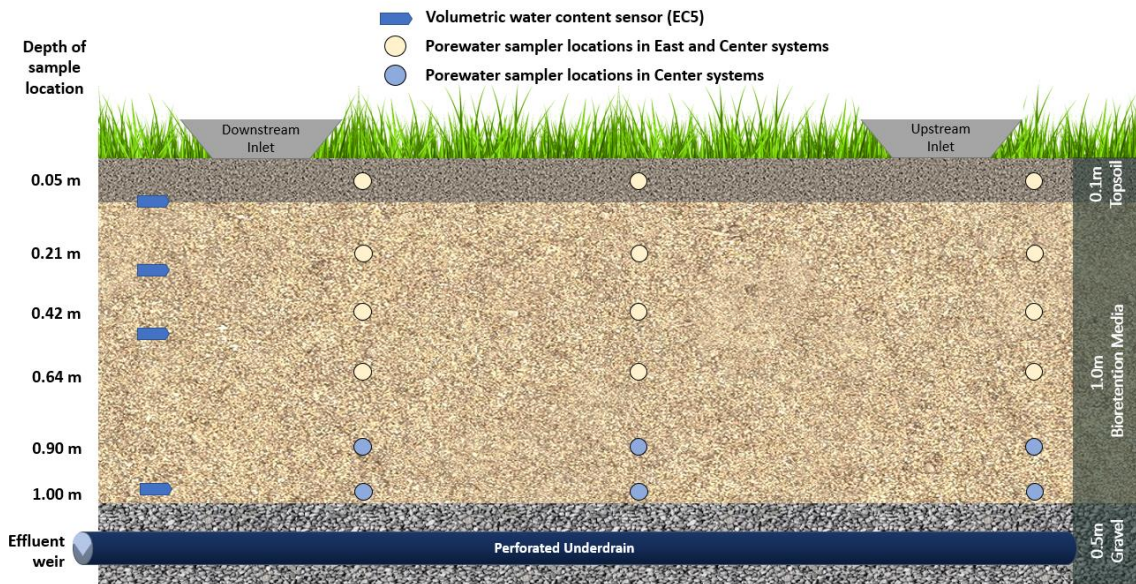


Figure 4-1: Cross-section of bioretention system showing the layout of porewater samplers and volumetric water content sensors installed in the East and Center bioretention systems.

Porewater samples were collected from the MacroRhizon samplers by attaching 60 mL syringes with retainers to create a vacuum pressure and draw water from the porous media. Vacuum pressure was also applied to the suction lysimeters at the same time, but for these samplers, the water sample is drawn into the tubing during sampling events and stored within the suction lysimeter until collection. The vacuum pressure was applied to all MacroRhizon and suction lysimeter samplers for 6 hours or overnight until sufficient water volume (at least 30 mL) was obtained. pH, electrical conductivity (EC), and oxidation-reduction potential (ORP) were measured immediately in the field using a HACH HQ40D portable meter with Intellical™ PHC201, CDC401, and MTC101 probes, respectively. Although the MacroRhizon and suction lysimeter samplers draw water through 0.15 μm ceramic tips, all samples were filtered through 0.45 μm cellulose acetate filter membranes for consistency. Samples were transferred from the collection syringes to 60 mL HDPE bottles and transported to the laboratory within two hours. SRP analysis was conducted within 48 hours of sample collection, with the remainder of the sample

frozen until further analysis. The analytical methods used for SRP, cations/metals, and anions are detailed in Section 3.2.1.2 and Appendix B Table B-1.

Soil cores were collected from an adjacent bioretention system (same engineering design and soil media) using a 5 cm diameter soil corer before all bioretention systems started receiving road runoff (cores collected on 31 August 2018). Soil moisture conditions were dry during soil core collection as there was no precipitation for at least two days prior. Topsoil and soil media samples were collected from multiple depths to provide an initial P content of the topsoil and soil media. The sediments were analyzed using a two-step modified sequential P extraction based on the Hedley et al. (1982) and Tiessen and Moir (1993) methods to quantify the soluble and loosely bound P fractions in the media and the topsoil. For this analysis the sediments were first oven dried for at least 24 hours at 105°C and the soil moisture content was determined using the oven dry method. Following this, 2.0 g of dry sediment was added to 60 mL of double-distilled water and shaken on a shaker table for 16 hours. The samples were then centrifuged for 15 minutes at 3200 RPM and the extracted water was filtered through a 0.45 µm cellulose acetate membrane filter. Finally, 60 mL of 0.5M NaHCO₃ was added to the sediment retained from the first step, before being shaken, centrifuged, and filtered following the same procedure. The supernatant of both steps was analyzed for TDP (Appendix B Table B-1).

Soil moisture content was continuously measured using a vertical array of Decagon ECH₂O EC-5 moisture sensors installed in each bioretention system. Before field installation, each sensor was calibrated in the laboratory with bioretention media using the empirical two-point alpha-mixing model as outlined in Sakaki, Limsuwat, Smits, & Illangasekare, (2008). Three sensors were installed near the downstream inlet of the Center bioretention system with the sensors located within the topsoil layer (0.1 m), mid-media depth (0.4 m), and above the gravel drainage layer (1.0 m). Soil moisture sensors were located at 0.05 m (topsoil), 0.25 m, 0.5 m, and 1.0 m depths below the ground surface near the downstream inlet in the East system. All sensors were connected to a CR10x Campbell Scientific data logger and readings were recorded every 15 minutes from October 2018 to October 2019. More details on the calibration and installation of

the soil moisture sensors are provided in Appendix G. The continuous in situ soil moisture measurements were validated by comparing measurements with the moisture content measured on intact soil media cores collected from the field (gravimetric oven dry method).

4.3 Results and Discussion

4.3.1 SRP distribution in bioretention systems

Monitoring of the influent and effluent of the East bioretention system showed that while some TP may have been retained within the system, there was net export of TDP from the system, mostly in the form of SRP, over the monitoring period. Considering the 24 precipitation events for which influent and effluent samples were collected, the cumulative mass of TP in the influent (56 ± 20 g P) was similar to the mass of TP in the effluent (53 ± 3 g P). In contrast, the cumulative TDP and SRP concentrations were greater in the effluent (39 ± 2 g P and 35 ± 2 g P, respectively) than in the influent (26 ± 10 g P and 14 ± 5 g P, respectively). The retention of TP relative to TDP and SRP is thought to be due to retention of PP due to physical filtration and sedimentation. Analysis of the seasonal changes in the influent and effluent P mass trends revealed that TP, TDP and SRP release from the systems was higher in mid-spring compared to the remainder of the monitoring period (Section 3.3.1.3). It is possible that exposure of the bioretention systems to prolonged high NaCl-based road de-icing salts may have contributed to this high TDP and SRP release in mid-spring (Section 3.3.4). The data analysis in this Chapter focuses on the summer and fall monitored events where the SRP distributions are not thought to be impacted by the winter and early spring salt loadings to the systems.

Porewater SRP concentrations in the East and Center bioretention cells reveal high spatial variability in the distribution of SRP including non-monotonic concentration trends with depth (Figure 4-2). This indicates that the bioretention media is not consistently releasing or retaining SRP with increasing infiltration depth. Mann-Whitney U tests of the SRP concentrations from all profiles and depths for all sampled events in summer and fall (17 July to 2 October, n=5) indicate that although there are significant differences between

some depths (for example, between 42 cm and 90 cm, $U=0.021$), the observed differences are not systematic nor indicate increasing P retention with depth (Appendix H Table H-1). Considering all sampled events in summer and fall at all profile locations, the mean SRP concentrations at 0 cm (pond water), 5 cm, 21 cm, 42 cm, 64 cm, 90 cm, and 100 cm were $98 \pm 42 \mu\text{g P/L}$, $170 \pm 174 \mu\text{g P/L}$, $72 \pm 32 \mu\text{g P/L}$, $118 \pm 100 \mu\text{g P/L}$, $156 \pm 356 \mu\text{g P/L}$, $86 \pm 93 \mu\text{g P/L}$ and $77 \pm 51 \mu\text{g P/L}$, respectively. Although not significantly different due to the high variability in SRP concentrations between precipitation events and depth profiles, the mean SRP concentration was highest within the topsoil layer at a depth of 5 cm compared to concentrations within the soil media and the infiltrating pond water. Unlike the bioretention media which was designed to meet the Credit Valley Conservation (2010) guidelines for P-index, the topsoil was locally sourced and not subject to soil testing prior to installation.

Mean soluble (NaHCO_3 -extractable) P concentrations from soil cores collected before the bioretention systems received road runoff were $337 \pm 209 \text{ mg P/kg}$ ($n = 5$) and $147 \pm 89 \text{ mg P/kg}$ ($n = 5$) for the topsoil and soil media, respectively. As such, the topsoil initially contained considerably higher soluble P compared with the soil media. The highest extractable soluble P was observed in the same location (2-5 cm depth, $504 \pm 130 \text{ mg P/kg}$) as the highest SRP porewater concentrations (5 cm depth). The solid phase extraction results combined with measured porewater distributions highlight the need for careful selection of the topsoil or mulch that is used on the surface of bioretention systems as this surface layer may act as a source of SRP and may alter the biogeochemical conditions within the underlying bioretention media layer, which may further promote SRP release. For example, the topsoil used on the monitored systems was observed to have a higher clay content compared to the underlying soil media. This may reduce the infiltration capacity of the bioretention systems and transport of oxygen to the underlying media, as well as promote cracking and preferential flow paths in dry summer conditions.

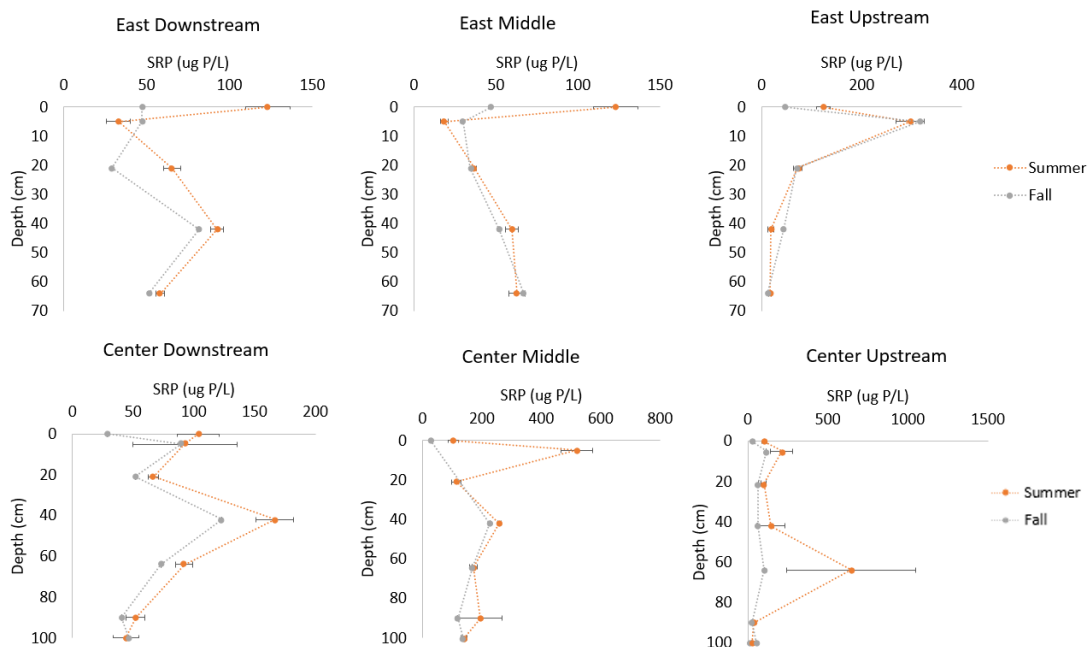


Figure 4-2: Porewater SRP concentrations for profiles in the East and Center bioretention system from summer (n=4) and fall 2019 (n=1). Pond water concentrations are shown at a depth of 0 cm.

In addition to the SRP concentrations varying non-monotonically with depth, the SRP concentration trends along each vertical profile varied between the different profile locations. For instance, considering samples collected from within the soil media only (i.e., below 5 cm), the SRP concentrations increased with depth at some profile locations (East Middle), decreased with depth at some profile locations (East Upstream), and were highest at intermediate depths at other profile locations (East Downstream, Centre Downstream, Centre Upstream). SRP data from all depths in summer and fall indicate that the SRP concentrations at the Center Middle profile were significantly different from all other profiles (Mann-Whitney U test, $p < 0.001$; see Appendix H Table H-2 for statistical analysis results). The Center Middle profile had significantly higher SRP concentrations (mean = $213 \pm 133 \mu\text{g P/L}$) than all other profiles, including those within the same bioretention system (Center Upstream mean = $179 \pm 375 \mu\text{g P/L}$, Center Downstream mean = $85 \pm 53 \mu\text{g P/L}$). In contrast, the SRP concentrations measured along the three vertical profiles in the East bioretention system were not significantly

different ($p > 0.05$) from each other (mean = $103 \pm 119 \mu\text{g P/L}$, $45 \pm 18 \mu\text{g P/L}$, and $60 \pm 23 \mu\text{g P/L}$ for the East Upstream, Middle, and Downstream locations, respectively).

Visual observations showed that there was limited ponding and infiltration around the middle Centre profile location (due to surface topography) compared to the other locations. It is possible that the higher SRP concentrations along the Centre Middle profile were associated with less infiltration resulting in longer porewater residence times and possibly more reducing conditions. Unfortunately, the field monitoring system was not designed to test this theory.

The observed heterogeneous distributions of SRP within the bioretention systems vary from previous studies that used only sediment chemical extractions to investigate P retention in bioretention systems. For instance, a recent mesocosm study by Song & Song (2018) observed sediment-bound P (extractable P, Fe-bound P, and Al-bound P) was highest at the surface and decreased with depth to 35 cm. Similarly, a field study by Komlos & Traver (2012) observed the highest sediment-bound P at shallow depth (0 – 5 cm depth), with these sediment concentrations generally decreasing with depth.

Assumptions of a homogeneous soil media mix and adsorption/desorption of SRP to/from the sediments as a function of available sorption sites (and thus infiltration depth) alone - as is commonly concluded from sediment extraction analysis (from field scale systems) and laboratory column experiments - are inconsistent with our observed heterogeneous porewater SRP distributions.

4.3.2 Relationship between SRP and other dissolved constituents

Porewater samples from 10 June, 19 August, and 2 October 2019 were analyzed for dissolved constituents often associated with the retention-release of SRP in porous media (Al, Fe, Mn, Ca). Concentrations of all constituents ranged over several orders of magnitude and the correlations between SRP, and Al, Fe, Mn, and Ca concentrations were tested for the significance of relationship for each profile independently using the Spearman rank test (critical p-value of 0.05) (Figure 4-3). Al and SRP exhibited a strong, significant, and positive correlation in the East Upstream profile ($\rho = 0.952$, $p = 0.00006$), but were not correlated for all other profiles. Fe and SRP were strongly correlated in the

Center Middle profile ($\rho=0.741$, $p=0.002$) and moderately correlated in the Center Upstream profile ($\rho=0.579$, $p=0.022$), but were not significantly correlated for all other profiles. The observed positive significant correlations suggest that Al- and Fe-oxide reductive dissolution, that may occur in response to changing pH and redox conditions, likely plays some role in the retention-release of SRP in the bioretention systems. The lack of correlation at many locations reveals the potential importance of other processes as well. Ca was significantly correlated with SRP for all profiles except Center Downstream. However, this correlation ranges from a strong negative correlation (East Upstream, $\rho=-0.929$, $p=0.0003$) to a strong positive correlation (East Downstream, $\rho=0.762$, $p=0.001$), suggesting this is not a consistent removal mechanism. However, the Ca concentrations (ranged from 13 to 197 mg Ca/L) were at least an order of magnitude higher than the SRP concentrations (ranged from 10 to 3,032 $\mu\text{g P/L}$), which makes it challenging to identify possible SRP and Ca co-precipitation and dissolution using porewater data alone as significant changes in SRP concentrations (in μg) may not result in detectable changes in Ca concentrations (in mg). Mn and SRP correlations were also highly variable between profiles. See Appendix H Tables H-3, H-4 for a summary of statistical analyses.

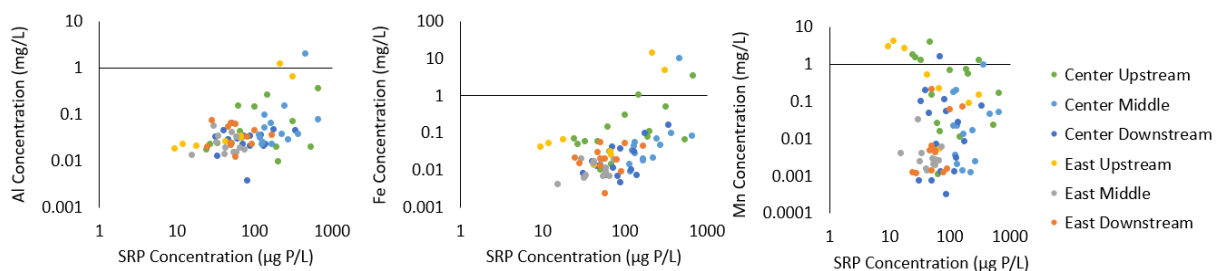


Figure 4-3: Porewater SRP and dissolved Al, Fe, and Mn from all profiles and depths in the East and Center bioretention systems collected on 10 June, 19 August, and 2 October 2019. The different coloring of the markers indicate the profile location for the porewater sample.

The role of Al- and Fe-oxide dissolution-precipitation on SRP retention-release not only varies between profile locations but also with depth in the bioretention systems. Al and SRP concentrations were strongly and positively correlated at a depth of 5 cm ($\rho=0.824$, $p=0.0003$) and moderately correlated at 42 cm depth ($\rho=0.412$, $p=0.048$), but not correlated at all other depths. Fe and SRP concentrations were strongly and positively correlated at 5 cm and 21 cm depths ($\rho=0.786$, $p=0.001$ and $\rho=0.818$, $p=0.0001$, respectively), but not correlated at all other depths. Significant correlations existed between SRP and Fe, Al, and Mn at a depth of 5 cm – this depth is within the topsoil layer which has different physical and chemical properties (i.e. porosity, Al, Fe, Mn contents, clay content, drainage capacity, and interactions with vegetation), compared to the underlying soil media. Mn and SRP correlations were highly variable at all depths, but moderately and positively correlated at 5 cm and 21 cm ($\rho=0.687$, $p=0.008$ and $\rho=0.504$, $p=0.042$, respectively). The only depth at which Ca and SRP concentrations were significantly correlated was 42 cm ($\rho=-0.478$, $p=0.05$; see Appendix H Tables H-5, H-6 for all statistical analysis results). Despite some significant correlations observed, the lack of consistency at different locations (profile locations and depths) emphasize the complexity and heterogeneity of the processes governing SRP within the bioretention systems.

The concentration depth profiles for SRP, Fe, Al, ORP and pH for the Centre system are shown in Figure 4-4 and Figure 4-5 for precipitation events on 19 August 2019 and 2 October 2019 to further examine the relationships between these constituents (Al and Fe data is only available for these events). Similar to the SRP vertical profiles, Al, Fe, pH and ORP trends are non-monotonic with depth. For some locations and sampling events, the relationship between Al, Fe and SRP is directly evident. For instance, Al, Fe, and SRP behave similarly at the Center Upstream profile, particularly around mid-depth (42 and 64 cm). The increase in Al, Fe, and SRP at 64 cm depth along this profile also coincides with an increase in pH at this depth (Figure 4-5a), suggesting that pH changes may be driving the dissolution of Al- and Fe-oxides, and therefore the release of SRP at mid-depth. While Fe- and Al-oxide dissolution can also be triggered by the onset of reducing conditions, there is no relationship between SRP concentrations and ORP at this

profile location (or other locations). In fact, ORP measurements for all profiles indicate that the conditions in the bioretention system are generally oxidizing conditions (> 50 mV) during precipitation events, and therefore ORP may not be a key control on SRP retention-release including the dissolution of Fe and Al-oxides (Figure 4-5b). For some profile locations, the SRP is not related to Al, Fe and pH revealing the potential importance of other processes in addition to adsorption-desorption to Fe- and Al-oxide surfaces governing SRP behaviour. For instance, the Centre Downstream profile shows a large increase in SRP concentration at mid-depth (42 cm) but there is no increase in the Al and Fe concentrations (Figure 4-4) and the pH remains stable with depth. While the ORP is slightly lower at 42 cm compared to other depths at this location for the 19 August precipitation event (Figure 4-5b), there is no increase in Al or Fe concentrations, suggesting conditions are not sufficiently reducing for metal oxide dissolution. The Al, Fe and SRP vertical profile distributions for the East system are provided in Appendix H Figure H-1, with the overall findings similar to the Centre system (only some profiles have similar vertical distributions of SRP, Al, and Fe).

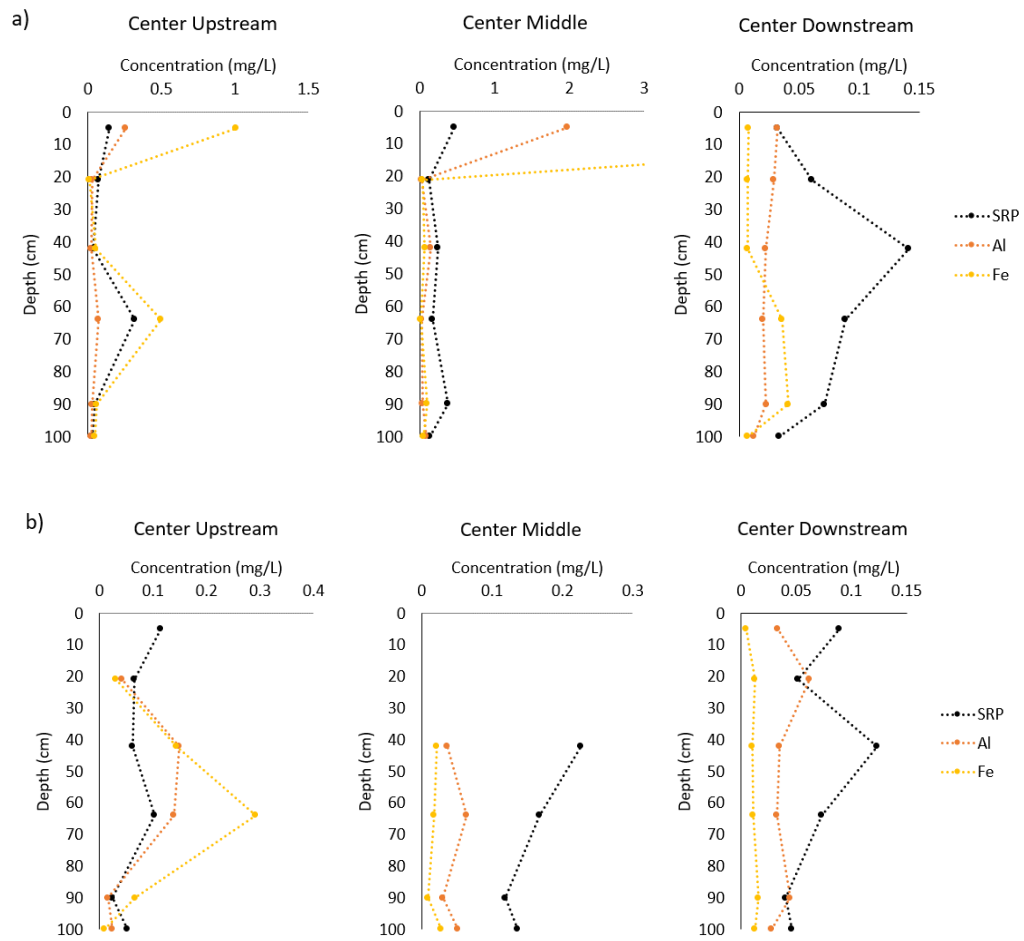


Figure 4-4: Porewater SRP, Al, and Fe concentrations along the Upstream, Middle, and Downstream profiles in the Centre bioretention system during precipitation events on a) 19 August and b) 2 October 2019.

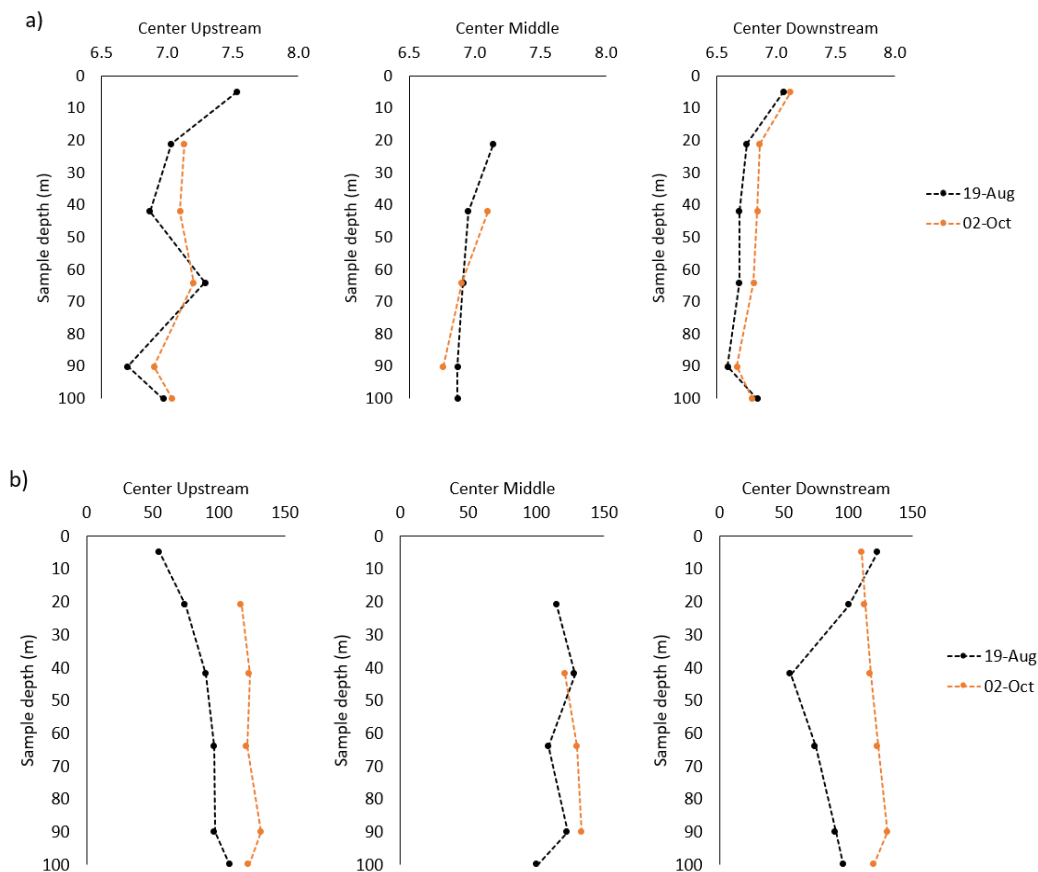


Figure 4-5: a) pH and b) ORP measurements for the Upstream, Middle and Downstream profiles in the Center bioretention system during precipitation events on 19 August and 2 October 2019.

4.3.3 Relationship between SRP and soil moisture fluctuations

Soil moisture fluctuations can influence SRP retention in porous media by increasing porewater exchange, changing redox conditions, and by causing osmotic shock to microbial biomass (Ding et al., 2019; Dupas et al., 2015; Gu et al., 2017; Mullins et al., 2020; Parsons et al., 2017). For instance, a recent mesocosm study examining SRP behaviour in the transitional zone between the land and lakes showed that high frequency drying and wetting cycles can increase the SRP release from sediments due to increased porewater exchange (Ding et al., 2019). Also, rapid fluctuations in water saturation in riparian zones are thought to cause osmotic shock and death to microbial biomass leading to SRP release (Dupas et al., 2015; Turner and Haygarth, 2001). As bioretention systems

are exposed to drying and wetting periods, it is possible that dynamic soil moisture fluctuations may be affecting the behaviour of SRP. This has not previously been examined in field bioretention studies, with few studies measuring soil moisture within field scale bioretention systems, and no studies simultaneously measuring the SRP distributions.

Soil moisture content was monitored in the East and Center bioretention systems from October 2018 to October 2019 with an example of the data for the Centre system shown in Figure 4-6 to illustrate the soil moisture dynamics during summer. As expected, the soil moisture content varied in direct response to precipitation events. The soil moisture dynamics varied between the monitored depths within the bioretention system and also between the topsoil and soil media layers. The topsoil had higher soil moisture content following precipitation events with the measured soil moisture content showing a typical surface soil drying curve between precipitation events (high evapotranspiration during the day and low evapotranspiration overnight). However, compared to the bioretention media, the topsoil had a higher silt and clay content resulting in higher moisture retention and slower initial drainage. Importantly, in both the East and Center bioretention system, the topsoil and 100 cm monitoring locations were consistently more saturated than at mid-depth, with the mid-depth locations often having the highest soil moisture content variation between precipitation events (except during prolonged drying periods when the shallow topsoil has the greatest variation, Figure 4-6, Appendix G Figure G-2). The change in soil moisture content that occurs in response to precipitation was calculated for three typical medium precipitation events (10 July, 17 July, 8 August 2019) (Appendix G Table G-2). For the Centre system, the average change in soil moisture content over a precipitation event in the topsoil and 40 cm layers ($6.6 \text{ m}^3/\text{m}^3$ and $5.4 \text{ m}^3/\text{m}^3$, respectively) was greater than at 100 cm ($2.5 \text{ m}^3/\text{m}^3$). It is possible the high porewater SRP concentrations (overall mean: $170 \text{ } \mu\text{g P/L}$, $118 \text{ } \mu\text{g P/L}$, and $156 \text{ } \mu\text{g P/L}$) observed at shallow and intermediate depths (topsoil, 42 cm, 64 cm, respectively) that were not related to changes in Fe, Al, ORP, and pH may be associated with the greatest fluctuations in soil moisture content between precipitation events (Figures 4-4 and 4-5). It is recommended future studies further explore the role of soil moisture dynamics and fluctuations within the bioretention systems on SRP release as it may be possible to

engineer the bioretention systems to limit soil moisture content fluctuations (e.g. using internal water storage zones (Eubanks et al., 2008)).

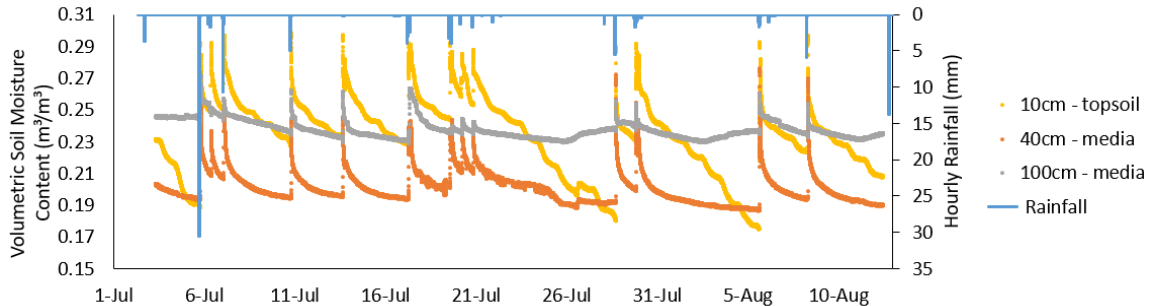


Figure 4-6: Volumetric water content in the Centre bioretention system in the topsoil layer (5 cm depth), and in the bioretention media layer (at 40 cm and 100 cm depths). The hourly precipitation depth is also shown.

4.4 Conclusions

Field-scale bioretention systems were observed to have heterogeneous spatial distributions of SRP and other constituents often associated with SRP mobility with vertical concentration profiles showing non-monotonic trends with depth. While SRP retention-release may be closely linked with Al- and Fe-oxide dissolution at some locations within the bioretention systems, SRP, Al and Fe were not consistently correlated, indicating the importance of other processes in governing the behaviour of SRP. Continuous soil moisture content measurements indicate that the moisture content fluctuations were greatest at shallow and intermediate depth within the bioretention systems. It is possible the greatest soil moisture content fluctuations at intermediate depth may be linked with the high SRP concentrations observed at this depth for many of the profile locations in the bioretention systems. The importance of the distribution and dynamics of soil moisture content within bioretention systems may be an important factor in the mobilization of SRP and this warrants further investigation.

This is the first study to our knowledge to present detailed analysis of porewater concentrations within field-scale bioretention systems. These study findings challenge

current understanding of P behaviour in bioretention systems whereby it is commonly considered that SRP adsorption to metal (Fe and Al) oxides, and particulate P filtration with depth are the major mechanisms governing P retention in bioretention systems. The field data highlight the complexity and heterogeneous behaviour of SRP in field-scale bioretention systems with SRP removal not increasing with increasing infiltration depth. This suggests that laboratory column experiments and field studies that only analyze the sediment for P content (using chemical extractions) may be over-simplifying the factors controlling P retention in field-scale bioretention systems. The data highlight the need for detailed high-resolution monitoring of the biogeochemical conditions within the bioretention systems, including the use of continuous redox, pH, and soil moisture probes. Future monitoring should also investigate the role of a topsoil or mulch layer on the overall in situ biogeochemical conditions and SRP behaviour. Finally, it is recommended that sequential sediment P extractions and porewater sampling completed over the same time period is needed to further understand the solid-aqueous phase P processes governing P retention. Identification of the different forms of sediment-bound P and how the relative pools of P change over the lifespan of a bioretention system is needed to further understand the processes governing P retention in these systems.

4.5 References

- Akhter, F., Hewa, G.A., Ahammed, F., Myers, B., Argue, J.R., 2020. Performance evaluation of stormwater management systems and its impact on development costing. *Water (Switzerland)* 12, 12–14. <https://doi.org/10.3390/w12020375>
- Blecken, G.T., Zinger, Y., Muthanna, T.M., Deletic, A., Fletcher, T.D., Viklander, M., 2007. The influence of temperature on nutrient treatment efficiency in stormwater biofilter systems. *Water Sci. Technol.* 56, 83–91. <https://doi.org/10.2166/wst.2007.749>
- Brown, R.A., Hunt, W.F., 2011. Impacts of Media Depth on Effluent Water Quality and Hydrologic Performance of Undersized Bioretention Cells. *J. Irrig. Drain. Eng.* 137, 132–143. [https://doi.org/10.1061/\(ASCE\)IR.1943-4774.0000167](https://doi.org/10.1061/(ASCE)IR.1943-4774.0000167)
- Carpenter, D.D., Hallam, L., 2010. Influence of planting soil mix characteristics on bioretention cell design and performance. *J. Hydrol. Eng.* 15, 404–416. [https://doi.org/10.1061/\(ASCE\)HE.1943-5584.0000131](https://doi.org/10.1061/(ASCE)HE.1943-5584.0000131)
- Cooper, J.E., Early, J., Holding, A.J., 1991. Mineralization of dissolved organic phosphorus from a shallow eutrophic lake. *Hydrobiologia* 209, 89–94. <https://doi.org/10.1007/BF00006920>
- Credit Valley Conservation, 2010. *Low Impact Development Stormwater Management Planning and Design Guide. Version 1.0.* Toronto and Region Conservation Authority and Credit Valley Conservation Authority.
- Davis, A.P., 2007. Field Performance of Bioretention: Water Quality. *Environ. Eng. Sci.* 24, 1048–1064. <https://doi.org/10.1089/ees.2006.0190>
- Debusk, K.M., Wynn, T.M., 2011. Storm-water bioretention for runoff quality and quantity mitigation. *J. Environ. Eng.* 137, 800–808. [https://doi.org/10.1061/\(ASCE\)EE.1943-7870.0000388](https://doi.org/10.1061/(ASCE)EE.1943-7870.0000388)

- Dietz, M.E., Clausen, J.C., 2006. Saturation to improve pollutant retention in a rain garden. *Environ. Sci. Technol.* 40, 1335–1340. <https://doi.org/10.1021/es051644f>
- Ding, B., Rezanezhad, F., Gharedaghlou, B., Van Cappellen, P., Passeport, E., 2019. Bioretention cells under cold climate conditions: Effects of freezing and thawing on water infiltration, soil structure, and nutrient removal. *Sci. Total Environ.* 649, 749–759. <https://doi.org/10.1016/j.scitotenv.2018.08.366>
- Ding, J., Hua, Z., Chu, K., 2019. The effect of hydrodynamic forces of drying/wetting cycles on the release of soluble reactive phosphorus from sediment. *Environ. Pollut.* 252, 992–1001. <https://doi.org/10.1016/j.envpol.2019.06.016>
- Dupas, R., Gruau, G., Gu, S., Humbert, G., Jaffrézic, A., Gascuel-Oudou, C., 2015. Groundwater control of biogeochemical processes causing phosphorus release from riparian wetlands. *Water Res.* 84, 307–314. <https://doi.org/10.1016/j.watres.2015.07.048>
- Eger, C.G., Chandler, D.G., Driscoll, C.T., 2017. Hydrologic processes that govern stormwater infrastructure behaviour. *Hydrol. Process.* 31, 4492–4506. <https://doi.org/10.1002/hyp.11353>
- Erickson, A.J., Gulliver, J.S., Weiss, P.T., 2012. Capturing phosphates with iron enhanced sand filtration. *Water Res.* 46, 3032–3042. <https://doi.org/10.1016/j.watres.2012.03.009>
- Eubanks, P.R., Jadlocki, S.J., Hathaway, J.M., Smith, J.T., Hunt, W.F., 2008. Pollutant Removal and Peak Flow Mitigation by a Bioretention Cell in Urban Charlotte, N.C. *J. Environ. Eng.*
- Fisher Landscaping, 2017. Sarnia Road Improvements- Bioretention Soil Test Results.
- Gu, S., Gruau, G., Dupas, R., Rumpel, C., Crème, A., Fovet, O., Gascuel-Oudou, C., Jeanneau, L., Humbert, G., Petitjean, P., 2017. Release of dissolved phosphorus from riparian wetlands: Evidence for complex interactions among hydroclimate

- variability, topography and soil properties. *Sci. Total Environ.* 598, 421–431.
<https://doi.org/10.1016/j.scitotenv.2017.04.028>
- Hager, J., Hu, G., Hewage, K., Sadiq, R., 2019. Performance of low-impact development best management practices: A critical review. *Environ. Rev.* 27, 17–42.
<https://doi.org/10.1139/er-2018-0048>
- Hedley, M., Stewart, J., Chauhan, B., 1982. No Title. *Soil Sci. Soc. Am.*
- Hsieh, C., Davis, A.P., Needelman, B.A., 2007. Bioretention Column Studies of Phosphorus Removal from Urban Stormwater Runoff. *Water Environ. Res.* 79, 177–184. <https://doi.org/10.2175/106143006X111745>
- Hunt, W.F., Davis, A.P., Traver, R.G., 2012. Meeting hydrologic and water quality goals through targeted bioretention design. *J. Environ. Eng. (United States)* 138, 698–707.
[https://doi.org/10.1061/\(ASCE\)EE.1943-7870.0000504](https://doi.org/10.1061/(ASCE)EE.1943-7870.0000504)
- Khan, U.T., Valeo, C., Chu, A., van Duin, B., 2012. Bioretention cell efficacy in cold climates: Part 2 - water quality performance. *Can. J. Civ. Eng.* 39, 1222–1233.
<https://doi.org/10.1139/l2012-111>
- Komlos, J., Traver, R.G., 2012. Long-Term Orthophosphate Removal in a Field-Scale Storm-Water Bioinfiltration Rain Garden. *J. Environ. Eng.* 138, 991–998.
[https://doi.org/10.1061/\(ASCE\)EE.1943-7870.0000566](https://doi.org/10.1061/(ASCE)EE.1943-7870.0000566)
- Kordana, S., Słyś, D., 2020. An analysis of important issues impacting the development of stormwater management systems in Poland. *Sci. Total Environ.* 727.
<https://doi.org/10.1016/j.scitotenv.2020.138711>
- Li, Davis, A., 2009. Water quality improvement through reductions of pollutant loads using bioretention. *J. Environ. Eng.* 135, 567–576.
[https://doi.org/10.1061/\(ASCE\)EE.1943-7870.0000026](https://doi.org/10.1061/(ASCE)EE.1943-7870.0000026)
- LID SWM Planning and Design Guide Contributors, 2020. Bioretention: Filter media

- LID SWM Planning and Design Guide [WWW Document]. Sustain. Technol. Eval. Progr. URL
https://wiki.sustainabletechnologies.ca/index.php?title=Bioretention:_Filter_media&oldid=10879 (accessed 5.5.20).
- Liu, J., Davis, A.P., 2014. Phosphorus speciation and treatment using enhanced phosphorus removal bioretention. *Environ. Sci. Technol.* 48.
<https://doi.org/10.1021/es404022b>
- Long, T., Wellen, C., Arhonditsis, G., Boyd, D., 2014. Evaluation of stormwater and snowmelt inputs, land use and seasonality on nutrient dynamics in the watersheds of Hamilton Harbour, Ontario, Canada. *J. Great Lakes Res.* 40, 964–979.
<https://doi.org/10.1016/j.jglr.2014.09.017>
- Lucas, W.C., Greenway, M., 2011. Phosphorus Retention by Bioretention Mesocosms Using Media Formulated for Phosphorus Sorption: Response to Accelerated Loads. *J. Irrig. Drain. Eng.* 137, 144–153. [https://doi.org/10.1061/\(ASCE\)IR.1943-4774.0000243](https://doi.org/10.1061/(ASCE)IR.1943-4774.0000243)
- Mackey, K.R.M., Van Mooy, B., Cade-Menun, B.J., Paytan, A., 2019. Phosphorus dynamics in the environment, 4th ed, *Encyclopedia of Microbiology*. Elsevier Inc.
<https://doi.org/10.1016/B978-0-12-809633-8.20911-4>
- Mangangka, I.R., Liu, A., Egodawatta, P., Goonetilleke, A., 2015. Performance characterisation of a stormwater treatment bioretention basin. *J. Environ. Manage.* 150, 173–178. <https://doi.org/10.1016/j.jenvman.2014.11.007>
- Marvin, J.T., Passeport, E., Drake, J., 2020. State-of-the-Art Review of Phosphorus Sorption Amendments in Bioretention Media: A Systematic Literature Review. *J. Sustain. Water Built Environ.* 6. <https://doi.org/10.1061/JSWBAY.0000893>
- McDowell, R.W., Sharpley, A.N., 2003. Phosphorus solubility and release kinetics as a function of soil test P concentration. *Geoderma* 112, 143–154.

[https://doi.org/10.1016/S0016-7061\(02\)00301-4](https://doi.org/10.1016/S0016-7061(02)00301-4)

- McManus, M., Davis, A.P., 2020. Impact of Periodic High Concentrations of Salt on Bioretention Water Quality Performance. *J. Sustain. Water Built Environ.* 6, 1–11. <https://doi.org/10.1061/JSWBAY.0000922>
- Mullins, A.R., Bain, D.J., Pfeil-McCullough, E., Hopkins, K.G., Lavin, S., Copeland, E., 2020. Seasonal drivers of chemical and hydrological patterns in roadside infiltration-based green infrastructure. *Sci. Total Environ.* 714, 136503. <https://doi.org/10.1016/j.scitotenv.2020.136503>
- O'Neill, S.W., Davis, A.P., 2012. Water treatment residual as a bioretention amendment for phosphorus. I: Evaluation studies. *J. Environ. Eng. (United States)* 138, 318–327. [https://doi.org/10.1061/\(ASCE\)EE.1943-7870.0000409](https://doi.org/10.1061/(ASCE)EE.1943-7870.0000409)
- Parsons, C.T., Rezanezhad, F., O'Connell, D.W., Van Cappellen, P., 2017. Sediment phosphorus speciation and mobility under dynamic redox conditions. *Biogeosciences* 14, 3585–3602. <https://doi.org/10.5194/bg-14-3585-2017>
- Passeport, E., Hunt, W.F., Line, D.E., Smith, R.A., Brown, R.A., 2009. Field study of the ability of two grassed bioretention cells to reduce storm-water runoff pollution. *J. Irrig. Drain. Eng.* 135, 505–510. [https://doi.org/10.1061/\(ASCE\)IR.1943-4774.0000006](https://doi.org/10.1061/(ASCE)IR.1943-4774.0000006)
- Prasad, R., Chakraborty, D., 2019. Phosphorus Basics: Understanding Phosphorus Forms and Their Cycling in the Soil, the Alabama Cooperative Extension System.
- Prestigiacomo, A.R., Effler, S.W., Gelda, R.K., Matthews, D.A., Auer, M.T., Downer, B.E., Kuczynski, A., Walter, M.T., 2016. Apportionment of bioavailable phosphorus loads entering Cayuga Lake, New York. *J. Am. Water Resour. Assoc.* 52, 31–47. <https://doi.org/10.1111/1752-1688.12366>
- Roy, A.H., Wenger, S.J., Fletcher, T.D., Walsh, C.J., Ladson, A.R., Shuster, W.D., Thurston, H.W., Brown, R.R., 2008. Impediments and solutions to sustainable,

- watershed-scale urban stormwater management: Lessons from Australia and the United States. *Environ. Manage.* 42, 344–359. <https://doi.org/10.1007/s00267-008-9119-1>
- Sakaki, T., Limsuwat, A., Smits, K.M., Illangasekare, T.H., 2008. Empirical two-point α -mixing model for calibrating the ECH 2O EC-5 soil moisture sensor in sands. *Water Resour. Res.* 44, 1–8. <https://doi.org/10.1029/2008WR006870>
- Shrestha, P., Hurley, S.E., Wemple, B.C., 2018. Effects of different soil media, vegetation, and hydrologic treatments on nutrient and sediment removal in roadside bioretention systems. *Ecol. Eng.* 112, 116–131. <https://doi.org/10.1016/j.ecoleng.2017.12.004>
- Song, Y., Song, S., 2018. Migration and transformation of different phosphorus forms in rainfall runoff in bioretention system. *Environ. Sci. Pollut. Res.* 1–8. <https://doi.org/10.1007/s11356-018-2405-4>
- Stagge, J.H., Davis, A.P., Jamil, E., Kim, H., 2012. Performance of grass swales for improving water quality from highway runoff. *Water Res.* 46, 6731–6742. <https://doi.org/10.1016/j.watres.2012.02.037>
- Steffen, M.M., Belisle, B.S., Watson, S.B., Boyer, G.L., Wilhelm, S.W., 2014. Status, causes and controls of cyanobacterial blooms in Lake Erie. *J. Great Lakes Res.* 40, 215–225. <https://doi.org/10.1016/j.jglr.2013.12.012>
- Street, L., 2014. A Balanced Diet for Lake Erie Reducing Phosphorus Loadings and Harmful Algal Blooms.
- Tiessen, H., Moir, J., 1993. Characterization of available P by sequential extraction, in: Carter, M.R. (Ed.), *Soil Sampling and Methods of Analysis*. Lewis Publishers, Boca Raton, pp. 75–86.
- Turner, B., Haygarth, P., 2001. Phosphorus solubilization in rewetted soils. *Nature* 411, 258. <https://doi.org/https://doi.org/10.1038/35077146>

- United States Environmental Protection Agency, 2004. National Water Quality Inventory: Report to Congress, 2004.
- Watson, S.B., Miller, C., Arhonditsis, G., Boyer, G.L., Carmichael, W., Charlton, M.N., Confesor, R., Depew, D.C., Höök, T.O., Ludsin, S.A., Matisoff, G., McElmurry, S.P., Murray, M.W., Peter Richards, R., Rao, Y.R., Steffen, M.M., Wilhelm, S.W., 2016. The re-eutrophication of Lake Erie: Harmful algal blooms and hypoxia. *Harmful Algae* 56, 44–66. <https://doi.org/10.1016/j.hal.2016.04.010>
- Wilson, C.E., Hunt, W.F., Winston, R.J., Smith, P., 2015. Comparison of Runoff Quality and Quantity from a Commercial Low-Impact and Conventional Development in Raleigh, North Carolina. *J. Environ. Eng.* 141. [https://doi.org/10.1061/\(ASCE\)EE.1943-7870.0000842](https://doi.org/10.1061/(ASCE)EE.1943-7870.0000842)
- Zhou, Z., Xu, P., Cao, X., Zhou, Y., Song, C., 2016. Efficiency promotion and its mechanisms of simultaneous nitrogen and phosphorus removal in stormwater biofilters. *Bioresour. Technol.* 218. <https://doi.org/10.1016/j.biortech.2016.07.039>

Chapter 5

5 Summary and Recommendations

5.1 Summary

Urban stormwater runoff is a major contributor to the degradation of surface water bodies worldwide as stormwater commonly has high contaminant loads, including total suspended solids (TSS), heavy metals, and nutrients (phosphorus [P] and nitrogen [N]). Prior studies have reported variable performance of bioretention systems with respect to their ability to reduce P loads in urban stormwater runoff. As such, the biogeochemical processes governing the fate of P within field-scale systems are unclear. To improve design of these systems there is a need to generate fundamental understanding of the fate of P within these systems including the underlying biogeochemical processes. While this study was performed in a cold-climate location and reveals the potential adverse impact of road de-icing salts on P retention in bioretention systems, the results may be broadly applicable to urban areas that experience salinization, for the evaluation of other stormwater LID features (e.g., infiltration trenches), or for systems installed in warmer climates. The study objectives were met through intensive monitoring and analysis of two field-scale bioretention systems.

Assessment of the seasonal performance of the field-scale bioretention systems revealed high release of P, mostly in the form of soluble reactive P (SRP), from the systems in spring compared to other seasons. The timing of P release in spring is of particular concern as high spring P loads to surface waters have been implicated in the proliferation of large algal blooms in summer (Irvine et al., 2019). Considering field data collected over a 12-month period, the bioretention systems were found to provide net retention of TP (3 ± 20 g P) and DOP (4 ± 5 g P), but a net release of SRP (21 ± 5.4 g P) and TDP (12 ± 10 g P). The behaviour of SRP appeared to govern the overall annual behaviour of TDP as SRP accounted for the majority of TDP. Porewater

samples collected during precipitation events in spring, summer and fall showed although adsorption to Al- and Fe-oxides may be an important P retention mechanism, this mechanism it is not likely responsible for the observed seasonal trends in P retention. The observed seasonal trends of the retention of the different forms of P highlight the complexity of the mechanisms that govern P fate in bioretention systems installed in cold climates and the need to consider temporal variability in field studies quantifying the ability of LID features to retain P.

The second objective to evaluate the effect of high salt (NaCl) loading on P retention in field-scale bioretention systems was addressed by combining the field monitoring data with laboratory column experiments designed to isolate the effects of NaCl loading on P retention in bioretention media. The laboratory column experiments revealed that prolonged input of high NaCl loading in winter may cause high spring P release with a delay between the initiation of high salt inputs and increased P release. This may be due to competitive adsorption and anion exchange processes, mobilization and mineralization of organic matter, vegetation toxicity, or impacts to the soil media's cation exchange capacity. However further work is required to identify the processes controlling the influence of high road salt loads on P retention in bioretention media, as well as to determine if the observed phenomena occurs for other bioretention media compositions.

The third study objective was to evaluate the spatial distribution of SRP within field-scale bioretention systems and the investigation the possible hydro-biogeochemical processes that influence P retention. This objective was completed through detailed porewater sampling and analysis, and soil moisture content monitoring in the field-scale bioretention systems. The SRP distribution within the bioretention systems was found to be highly heterogeneous with SRP concentrations varying non-monotonically with depth. Concentrations of dissolved constituents often associated with P retention-release in porous media suggest that SRP concentrations appear to be linked with SRP adsorption-desorption from Al- and Fe-oxides at some locations, but this mechanism does not govern P behaviour throughout the bioretention systems. Fluctuations in soil moisture content were found to be high at intermediate depth within the systems which may explain high

SRP concentrations within the bioretention systems at intermediate depth. Soil moisture fluctuations can influence P retention by increasing porewater exchange, changing redox conditions, and causing osmotic shock to microbial biomass. Overall, the field data highlight the complexity of the biogeochemical processes which affect the fate and transport of P within field-scale bioretention systems. The high spatiotemporal variability observed in the in situ P behaviour suggests the need for more intensive monitoring of bioretention systems in time and space to better understand the processes governing P retention.

5.2 Recommendations

The findings from this thesis highlight the complex behaviour of P within field scale bioretention systems including the potential impacts of high road salt application as well as the heterogeneous biogeochemical processes occurring within the systems that affect P retention and release. It is recommended that future research examine the following areas to improve understanding of P retention in bioretention systems in order to optimize the design of these systems:

- Monitor field bioretention cells over multiple years with increased sampling over all seasons. A longer monitoring period is needed to confirm the observed trend of high release of P, mostly SRP, in spring, and the potential impact of high road salt inputs.
- Conduct column experiments to investigate the influence of NaCl loading on P retention on several different field-applied bioretention media mixes. Field bioretention systems often use different media compositions that adhere to the bioretention design guidelines and as such there is a need to test the influence of NaCl loading on other bioretention media mixes. For future column experiments, it is recommended other parameters are measured including solid phase analysis, organic matter content and type, particle size analysis, and cation concentrations to better understand the processes governing the interactions between NaCl and P in the bioretention media.
- Investigate the impact of the topsoil or mulch layer on the biogeochemical conditions within the engineered soil media layer. While this study observed statistically

significant differences between P, Al and Fe concentrations in the topsoil and media layers, this currently study did not explore the impact of the topsoil layer characteristics on the conditions within the soil media layer and how this may affect P behavior.

- Improve the influent water quantity monitoring system to reduce uncertainties in quantification of the influent flow rates and thereby the water and P balances for the bioretention systems. Furthermore, measuring exfiltration to the native soil would also reduce uncertainties in the water and P balance calculations and provide insight into the implications of bioretention systems on groundwater P contamination.
- Use non-invasive methods such as geophysics to characterize the movement of the infiltrating stormwater within the bioretention systems as well as physical subsurface conditions surrounding the systems. Non-invasive methods would minimize disruption to the bioretention systems yet could provide spatially continuous time-lapse information.
- Monitor field-scale bioretention systems over time with detailed sediment extractions coupled with porewater samples. More detailed approach to understanding the P retention processes and the changes in P distribution between phases can provide greater insight into the mechanisms governing P behaviour than sediment or porewater analysis alone.
- Explore the use of continuous in situ water quality probes within the bioretention systems (e.g., for continuous redox and pH measurements) in addition to the volumetric water quantity probes used in this study. Continuous measurements at high spatial resolution would provide greater understanding of the dynamic biogeochemical conditions within the systems including capturing the dynamics of the wetting and drying cycles.
- Apply the field data to develop a numerical reactive transport model that can be applied to provide further understanding of factors controlling the P retention in bioretention systems and can be used to inform engineering bioretention system design.

5.3 References

Irvine, C., Macrae, M., Morison, M., Petrone, R., 2019. Seasonal nutrient export dynamics in a mixed land use subwatershed of the Grand River, Ontario, Canada. *J. Great Lakes Res.* 45, 1171–1181. <https://doi.org/10.1016/j.jglr.2019.10.005>

Appendices

Appendix A: Supporting information on field bioretention system monitoring

Project: Sarnia Road Improvements - Bioretention Soil Test Results

Soil Supplier	JRFisher	JRFisher
Report	C17237-103661-1	C17237-103661-2
Lab Number	45734-C	45735-D
Date:	Sep-22-17	Sep-22-17

Criteria	Design Value ¹		
• Soil Composition (percent by weight)			
o Gravel (Coarse > 50 mm)	-		
o Gravel (Fine and Coarse < 50 mm)	-		
o Sands	85% to 88%	90.2%	92.2%
o Fines	8% to 12%	9.8%	7.8%
Silt		6.0%	4.0%
Clay		3.8%	3.8%
• Organic Matter	3% to 5%	3.3%	3.4%
• Phosphorus Index (P-index) value	10 to 30 PPM		
Bicarb		9	11
Bray-P1		13	14
• Cationic Exchange Capacity (CEC) in mg/100g	> 10 meq/100g	38.2	38.2
• pH	5.5 to 7.5	7.5	7.4
• Infiltration rate	>25mm/hr	N/A	N/A
Soil Textural Class	Loamy Sand	Sand	Sand

1. Design Values as per the CVC's specifications - Low Impact Development Stormwater Management Planning and Design Guide
Does not meet Design Value

Infiltration Testing:

Soil Supplier:	JRFisher
Report:	C17256-70020-1
Date:	27-Sep-17
Infiltration Rate:	26.52 in/hr
	673 mm/hr

Figure A-0-1: Initial bioretention soil media test results (Fisher Landscaping, 2017)

Additional information on monitoring instrumentation in bioretention systems

Hydraulic monitoring of the bioretention systems was completed through influent and effluent measurements. Precipitation depth and curbside weir boxes were used to characterize input water volume. Precipitation depth and panel temperature were recorded every 5 minutes from December 2018 to February 2020 using two rain gauges located at Western University. The tip volume of the Texas Electronics rain gauge was calculated to be 0.147mm/tip. Some data is missing from due to volatile and ring memory technical issues. The Weather Measure WEATHERtronics rain gauge as calculated to be have a tip volume of 0.216mm/tip. It is noted that none of the rain gauges were heated, therefore data is approximated during the winter months. The definition of a rain event ensured that residual water after a rain event would not be classified as its own event. If two distinct rain events by definition occurred in close proximity and resulted in a hydrograph with a single indistinct peak, it was analyzed as one rain event.

Stainless steel weir plates were installed onto concrete boxes at both curb inlets in the East bioretention system to quantify the water volume entering the system from the road. The 75-degree V-notch weir plate, as shown in Figure A-2, measured 16 cm high and had a 4 cm threshold height. The plate was laser cut into 1/8' thick stainless steel by the University Machine Services at Western University. The 0.55m x 0.4m weir box provided backwater volume to stabilize incoming runoff. The total pressure readings from the Diver data loggers installed in the weir were offset using barometric pressure data recorded using a Level TROLL 700 Data Logger located on the CMLP roof at Western University to calculate the depth of water.



Figure A-2: Influent weir installed at curb inlet of the East bioretention system

The effluent weir was designed with a 14 cm, 5-degree lower v-notch, and a 90-degree upper v-notch. The two-stage V-notch design allowed for continuous sensitive measurements for low-flow events as well as the capacity to measure high-flow events (Figure A-3). A threshold of 3.5 cm created backwater volume in the sloped underdrain to stabilize the flow. The weir plates were laser cut into clear PETG by University Machine Services at Western University (Figure A-4). A field calibration shown in Figure A-3 was performed during a precipitation event on 27 August 2019 to correlate the measured water level with flow rate, and the calibration equation was applied to all recorded flow measurements. The 2.0 psi pressure transducer was installed upright and protected from moisture using a tubing membrane.

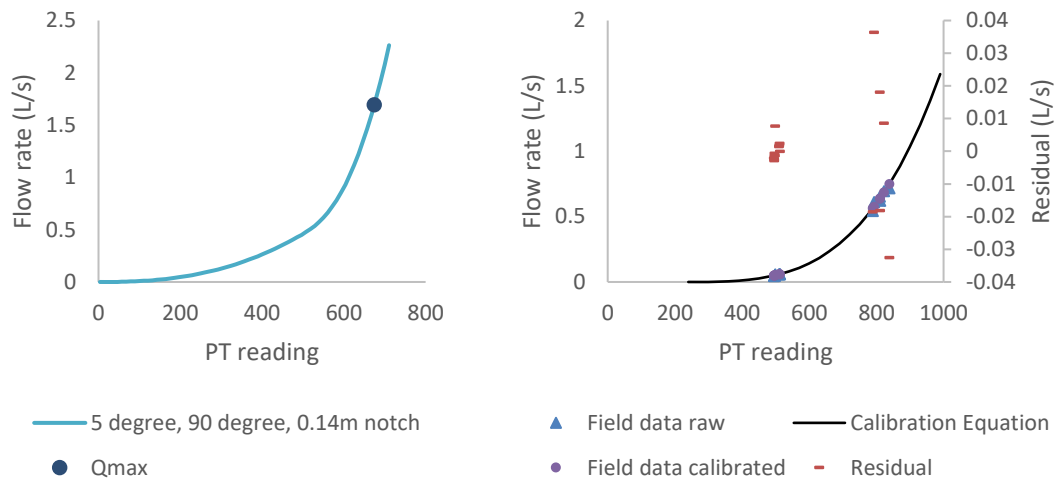


Figure A-3: (a) Design flow rate for effluent weir, and (b) field calibration of effluent weir completed on 27 August 2019.



Figure A-4: Installed effluent weir with pressure transducer and automatic sampler port.

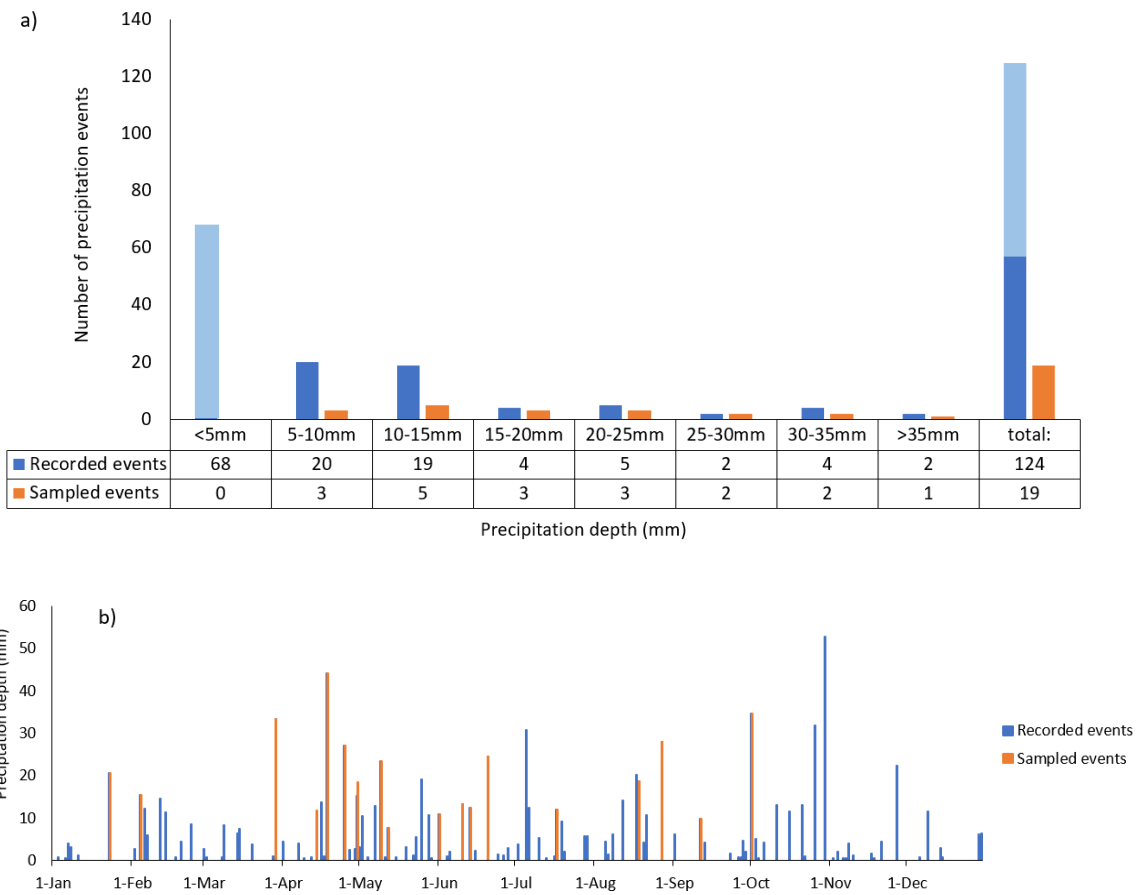


Figure A-5: Distribution of sampled events in 2019 considering (a) precipitation depth and (b) seasonality and frequency

Appendix B: Analytical methods for the determination of water quality parameters

Table B-1: Analytical methods for the determination of water quality parameters

Analyte	Analysis Method	Method	Detection limits	Storage conditions
Electrical Conductivity (EC) and pH	HACH HQ40D portable multi meter, Intellical™ CDC401 probe and Intellical™ PHC201 probe	N/A	N/A	Measured immediately, or within 14 hours, stored at 4°C.
Soluble Reactive Phosphorus (SRP)	LaChat QuikChem 8500 Flow Injection Analysis	10-115-01-1-M	1-100 ug P/L	Stored at 4°C for analysis within 48 hours of collection
Total (Dissolved) Phosphorus (TP and TDP)	HACH Total Phosphorus UV-Vis Method 8190	Standard method 4500-P E	0.1 to 2.0 mg P/L	Stored frozen at -17°C
Chloride (Cl)	Waters High-Performance Liquid Chromatography (HPLC)	432 w/ 717	2.5 mg/L to 100 mg/L	Stored frozen at -17°C
Al, Ca, Fe, Mn, Na	Vista-PRO CCD Simultaneous ICP_OES by Varian	Standard method 3120B	1 to 100 mg/L	Stored frozen at -17°C, acidified with HNO ₃ before analysis

Appendix C: P concentrations and mass loading

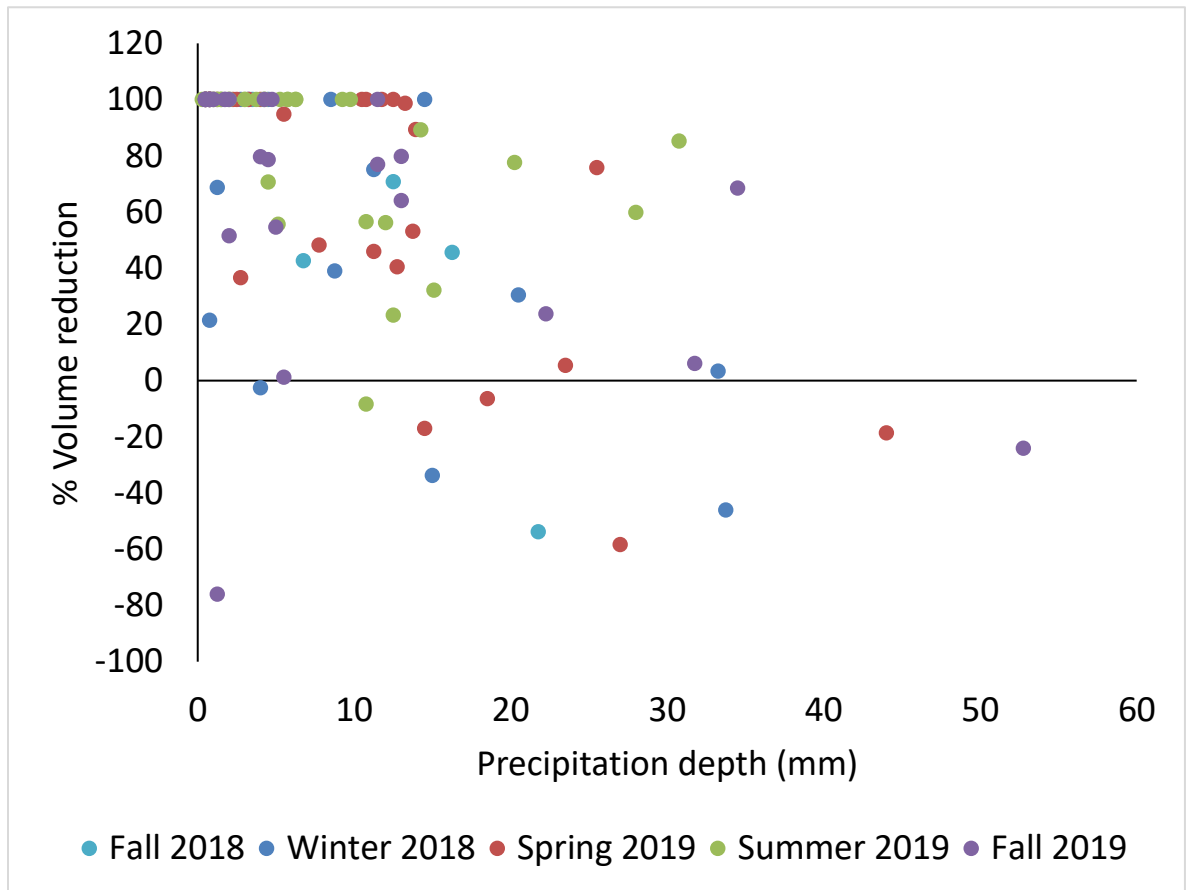


Figure C-1: Relationship between percent volume reduction and precipitation depth

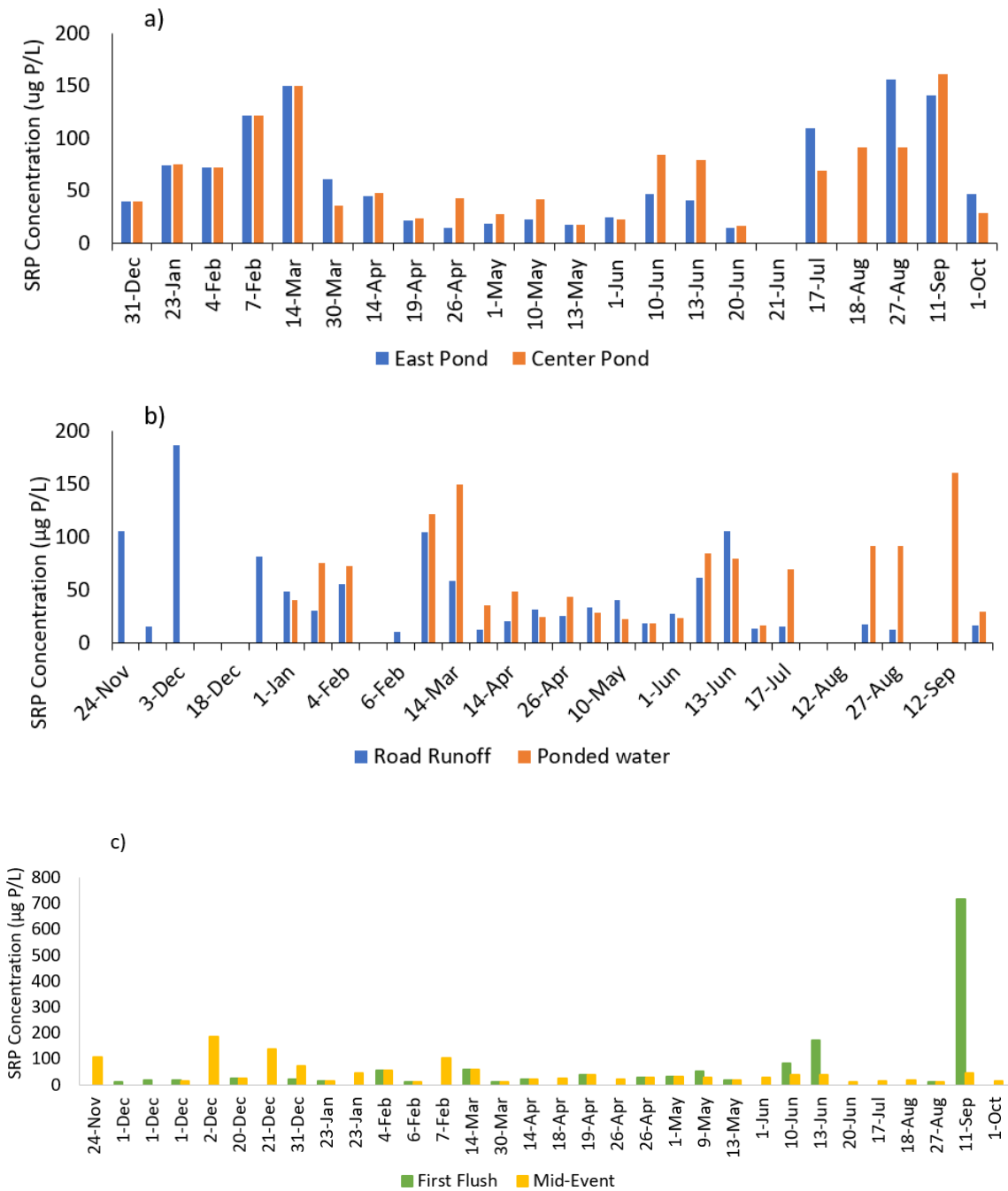


Figure C-2: (a) Pond water SRP concentrations for the ponded water on the East and Center systems (b) SRP concentrations for road runoff and ponded water from November 2018 to October 2019 (c) SRP concentrations for samples collected during the first flush and in the middle of the precipitation event

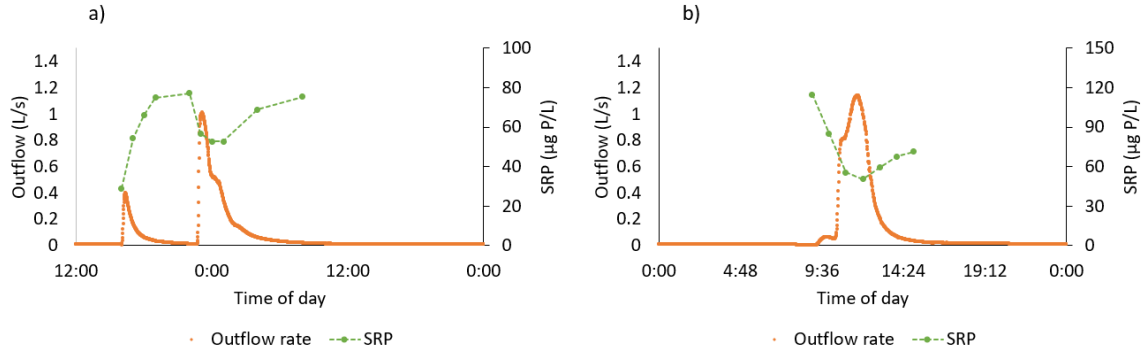


Figure C-3: Stability of effluent SRP concentrations over the duration of the precipitation event on (a) 18 August 2019 and (b) 27 August 2019

Hourly samples collected from the effluent indicate a relatively stable effluent. Stagnant water that is collected from the underdrain immediately before drainage occurs can have a small impact on the first samples of the drainage event. There is also some dilution of SRP concentrations that occurs during high peak flows, but overall a single sample is representative of the concentrations that occur throughout the drainage period. For example, the mean SRP concentration of samples collected during the 18 August precipitation event was $64 \pm 9.7 \mu\text{g P/L}$.

Table C-1: Mass retention of TP, TDP, DOP, and SRP. Total by season, and mean retention per event sampled

	TP	TP standard deviation	TDP	TDP standard deviation	SRP	SRP standard deviation	DOP	DOP standard deviation
Total P retention- Winter 2018 (mg)	7.5	2.6	-1.7	0.7	-3.0	0.3	0.5	0.5
Total P retention- Spring 2019 (mg)	-6.3	3.76	-12.4	1.80	-18.5	1.01	2.6	1.00
Total P retention- Summer 2019 (mg)	3.2	1.35	0.8	0.69	-0.6	0.19	0.4	0.53
Total P retention- Fall 2019 (mg)	-0.3	0.36	0.3	0.36	0.0	0.14	0.0	0.22

	TP	TP standard deviation	TDP	TDP standard deviation	SRP	SRP standard deviation	DOP	DOP standard deviation
Mean P retention per event- Winter 2018 (mg)	1.87	0.65	-0.42	0.18	-0.74	0.08	0.14	0.11
Mean P retention per event- Spring 2019 (mg)	-0.57	0.34	-1.13	0.16	-1.68	0.09	0.24	0.09
Mean P retention per event- Summer 2019 (mg)	0.64	0.27	0.17	0.14	-0.13	0.04	0.09	0.11
Mean P retention per event- Fall 2019 (mg)	-0.28	0.36	0.27	0.36	0.03	0.14	0.02	0.22

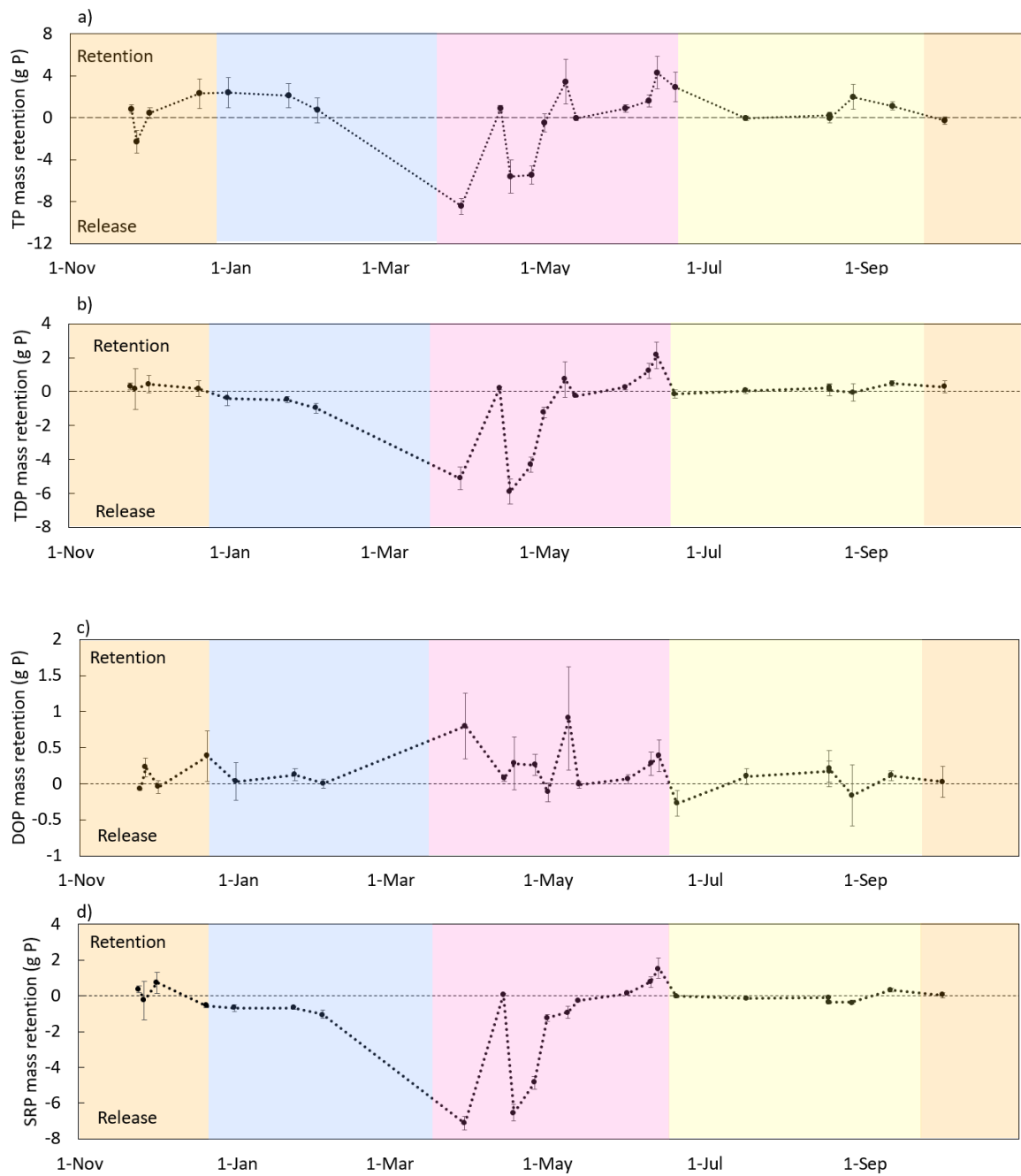


Figure C-4: Mass retention of (a) TP, (b) TDP, (c) DOP, and (d) SRP for the East bioretention system from November 2018 to October 2019. The pink region represents Spring 2019.

Appendix D: Statistical analysis of effluent P concentrations and loads

Statistical analysis of effluent P concentrations between seasons

Table D-1: Mann-Whitney U test results for statistical differences in (a) TP, (b) TDP, (c) DOP, (d) SRP effluent concentrations across seasons. P values <0.05 indicate concentrations are statistically different between seasons. P values >0.05 indicate there is not enough data to statistically conclude that the P concentrations during each season are different

a)

TP	Fall 2018	Winter 2018	Spring 2019	Summer 2019	Fall 2019
Fall 2018		0.60	0.12	0.48	0.65
Winter 2018			0.04	0.25	0.48
Spring 2019				0.014	0.22
Summer 2019					0.48
Fall 2019					

b)

TDP	Fall 2018	Winter 2018	Spring 2019	Summer 2019	Fall 2019
Fall 2018		0.86	0.016	1	0.65
Winter 2018			0.031	0.77	0.48
Spring 2019				0.03	0.12
Summer 2019					0.48
Fall 2019					

c)

DOP	Fall 2018	Winter 2018	Spring 2019	Summer 2019	Fall 2019
Fall 2018		0.48	0.71	0.29	0.18
Winter 2018			1.24	0.56	0.16
Spring 2019				0.28	0.38
Summer 2019					0.48
Fall 2019					

d)

SRP	Fall 2018	Winter 2018	Spring 2019	Summer 2019	Fall 2019
Fall 2018		1	0.17	0.48	0.18
Winter 2018			0.12	0.021	0.16
Spring 2019				0.031	0.12
Summer 2019					0.16
Fall 2019					

Table D-2: Seasonal P effluent concentration calculations. S.D. represents Standard Deviations

	SRP outflow [] (ug P/L)	S.D.	TP outflow [] (mg P/L)	S.D.	TDP outflow [] (mg P/L)	S.D.	DOP outflow [] (mg P/L)	S.D.
Fall 2018	95.4	35.0	0.14	0.05	0.11	0.02	0.01	0.01
Winter 2018	97.6	23.1	0.15	0.06	0.12	0.03	0.02	0.02
Spring 2019	151.9	68.9	0.23	0.08	0.18	0.04	0.03	0.04
Summer 2019	67.5	5.1	0.15	0.02	0.11	0.03	0.05	0.03
Fall 2019	45.5	0.0	0.16	0.00	0.09	0.00	0.04	0.00

Table D-3: Kruskal-Wallis H test for P effluent concentrations between seasons

	H	p-value
SRP	9.62	<0.05
TP	8.78	<0.1
DOP	2.94	>0.5
TDP	10.8	<0.05

Table D-4: Spearman rank correlations between P effluent concentrations and rainfall depth. P values <0.05 indicate correlations are statistically different.

	ρ	P	Correlation
TP	-0.125	0.56	insignificant low negative
TDP	0.029	0.89	insignificant low negative
SRP	0.166	0.44	insignificant low negative
DOP	-0.257	0.22	insignificant low negative

Statistical analysis of net P loads between seasons

Table D-5: Mann-Whitney U test results for statistical differences in (a) TP, (b) TDP, (c) DOP, (d) SRP mass retention across seasons. P values <0.05 indicate retentions are statistically different between seasons. P values >0.05 indicate there is not enough data to statistically conclude that the P retentions during each season are different

a)

TP	Fall 2018	Winter 2018	Spring 2019	Summer 2019	Fall 2019
Fall 2018		0.077	0.59	0.65	0.65
Winter 2018			0.90	0.05	0.16
Spring 2019				0.69	0.88
Summer 2019					0.38

b)

TDP	Fall 2018	Winter 2018	Spring 2019	Summer 2019	Fall 2019
Fall 2018		0.077	0.39	0.30	0.65
Winter 2018			0.60	0.086	0.16
Spring 2019				0.69	0.88
Summer 2019					0.38

c)

DOP	Fall 2018	Winter 2018	Spring 2019	Summer 2019	Fall 2019
Fall 2018		0.29	0.14	0.30	0.65
Winter 2018			1	0.81	1
Spring 2019				0.69	0.88
Summer 2019					0.38

d)

SRP	Fall 2018	Winter 2018	Spring 2019	Summer 2019	Fall 2019
Fall 2018		0.034	0.24	0.30	0.65
Winter 2018			0.70	0.014	0.16
Spring 2019				0.69	0.88
Summer 2019					0.38

Table D-6: Seasonal P mass retention calculations. S.D. represents Standard Deviations

	mean SRP mass retention (g P)	S.D.	mean TP mass retention (g P)	S.D.	mean TDP mass retention (g P)	S.D.	mean DOP mass retention (g P)	S.D.
Fall 2018	0.28	1.01	-0.36	1.02	0.30	1.07	0.08	0.11
Winter 2018	-0.74	0.22	1.87	1.84	-0.42	0.50	0.32	0.32
Spring 2019	-1.68	0.35	-0.57	1.56	-1.13	0.73	0.47	0.43
Summer 2019	-0.09	0.12	0.64	0.85	0.17	0.43	0.28	0.33
Fall 2019	-0.06	0.33	-0.28	0.51	0.27	0.51	0.24	0.30

Table D-7: Kruskal-Wallis H test for P mass retention between seasons

	H	p-value
SRP	4.91	0.5 to 0.25
TP	3.91	<0.5
DOP	2.12	<0.75
TDP	4.02	<0.5

Table D-8: Spearman rank correlations between P effluent concentrations and rainfall depth

	ρ	P	Correlation
TP	-0.177	0.41	No
TDP	-0.490	0.015	significant low/ moderately negative
SRP	-0.624	0.001	significant/ moderately negative
DOP	0.461	0.022	significant low/ moderately positive

Appendix E: Statistical analysis for seasonal porewater samples

Table E-1: Spearman rank correlations between porewater elements and SRP

	Al	Ca	Cl	Fe	Mn	Na
01-Jan-19	N/A	N/A	-0.1667	N/A	N/A	N/A
07-Feb-19	N/A	N/A	-0.486	N/A	N/A	N/A
30-Mar-19	0.641	-0.306	-0.333	0.522	0.385	-0.541
10-Jun-19	0.513	-0.432	0.773	0.770	0.356	0.436
19-Aug-19	0.628	-0.122	0.358	0.475	0.057	0.400
02-Oct-19	0.25092	-0.174	0.385	0.0269	-0.368	0.162

Table E-2: P-values for significance of correlations between porewater elements and SRP

	Al	Ca	Cl	Fe	Mn	Na
01-Jan-19	N/A	N/A	-0.167	N/A	N/A	N/A
07-Feb-19	N/A	N/A	-0.486	N/A	N/A	N/A
30-Mar-19	0.007	0.249	0.023	0.090	0.322	0.030
10-Jun-19	0.021	0.057	0.00006	0.00007	0.123	0.055
19-Aug-19	0.0002	0.520	0.052	0.008	0.766	0.028
02-Oct-19	0.207	0.385	0.047	0.894	0.059	0.420

Table E-3: Porewater concentrations. SRP concentrations are in $\mu\text{g P/L}$ while other elements are in mg/L

	SRP	Al	Ca	Cl	Fe	Mn	Na
01-Jan-19	202.6	N/A	N/A	2930.2	N/A	N/A	N/A
07-Feb-19	109.3	N/A	N/A	6915.6	N/A	N/A	N/A
30-Mar-19	292.4	0.083	102.262	2581.4	0.393	0.056	1718.660
10-Jun-19	207.0	0.043	64.310	53.84	0.216	0.119	80.400
19-Aug-19	110.0	0.144	86.550	23.98	0.862	0.554	123.411
02-Oct-19	82.0	0.069	84.784	19.78	0.203	0.284	86.355

Table E-4: Standard deviations of porewater concentrations. SRP deviations are in $\mu\text{g P/L}$ while other elements are in mg/L

	SRP	Al	Ca	Cl	Fe	Mn	Na
01-Jan-19	107.9	N/A	N/A	4285.9	N/A	N/A	N/A
07-Feb-19	56.6	N/A	N/A	3171.9	N/A	N/A	N/A
30-Mar-19	216.0	0.176	75.277	2251.2	1.328	0.120	1147.253
10-Jun-19	194.7	0.071	51.174	127.5	0.725	0.182	59.838
19-Aug-19	110.5	0.400	43.049	45.92	2.963	1.011	177.177
02-Oct-19	65.4	0.113	46.192	30.70	0.860	0.820	112.908

Table E-5: Kruskal-Wallis test for statistical difference of P mass retention between seasons

	SRP	Al	Ca	Fe	Mg	Mn	Na	Cl
Degrees of freedom	5	3	3	3	3	3	3	5
H- value	29.5	9.01	4.20	7.24	6.27	5.74	37.4	66.6
p-value	<0.05	<0.05	<0.25	<0.1	0.1	<0.25	<0.05	<0.05
Statistical difference between seasons?	Yes	Yes	No	No	No	No	Yes	Yes

Appendix F: Calculations for SRP release at the column and field scales

Table F-1: Summary calculations of chloride mass per volume of pore spaces before divergence of TP release in columns treated with salted road runoff

Column experiment	Value	Assumptions
Volume of media in column (m ³):	5.11E-04	0.05 m diameter, 0.26 m height
Volume of Pore space in column (m ³)	1.33E-04	0.26 porosity
Volume of Pore space in column (L)	1.33E-01	
Infiltration rate (L/day)	1.44	
Pore volumes/day	10.84	
Time to divergence (days)	20	
Pore volumes flushed before divergence	216.8	
Influent Cl concentration (mg/L)	1200	
Influent Cl infiltration rate (mg/day)	1728	
water volume to flush total column pore space 210 times (L)	27.90	
Cl mass in total column pore space flush (mg)	33480.7	
Cl mass per [total pore space] flush (mg)	159.4	

Table F-2: Summary calculations of chloride mass per volume of pore spaces before divergence of TP release in the East bioretention system based on column-scale chloride loading

East bioretention system		Assumptions
Volume of media in East system (m ³):	53	53 m ² footprint, 1 m media depth
Volume of pore space in system (m ³):	13.78	0.26 porosity
Volume of pore space in system (L):	13780	
Volume of 210 [total system pore spaces] (m ³):	2893.8	
Volume of 210 [total system pore spaces] (L):	2893800	
Cl mass per 210[total pore space] flush	4.61E+08	

Table F-3: Summary of calculations for cumulative chloride loading from the East bioretention system from Winter 2018

Date of drainage	Total Effluent Volume (L)	First Flush Chloride Concentration (mg/L)	First Flush Cl loading (mg)	Cumulative Influent Cl loading - First Flush (mg)	Mid-Event Chloride Concentration (mg/L)	Mid-Event Cl loading (mg)	Cumulative Influent Cl loading - Mid-Event (mg)
24-Nov-18	2770	20	5.54E+04	5.54E+04	20	5.54E+04	5.54E+04
26-Nov-18	23921	63	1.50E+06	1.55E+06	63	1.50E+06	1.55E+06
01-Dec-18	9029	959	8.66E+06	1.02E+07	959	8.66E+06	1.02E+07
20-Dec-18	6319	1366	8.63E+06	1.88E+07	1366	8.63E+06	1.88E+07
28-Dec-18	3817	5000	1.91E+07	3.79E+07	1500	5.73E+06	2.46E+07
31-Dec-18	14344	24073	3.45E+08	3.83E+08	159	2.28E+06	2.68E+07
08-Jan-19	3256	12000	3.91E+07	4.22E+08	500	1.63E+06	2.85E+07
23-Jan-19	10161	7961	8.09E+07	5.03E+08	2378	2.42E+07	5.26E+07
4-Feb-19	33107	202	6.69E+06	5.10E+08	202	6.69E+06	5.93E+07
14-Feb-19	2201	150	3.30E+05	5.10E+08	70	1.54E+05	5.95E+07
Mean		5179			722		

Appendix G: Supplementary material for soil moisture content monitoring

Soil moisture probe calibration and installation methods

The Decagon EC-5 soil moisture probes use excitation voltages to measure the dielectric constant of soils and media. Each probe was calibrated twice in the lab using Equation G-1:

$$\theta = \frac{ADC^{\alpha} - ADC_{dry}^{\alpha}}{ADC_{sat}^{\alpha} - ADC_{dry}^{\alpha}} \phi \quad (G-1)$$

Where θ = the volumetric soil moisture, $\alpha=2.5$, ϕ =porosity (set to 0.28 for bioretention media), ADC_{dry} = ADC counts in air-dry soil, and ADC_{sat} = ADC counts in water-saturated soil. ADC counts are determined using the raw mV reading from the sensor. Table G-1 includes the lab experimental calibration data. Although the two-point Sakaki calibration method does not require a unique calibration for each soil type, select sensors were re-calibrated using a native topsoil to account for the physical differences between the topsoil and media layers.

Table G-1: Decagon EC-5 soil moisture probe calibration readings

Installation location	mV		ADC counts	
	Air-Dry	Saturated	Air-Dry	Saturated
East, topsoil	370.2	663.7	55321.4	30855.6
Center, topsoil	444.5	639.0	46071.6	32052.6
Center, 40cm	442.9	648.4	46240.7	31586.7
Center, 100cm	445.3	643.3	45991.5	31837.1
East, 25cm	425.4	674.6	48140.1	30359.9
East, 50cm	439.5	642.3	46595.8	31884.2
East, 100cm	438.3	628.9	46728.7	32567.4

Deep sensors were installed in individual one-inch boreholes using an insertion tool and then backfilled with media to reduce soil disturbance and preferential flow paths. Shallow sensors were installed vertically in the side of boreholes to minimize disturbance to infiltration pathways and ponding on the sensor prongs. All cables were buried and connected to a Campbell Scientific CR10x data logger through the monitoring chamber. The volumetric water content was determined every 5 to 15 minutes throughout the study period. However, high chloride loadings due to road salt application caused some interference in the volumetric water content readings in winter.



Figure G-1: Decagon EC-5 soil moisture probe

Soil moisture content dynamics in the bioretention systems

Table G-2: Soil moisture content for select rain events in the Center bioretention system

Location	Rainfall date	Pre-precipitation soil moisture (m³/m³)	Max-precipitation soil moisture (m³/m³)	Change in soil moisture (m³/m³)	Average change in soil moisture (m³/m³)
Topsoil	10 July, 2019	22.9	29.8	6.9	6.6
	17 July, 2019	23.1	29.0	5.9	
	8 August, 2019	22.6	29.6	7.1	
40cm	10 July, 2019	19.6	24.4	4.7	5.4
	17 July, 2019	19.5	23.9	4.4	
	8 August, 2019	19.5	26.7	7.2	
100cm	10 July, 2019	23.7	26.3	2.6	2.5
	17 July, 2019	23.6	26.4	2.9	
	8 August, 2019	23.6	25.5	2.0	

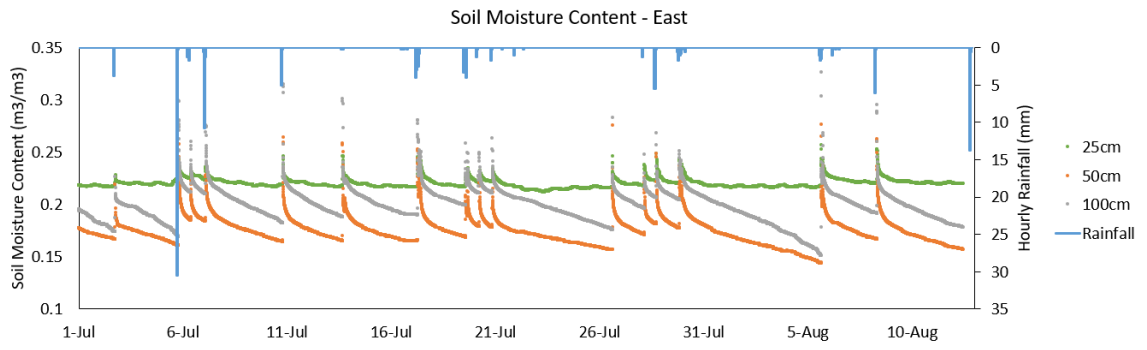


Figure G-2: Soil moisture content and precipitation depth in the East bioretention system

Appendix H: Distribution and statistical analysis of dissolved constituents in porewater

Statistical analysis of dissolved constituents in porewater

Table H-1: Mann-Whitney U test results for statistical differences in SRP porewater concentrations by profile. p values <0.05 indicate SRP concentrations are statistically different between profiles. p values >0.05 indicate there is not enough data to statistically conclude that the SRP concentrations at the two profiles are different

Profile	Center Middle	Center Downstream	East Upstream	East Middle	East Downstream
Center Upstream	0.0003	1.000	0.138	0.015	0.138
Center Middle		0.000002	0.001	2E+08	3E+08
Center Downstream			0.188	0.001	0.184
East Upstream				0.705	0.543
East Middle					0.062

Table H-2: Mann-Whitney U test results for statistical differences in SRP porewater concentrations between depths. p values <0.05 indicate SRP concentrations are statistically different with depth. p values >0.05 indicate there is not enough data to statistically conclude that the SRP concentrations at the two depths are different

Depth	21cm	42cm	64cm	90cm	100cm
5cm	0.725	0.502	0.346	0.376	0.370
21cm		0.032	0.046	0.111	0.179
42cm			0.145	0.021	0.036
64cm				0.025	0.048
90cm					0.870

Table H-3: Spearman-rank correlations between porewater SRP and other dissolved constituents analyzed by profile location. Moderate correlation is 0.4 to 0.69, strong correlation is 0.7 to 0.89, and very strong correlation is 0.9 to 1.0.

Profile	Al	Fe	Mn	Ca
Center Upstream	0.254	0.579	-0.436	-0.907
Center Middle	0.495	0.741	0.020	-0.556
Center Downstream	0.097	0.347	-0.079	-0.300
East Upstream	0.952	0.310	-0.881	-0.929
East Middle	-0.074	0.186	-0.175	0.662
East Downstream	0.000	0.101	0.699	0.792

Table H-4: p-values (significance) for correlations between porewater elements and SRP analyzed by profile location. Correlations are considered statistically significant for p-values <0.05.

Profile	Al	Fe	Mn	Ca
Center Upstream	0.360	0.022	0.101	0.000001
Center Middle	0.069	0.002	0.946	0.036
Center Downstream	0.720	0.185	0.769	0.257
East Upstream	0.0001	0.448	0.002	0.0003
East Middle	0.820	0.561	0.584	0.016
East Downstream	1.000	0.753	0.009	0.001

Table H-5: Spearman-rank correlations between porewater SRP and other dissolved constituents analyzed by depths. Moderate correlation is 0.4 to 0.69, strong correlation is 0.7 to 0.89, and very strong correlation is 0.9 to 1.0.

Depth	Al	Fe	Mn	Ca
5cm	0.824	0.786	0.687	-0.462
21cm	-0.397	0.818	0.509	-0.024
42cm	0.483	0.324	-0.255	-0.478
64cm	0.412	0.362	-0.062	-0.456
90cm	0.371	0.029	-0.429	0.257
100cm	0.250	0.550	-0.233	-0.217

Table H-6: p-values (significance) for correlations between porewater elements and SRP analyzed by depth. Correlations are considered statistically significant for p-values <0.05.

Depth	Al	Fe	Mn	Ca
5cm	0.0003	0.001	0.008	0.108
21cm	0.125	0.0001	0.042	0.931
42cm	0.048	0.203	0.322	0.050
64cm	0.110	0.166	0.820	0.073
90cm	0.454	0.956	0.379	0.614
100cm	0.512	0.115	0.541	0.572

Distribution of dissolved constituents in porewater in the East bioretention system

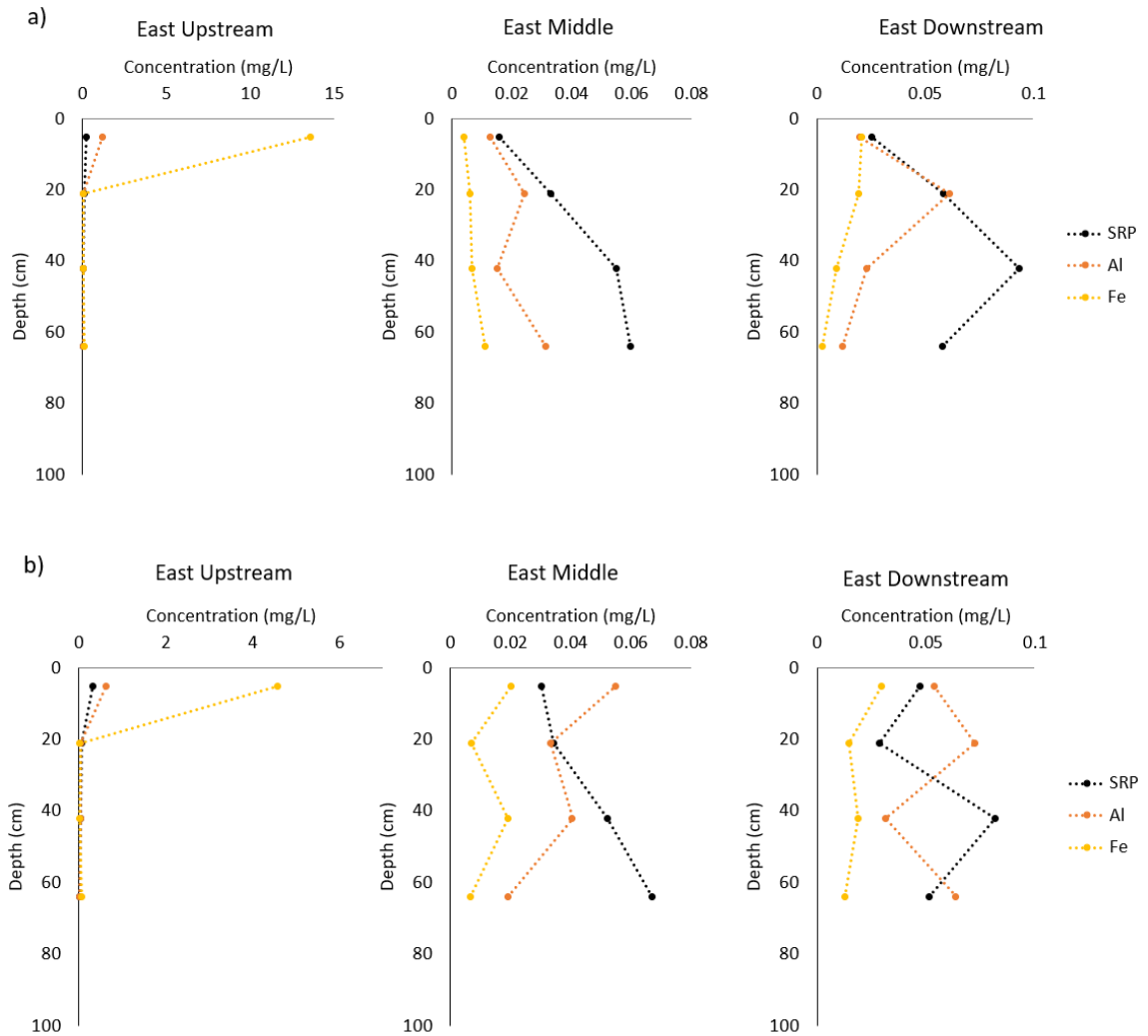


Figure H-1: Porewater SRP, Al, and Fe concentrations in the East Upstream, Middle, and Downstream profiles for precipitation events on (a) 19 August and (b) 2 October 2019

Curriculum Vitae

Name: Jaeleah Goor

Post-secondary Education and Degrees: The University of Western Ontario
London, Ontario, Canada
2013-2017 B.E.Sc.

The University of Western Ontario
London, Ontario, Canada
2017-2020 M.E.Sc

Honours and Awards: The R.M. Quigley Award
2019

Environment & Sustainability Award of Excellence
2018, 2019

Related Work Experience Graduate Teaching Assistant
The University of Western Ontario
2017-2018